5-2021

Musculoskeletal Modeling Analysis of Knee Joint Loading During Uphill and Downhill Waling In Patients with Total Knee Replacement

Tanner A. Thorsen
University of Tennessee, tthorsen@vols.utk.edu

To the Graduate Council:

I am submitting herewith a dissertation written by Tanner A. Thorsen entitled "Musculoskeletal Modeling Analysis of Knee Joint Loading During Uphill and Downhill Waling In Patients with Total Knee Replacement." I have examined the final electronic copy of this dissertation for form and content and recommend that it be accepted in partial fulfillment of the requirements for the degree of Doctor of Philosophy, with a major in Kinesiology and Sport Studies.

Songning Zhang, Major Professor

We have read this dissertation and recommend its acceptance:

Joshua T. Weinhandl, Jeffery A. Reinbolt, Jared M. Porter

Accepted for the Council:

Dixie L. Thompson

Vice Provost and Dean of the Graduate School

(Original signatures are on file with official student records.)

Musculoskeletal Modeling Analysis of Knee Joint Loading During Uphill and Downhill Walking in Patients with Total Knee Arthroplasty

A Dissertation Presented for the

Doctor of Philosophy

Degree

The University of Tennessee, Knoxville

Tanner A. Thorsen

May 2021

DEDICATION

This dissertation is first dedicated to my wife, Christine. Without your belief in and continual support of me through these ten years of marriage, often at your own disproportionate personal sacrifice, I would have never made it this far. Also, to our children, Trace, Harper, and Cole who greeted me with excitement and love each day as I came home, running out to the driveway ready to give hugs even before I could get my door open.

ACKNOWLEDGEMENTS

There are many people who have immensely helped me with this project, and, without them I could not have even begun this endeavor. I first had many peers who helped me, Erik Hummer, Lauren Schroder, Jake Melaro, and Shelby Peel for their many ideas and good humor that was needed through the pandemic. Without these individuals, I never would have been able to finish.

I would like to also thank my committee members for their hard work on this dissertation. In these unique times that we are in, Dr. Jared Porter, Dr. Jeffery Reinbolt, and Dr. Joshua Weinhandl, were there as I first proposed an intervention study, and then re-proposed this current simulation-based project. At every step of the way, they offered valuable counsel, taught me much about research, and willingly mentored me.

I would finally like to express my gratitude for my advisor, Dr. Songning Zhang. Over the past five years I have felt his support in too many ways to count. He has taught me to think critically and thoroughly, but more importantly, he has shown me how to be a mentor and a friend. He has worked tirelessly to ensure my success as a student and his support, encouragement, and feedback have made me a better researcher and scholar. Thank you!

ABSTRACT

The purposes of these studies were to determine differences in total (TCF), medial (MCF) and lateral (LCF) tibiofemoral compartment compressive forces and related muscle forces between limbs (replaced, non-replaced, and control), and different slopes during uphill [0° (level), 5°, 10°], and downhill [0° (level), 5° 10°] using statistical parametric mapping (SPM). Static optimization was used to determine muscle and compressive forces for 9 patients with total knee arthroplasty (TKA) and 9 control participants during walking trials. Total , loading-response, and push-off TCF impulse were calculated. A 3×3 [Limb (replaced, non-replaced, control] × Slope (0°, 10°, 15°)] SPM{F} repeated measures ANOVA was conducted independently for both uphill and downhill walking. Independent 3×3 (Limb × Slope]) mixed-model ANOVA were used to detect differences for TCF impulse for both up- and downhill walking.

For study one, significant between-limb differences were observed for MCF during 23-30% stance between replaced and control limbs. Significant differences between slopes were observed for all variables, except knee flexor muscle force. TCF impulse indicates that joint load is greater for all limbs as slope increases. A small sample size of patients with TKA who utilize different gait strategies may have rendered difference between limbs non-significant.

For study two, significant differences were found for TCF, MCF, and knee flexor muscle forces between replaced and control limbs during early loading-response (1-5% stance). No significant differences were found between limbs for MCF or LCF, suggesting that TKA may have been successful in correcting errant frontal plane alignment. Loading-response TCF impulse increased with increasing slope yet push-off

TCF impulse decreased with increasing decline slope suggesting decreased knee joint loading during push-off while not having to overcome gravity.

Uphill walking may be an effective exercise for high intensity early and long-term rehabilitation programs with increased muscular demand and quadriceps strengthening as slope increases while promoting the reacquisition of normal gait patterns following TKA. Downhill walking facilitates increased muscular demand and quadriceps strengthening via eccentric contractions while regaining normal gait patterns following TKA. Downhill walking, therefore, may be an effective exercise for high intensity early and long-term rehabilitation.

TABLE OF CONTENTS

LIST OF TABLES

LIST OF FIGURES

CHAPTER I

INTRODUCTION

Background

Uphill walking is a necessary part of daily living and has become popular in exercise and rehabilitation for patients with total knee arthroplasty (TKA) (Ehlen et al., 2011; Meier et al., 2008; Silder et al., 2012). The biomechanics of uphill walking in young, healthy populations has been documented in the literature. Kinematically, uphill walking has been shown to produce a greater knee flexion angle at heel strike (Alexander and Schwameder, 2016; Hong et al., 2014; Lay et al., 2006; McIntosh et al., 2006) and during early stance (Franz and Kram, 2014; Lay et al., 2006; McIntosh et al., 2006), but with reduced knee flexion range of motion (ROM), compared to level walking. This may be in part due to a greater knee flexion angle at heel strike, as well as reduced knee extension nearing toe-off, in order to raise the lower limb with sufficient clearance on the inclined surface (Franz and Kram, 2014; Lay et al., 2006; McIntosh et al., 2006). Uphill walking has also been shown to generate greater peak knee extension moment (KEM) (Alexander and Schwameder, 2016; Lay et al., 2006; McIntosh et al., 2006; Redfern and DiPasquale, 1997). Previous studies of uphill walking in young healthy individuals have also shown that walking up inclines greater than 10° actually reduces frontal plane joint loading represented by the internal knee abduction moment (KAbM), which may have implications for TKA rehabilitation (Haggerty et al., 2014; Lange et al., 1996).

Wen et al. (2019) conducted one of the first biomechanical studies of uphill walking in which patients with TKA and heathy controls performed walking trials on slopes of 0° (level walking), 5°, 10°, and 15°. For all slopes, TKA patients had smaller

knee extension ROM and lower KEM than did healthy controls in both the replaced and non-replaced limbs. At every inclination, both the replaced and non-replaced limbs, patients with TKA demonstrated significantly lower knee extension ROM compared to healthy controls. Knee flexion ROM, however, was only different between slopes and not between replaced, non-replaced, or control limbs. The replaced limb of TKA patients exhibited lower peak KEM at 10° and 15° incline compared to the non-replaced limb. Between slopes, the replaced limb demonstrated that peak KEM was lower during level and 5° uphill walking (0.33 ± 0.21 and 0.30 ± 0.22 Nm, respectively) compared to 10° and 15° uphill walking (0.39 ± 0.27 and 0.45 ± 0.28 Nm, respectively). More importantly, there was a significant limb × slope interaction, suggesting that the non-replaced limb demonstrated greater increases in peak KEM from 0° (0.35 ± 0.24 Nm) to 15° (0.61 ± 0.33 Nm) than the replaced limb. Peak vertical ground reaction forces (GRF) and peak loading-response KAbM were also lower in all uphill walking conditions for all participants compared to level walking.

Wen et al. (2021) also performed the first biomechanical analysis of downhill walking in patients with TKA. Wen and colleagues reported increased knee flexion ROM with decreasing slope. Peak loading-response vertical GRF was lower in level walking and -5° relative to -10° and -15° (Wen et al., 2021). For patients with TKA, it was found that at all slopes loading-response peak vertical GRF was lower in the replaced limb than the non-replaced limb. For both the TKA group and the healthy control group, peak push-off vertical GRF was greater in the level walking and -5° slope compared to the -10° and -15° slopes. During downhill walking, peak KEM increased with decreased slope, and the non-replaced limb of patients with TKA experienced greater peak loading-response KEM

than the replaced limb during all downhill conditions. Interestingly, the non-replaced limb of patients with TKA also demonstrated lower peak loading-response KEM than the healthy control group.

Previous research has shown that joint loading variables such as KEM and KAbM have been correlated to medial compartment tibiofemoral compressive force in level walking (Walter et al., 2010). However, these variables alone do not directly indicate the magnitude of tibiofemoral compressive forces. Understanding knee joint contact forces can provide valuable insights for rehabilitation protocols and prosthesis design. The magnitude and behavior of tibiofemoral joint compressive forces during uphill walking as compared to level walking remains unknown in the literature. *In vivo* tibiofemoral compressive forces measured with an instrumented knee replacement suggest that the knee can experience joint loading that exceed two times of body weight (BW) during stance of level walking (Mundermann et al., 2008; Zhao et al., 2007a). Knee joint prostheses instrumented with force measurement capacity is expensive and impractical for normal clinical use. However, *in vivo* measurements only report forces from the instrumented knee prostheses, and not the contralateral non-replaced knee, and medial and lateral compartment-specific compressive forces are less frequently reported (Fregly et al., 2012). Understanding joint contact forces of the contralateral limb contributes important information to the wholistic understanding of bipedal ambulation following TKA. It has been shown that patients with TKA ambulate with biomechanical deficits during level walking and during stair negotiation following surgery, which likely may affect the loading of the contralateral limb and may perpetuate OA progression and explain the large prevalence of contralateral TKA following unilateral arthroplasty

(Aljehani et al., 2019; Standifird et al., 2016). These deficits may include reduced KEM in the replaced limb (Wen et al., 2019), shorter stride length (Benedetti et al., 2003), decreased knee flexion ROM, peak knee flexion angle (Benedetti et al., 2003), and reduced vertical GRF in the replaced limb (Kramers-de Quervain et al., 2012).

In light of the limitations of instrumented knee joint prostheses, musculoskeletal modeling and simulation provide tools that allow for the estimation of tibiofemoral compressive forces and related muscle forces without need of *in vivo* measurements (Delp et al., 2007; Lerner et al., 2015; Steele et al., 2012). One commonly used software that has this capability is OpenSim, a freely-available open source platform designed for the analysis of biological movement (Delp et al., 2007). Lerner et al. (2014) utilized the Joint reaction analysis tool in OpenSim to compute tibiofemoral joint compressive as participants walked with increased gait speed. Ten healthy participants walked on an instrumented treadmill at speeds of 0.75, 1.25, and 1.5 $m \cdot s^{-1}$. A generic OpenSim model with 12 segments, 19 degrees of freedom, and 92 muscles was modified to include a planar patellofemoral joint. They reported peak loading-response compressive forces increased over 50%, from 2.0 BW to 3.0 BW as walking speed increased. Peak push-off compressive forces also increased significantly with walking speed, from 2.4 BW to 2.8 BW.

Advances in musculoskeletal modeling and simulation have afforded researchers the capability of estimating compartment-specific tibiofemoral contact forces. Utilizing an electromyography (EMG) driven musculoskeletal modeling and simulation strategy, Saxby et al. (2016) had sixty older adults walk overground at a self-selected pace (1.44 ± 0.22 $m \cdot s^{-1}$) while kinematics, kinetics, and EMG of specific lower extremity

muscles were recorded. A generic OpenSim musculoskeletal model was modified by adding an internal/external rotation degree of freedom while the abduction/adduction degree of freedom remained locked. Medial and lateral tibiofemoral contact points were determined using a regression method based on femoral condyle width (Winby et al., 2009). Gait biomechanics and EMG data served as inputs for an EMG-driven model to estimate muscle and tibiofemoral contact forces (Gerus et al., 2013; Winby et al., 2009). They reported peak tibiofemoral compressive force of 2.8 BW while walking at a self-selected pace.

Lerner et al. (2015) implemented a static optimization approach with a novel musculoskeletal knee model that was capable of resolving total tibiofemoral compressive force (TCF) into the compartment-specific medial and lateral compressive forces (MCF and LCF). More importantly, this model accounted for patient-specific frontal plane alignment of the lower extremity as well as for patient specific condylar contact points. Two revolute joints which work only in the frontal plane connect the femur to the tibia. These revolute joints alone cannot allow frontal plane rotation of the knee joint, but, acting in parallel, act to share all loads that are transmitted through the joint thus allowing for the resolution of MCF and LCF. These resolute joints are placed specifically at the pre-determined, subject specific condylar contact points and thus can more accurately determine compressive forces as well as moments of force. This model estimated TCF 2.3 BW, as well as MCF of 1.3 BW and LCF of 1.0 BW during the stance phase of level walking. Given the nature of increased medial compartment joint loading (i.e., increased MCF) that was likely a contributing factor to knee osteoarthritis (OA) preceding TKA, investigation of the response of TCF, MCF, and LCF in uphill and downhill walking can

provide insight not only to overall joint loading but also changes in medial compartment joint loading consequential of TKA in both replaced and contralateral knees.

Discrete point analysis has been the most common form of data analysis in biomechanics. With discrete point analysis, the dimensionality of a time-series of a dependent variable against an independent variable (i.e., a join angle plotted across time), is reduced to single key data points (e.g., local minima or maxima) that are used to describe the entirety of the biological movement (Warmenhoven et al., 2018). One advantage of discrete point analysis it can very effectively convey certain information, such as changes in ROM. The ability, though, to examine a biomechanical variable throughout the entirety of a specified movement is of particular interest. Statistical Parametric Mapping (SPM) has gained popularity in biomechanical research , and had been implemented to assess the time-series of biomechanical variables throughout the entirety of a movement (Pataky et al., 2015). One benefit of SPM is that a temporally normalized dependent variable can be evaluated over a specific time continuum, rather than distilled into a discrete value (i.e., maximum, or minimum value) as in traditional statistical analysis. In SPM, a time series of the critical value thresholds is determined from the smoothness of the residuals of the data (Penny et al., 2011). Examples of these critical values include statistical tests such as the t-statistic for either Student's or Hotelling's T-Test, or the f-statistic for an analysis of variance. Then, Random Field Theory is used to minimize Type I error rates of the test-statistic time series' topological features. Finally, the probability that the test statistic time series field could have crossed the critical value threshold by chance is calculated using analytic expectation (Cao and Worsley, 1999).

Statement of Problems

The behavior of knee joint compressive forces throughout the entirety of stance in response to changes in slope during uphill and downhill walking in older adults who have undergone TKA remains unknown. The results of this study may help to inform TKA rehabilitation protocols and prosthesis design. Therefore, the purposes of these studies are as follows:

Study One

The aim of Study One was to determine differences in tibiofemoral joint compressive forces (TCF, MCF, LCF) between different limbs (replaced, non-replaced, and control), and different slopes ([0° (level), 5° and 10° (uphill)], and their interactions. We also explored differences in TCF impulse and muscle forces between different limbs and slopes.

Study Two:

The aim of Study Two was to determine differences in tibiofemoral joint compressive forces (TCF, MCF, LCF) between different limbs (replaced, non-replaced, and control), and different slopes ([0° (level), 5° and 10° (downhill)], and their interactions. We also explored differences in TCF impulse and muscle forces between different limbs and slopes.

Research Hypotheses

Study One

It was hypothesized that tibiofemoral compressive forces, TCF impulse, and knee joint-spanning muscle forces during uphill walking would be greater in the control limb, followed by the non-replaced limb of the TKA group, and lowest in the replaced limb of

the TKA group, and that compressive and muscle forces would increase with each slope. We also hypothesized an interaction would be present between limbs and slopes for tibiofemoral compressive forces and muscle forces.

Study Two

It was hypothesized that tibiofemoral compressive forces, TCF impulse, and knee joint-spanning muscle forces during downhill walking would be greater in the control group, followed by the non-replaced limb of the TKA group, and lowest in the replaced limb of the TKA group, and that compressive and muscle forces would increase with each slope. We also hypothesized an interaction would be present between limbs and for tibiofemoral compressive forces and muscle forces.

Delimitations

For the TKA group, the inclusion criteira included:

- Men and Women 50-75 years old.
- Minimum of 6 months post TKA surgery.
- Maximum of 5 years post TKA surgery.

For the TKA group, the exclusion criteira included:

- Diagnosed osteoarthritis of the hip or ankle of the same side as TKA or any major spinal disorder, including osteoarthritis of the spine, as reported by the patient.
- Diagnosed osteoarthritis of the contralateral ankle, knee or hip as reported by the patient.
- Previous replacement of any other lower extremity joint.

- Any arthroscopic surgery or intra-articular injections in any lower extremity joint within past 3months.
- Systemic inflammatory arthritis (rheumatoid arthritis, psoriatic arthritis) as reported by the patient.
- BMI greater than 38 kg/m^2
- Inability to walk without a walking aid.
- Neurologic disease (e.g., Parkinson's disease, stroke) as reported by the patient.
- Any visual conditions affecting gait or balance.
- Any major lower extremity injuries/surgeries.
- Women who are pregnant or nursing.
- Any cardiovascular disease or primary risk factor, which precludes participation in aerobic exercise as indicated by the Physical Activity Readiness Survey.

For the Control group, inclusion criteria included:

- Men and Women 50-75 years old.

For the Control group, exclusion criteria included:

- Knee pain experienced during routine activities of daily living.
- Diagnosis of arthritis of any form in any lower extremity joint, as reported by the patient.
- Previous replacement of any other lower extremity joint.
- Any arthroscopic surgery or intra-articular injections in any lower extremity joint within past 3months.

- Systemic inflammatory arthritis (rheumatoid arthritis, psoriatic arthritis) as reported by the patient.
- BMI greater than 38 kg/m^2
- Inability to walk without a walking aid.
- Neurologic disease (e.g., Parkinson's disease, stroke) as reported by the patient.
- Any visual conditions affecting gait or balance.
- Any major lower extremity injuries/surgeries.
- Women who are pregnant or nursing.
- Any cardiovascular disease or primary risk factor, which precludes participation in aerobic exercise as indicated by the Physical Activity Readiness Survey.

Limitations

- All data were previously collected in a laboratory setting.
    - All data were previously collected. Therefore, data collection procedures could not be changed.
    - Motion capture tracking markers for the foot segment were placed on the shoe. As such, these tracking markers may not truly reflect the movement of the foot within the shoe.
    - The accuracy of three-dimensional kinematics collected with a motion capture system is greatly influenced by the accuracy of the placement of anatomic markers on the surface of the skin at bony landmarks.
    - The ramp assembly required placement within the motion capture volume prior to any participant coming into the lab. As such, all incline and

decline conditions were always performed prior to level walking conditions.

- In order to obtain contact forces, we used OpenSim's joint reaction analysis which uses muscle forces that were solved for using static optimization. Muscle activations and forces from static optimization are not time dependent and may differ from *in vivo* activations and forces and even dynamic optimization techniques.
- Subject-specific medial and lateral condyle contact points, as well as subject specific frontal plane knee joint alignment were not implemented in this study, which could hamper accuracy of compressive force estimation (Lerner et al., 2015).

CHAPTER II

LITERATURE REVIEW

Abstract

The purposes of these studies are to determine differences in tibiofemoral joint compressive forces between different limbs (replaced, non-replaced, and control), and different slopes, and their interactions during uphill and downhill walking. We also explored differences in total tibiofemoral compressive force (TCF) impulse and muscle forces between different limbs and slopes. This chapter includes literature review of four primary topics. The first section contains a review of the pertinent literature comparing gait biomechanics between healthy individuals and those with total knee arthroplasty (TKA). Next, this chapter discusses the most common techniques and a brief review of *in-vivo* tibiofemoral joint compressive force measurement. Third, this chapter reviews the musculoskeletal modeling and simulation techniques that have been utilized to estimate tibiofemoral compressive forces. The final topic of this chapter discusses one-dimensional statistical parametric mapping; a hypothesis testing tactic whereby the entire waveform of a biomechanical variable, rather than discrete values, is statistically tested.

Comparison of TKA vs. Healthy Gait Lower Extremity Biomechanics

Understanding differences in gait following TKA during different modes of ambulation enhances surgical and rehabilitative outcomes for the patient. Walking is a basic human movement and is crucial to the successful performance of several common activities of daily living. In the subsequent sections, gait alterations due following TKA will be discussed for level walking, uphill walking, and downhill walking in comparison of the replaced limb, non-replaced limb, and healthy control limbs.

Level Walking

Kinematics

For most people, walking is a basic and integral aspect of daily life and is critical for increased quality of independent living. As such, determining the effect of TKA on kinematic and kinetic biomechanical variables is an important place to begin the assessment of surgical and rehabilitation outcomes. Important kinematic variables which merit discussion as it relates to TKA include knee flexion angle at initial heel strike, maximum knee flexion angle during the stance phase and the swing phase of gait, and total knee flexion range of motion (ROM).

Knee flexion angle at initial heel strike has been shown to be similar between replaced limbs, non-replaced limbs, and healthy control limbs (Benedetti et al., 2003; Kurihara et al., 2021; Levinger et al., 2013; McClelland et al., 2011). In a comparison of 32 patients with TKA and 28 age matched control participants, Levinger et al. (2013) reported knee flexion angle at heel strike of 14.1° pre-TKA, and a post-surgical knee flexion angle of 12.8°. When compared with the knee flexion angle at initial contact for the control group (9.3°) however, pre-TKA knee flexion angle at initial contact was

significantly greater. Benedetti et al. (2003) also demonstrated similar knee flexion angles at heel strike for the replaced and control limbs. In this comparison of 9 patients with TKA and 10 healthy control patients, knee flexion angle at heel strike 6 months post-TKA was reported as 3.4°, 2.3° at 12 months post-TKA and 4.2° at 24 months post-TKA, with the control group reported as 1.5°. Similar trends in knee flexion angle at initial contact have been shown by McClelland et al. (2011) who reported similar knee flexion at initial contact for their control group compared to the TKA group (7.08° vs 4.80°, non-significant). These data suggest that the knee flexion angle at heel strike does not change significantly between pre- and post-TKA patients or healthy controls.

During the loading-response phase of stance, the knee to flexes to provide stability in preparation for power generation during propulsion (McClelland et al., 2011). Many studies have reported that patients post-TKA present with reduced stance phase knee flexion (Ouellet and Moffet, 2002). Specifically, Ouellet et al. (2002) demonstrated that the replaced knee had peak knee flexion angle during stance reduced by nearly 9° compared to pre-TKA and 12° compared to healthy controls nearly 2 months after TKA. This reduced knee flexion deficit was accompanied with greater hip flexion and a more dorsiflexion ankle during stance. These results are supported by the work of McClelland et al. (2011), Levinger et al. (2013), and Saari et al. (2005) who reported reduced peak knee flexion angles following surgery.

In the sagittal plane, knee joint ROM is often computed as the difference of the knee angle at initial heel strike and the maximum knee flexion angle achieved during the stance phase. As might be expected with reduced peak knee flexion angles, smaller knee flexion ROM in patients following TKA has been reported. Levinger et al. (2013), for

example, reported that patients following TKA demonstrated a reduced knee flexion ROM of nearly 8° compared to healthy control knee flexion ROM of more than 11°. Benedetti et al. (2003) also reported decreased knee flexion ROM of 8° in patients following TKA when compared against healthy controls. From examination of knee flexion angle at initial heel strike and peak knee flexion angle during stance in conjunction with knee flexion ROM, it is evident that the diminished knee flexion ROM is a product of reduced peak knee flexion angles during stance and at initial heel strike. Previous work has suggested that patients of TKA implement an altered gait pattern, referred to as stiff-knee gait, whereby a diminished amount of weight bearing knee flexion is observed during the stance phase of gait (Milner and O'Bryan, 2008). Having defined knee flexion ROM as the difference between the peak knee flexion angle and peak knee extension angle, Wen et al. (2019) reported knee flexion ROMs during level walking for the replaced and non-replaced limbs of patients with TKA, as well as both limbs of participants of a control group. The replaced and non-replaced limbs saw a small and non-significant decrease in ROM (-40.8 ± 5.2° and -43.1 ± 6.1°, respectively, compared to -43.4 ± 5.2° and -44.7 ± 7.2°, for the healthy control limbs).

Joint kinematics in the frontal plane are also an important aspect to examine in patients following TKA. Frequently, TKA is the sought-after solution to joint pain and loss of function that result from knee osteoarthritis (OA). With the development of knee OA, anatomical and alignment changes are introduced to the knee joint such as joint space narrowing (Andriacchi et al., 2009), increased bone mineral density (Miyazaki et al., 2002), increased joint laxity (Lewek et al., 2004). The end result of these anatomical changes is that compressive forces of the medial compartment can become higher than

non-pathological knee joints. During adduction of the knee, the lateral compartment is off loaded, while at the same time the medial compartment is compressed. The degenerative cartilage changes in the medial compartment cause the joint space narrowing and a change of lower limb alignment to be more varus which causes more compression on the medial compartment, which increases the joint laxity of the knee joint (Lewek et al., 2004). It has been well documented that frontal plane kinematics play a critical role in the development of medial compartment knee OA.

Several researchers have demonstrated that peak knee adduction angles can successfully be restored to be comparable with healthy knees through TKA procedures (Mandeville et al., 2008; McClelland et al., 2011). Six-months following surgery, Mandeville et al. (2008) reported that patients who have undergone surgery exhibited peak frontal plane knee adduction angle of 5.81° while the healthy control group exhibited peak frontal plane knee adduction angle of 5.46°. Likewise, McClelland et al. (2011) reported similar knee adduction angles of TKA and healthy control group of 4.54° and 4.54° respectively.

While comparison of the replaced limb against healthy control limbs provides valuable information, inter-limb comparison of the replaced and non-replaced limbs also provide insight to gait adaptations post-TKA. Due to the bilateral effects of knee OA, unilateral TKA replaced knees cannot be compared against the non-replaced limb as an accurate control limb for comparison, however it is still important to make such comparisons (Aljehani et al., 2019). Milner et al. (2008) showed no difference stance phase peak knee adduction between the replaced limb, non-replaced limb, and control limbs (1.8°, 4.3°, and 2.4° respectively). In another study, frontal plane knee adduction

was significantly lower in the replaced limb compared to the non-replaced limb (0.9° vs. 3.6° respectively) during level walking (Alnahdi et al., 2011). These studies suggest encouraging results that the correction of errant frontal plane knee alignment during TKA can be translated to the dynamic task of walking.

Kinetics

Ground reaction force (GRF) is a measurement of the force applied to a body by the ground during the stance phase of gait and can be considered a useful indicator of total external loading to the body (Wahid et al., 2016; Yocum et al., 2018). For comparison amongst individuals, GRF is frequently reported as a percent of body weight (BW). Furthermore, the magnitude of GRF is directly associated with gait velocity. As gait velocity increases, the acceleration of the body as it contacts the ground increases, and therefore the force imparted on the ground by the body increases, thus resulting in an increased GRF. As such, it is common for BW-normalized GRF to be reported alongside gait velocity so as to understand the source of any differences.

For the TKA population, peak vertical GRF has been shown by some to decrease in the replaced limb following TKA (Burnett et al., 2015; Wahid et al., 2016; Yoshida et al., 2008). In addition to decreased GRF in the replaced limb compared to the non-replaced limb, patients of TKA have also been shown to exhibit lower GRF than healthy controls as well. Kramers-de Quervain et al. (2012) measured GRF prior to, and two years following TKA in a large sample of 111 patients. Two years following TKA, patients with TKA demonstrated significantly decreased GRF on the replaced limb compared against the non-replaced limb (1.06 vs. 1.10 BW, respectively). It has been speculated that the inter-limb GRF asymmetry encourages increased loading in the non-

replaced limb compared to the replaced limb, potentially leading to a primary TKA on the non-replaced limb (Sayeed et al., 2011; Zeni Jr et al., 2019).

Joint kinetic variables describe the forces acting on the joint during a specific activity. Common example of joint kinetic variables are joint moments, powers, and joint contact forces (which will be discussed in depth in a later section). A joint moment is defined as the product of a force and the perpendicular distance of the vector of that force to an axis of rotation. As with all moments of force, the torque applied by the force causes a rotation about the related axis. At the knee joint, the axis of rotation is the knee joint center. Common forces that act upon the knee joint stem from the GRF and acting muscle forces. For comparison amongst individuals of different body masses, joint moments are often normalized to body mass (Nm/kg) or the product of bodyweight and height (%BW × height).

During the stance phase of gait, the internal sagittal-plane knee joint moment represents the sum of moments produced by all muscles, often referred to as the net moment, acting on the knee in the sagittal-plane in response to the externally applied moment by GRF (Winter, 2009). If, for example, the resultant GRF vector was to pass posterior to the knee joint center, this torque application would promote angular rotation of the shank relative to the femur, or, in other words, knee flexion. A common method for calculating these external joint moments is inverse dynamics; whereby measured kinematics and the external GRF and anthropometric data can be used to calculated net joint torques starting with the most distal segment and working proximally (Winter, 2009). Typically, during healthy gait, the internal moment is primarily a knee extension moment (KEM) during stance phase (Nordin and Frankel, 2001; Winter, 2009).

In the sagittal plane, there are two knee joint moments, KEM, and the knee flexion moment. As joint moments are related to GRF, some have suggested that the asymmetrical trends of GRF in patients with TKA is also reflected in the behavior of joint moments (Benedetti et al., 2003). For gait biomechanics, KEM has been frequently used as an indication of overall loading at the knee joint level (Astephen et al., 2008; Benedetti et al., 2003; Kuster et al., 1997; McClelland et al., 2014; Ngai and Wimmer, 2015; Ro et al., 2018). For the TKA population specifically, overall joint loading is of particular interest as it has been related to increased wear and degradation of the prosthesis, joint loading asymmetry, and quadriceps avoidance gait (Benedetti et al., 2003; Ro et al., 2018). It should also be pointed out that other researchers have shown that similarities between GRF and joint moments are not always present. Wen et al. (2019) for example reported that peak vertical GRF decreased with increasing slope, yet KEM increased. Similar studies have reported supporting results (Franz and Kram, 2014; Hong et al., 2014; Lay et al., 2006). A proposed mechanism behind this increased KEM has suggested that altered uphill walking kinematics, specifically an increased knee extension ROM, require the quadriceps to produce more force to elevate the center of mass up the incline, thereby increasing KEM (Alexander and Schwameder, 2016; Wen et al., 2019).

Similar to vertical GRF, knee joint moments have been shown to be decreased for the replaced limb as compared to both the non-replaced limb and healthy controls. Yoshida et al. (2008) investigated gait biomechanics of patients immediately after TKA, 3 months post-TKA, and 12 months post-TKA. Surprisingly, they did not report any deficit of KEM in the replaced limb immediately following TKA and 3 months post-TKA

(28.2 vs 28.4 Nm respectively). At 12 months post-TKA, however, they reported smaller KEM of 19.9 ± 15.5 Nm in the replaced limb, compared to the non-replaced limb of 35.6 ± 18.4 Nm. Smith et al. (2006) investigated knee joint biomechanics on 34 participants 12 months post-TKA. They reported that in the TKA group, peak external knee flexion moment was smaller in patients with TKA (0.22 Nm/kg) as compared to their healthy control group (0.31 Nm/kg). Others, such as Mandeville et al. (2007) reported that mean KEM was decreased during stance for patients with TKA by nearly 2 %BW × height and Ouellet et al. (2002) reported significant decreases of 0.31 Nm/kg for KEM for patients with TKA who were 2 months post-TKA compared to healthy controls.

Of all the kinetic variables of the knee during gait, the frontal plane internal joint moment has received a great deal of attention for many years (Andriacchi et al., 2009; Hunt et al., 2006; Hurwitz et al., 1998; Lewek et al., 2004; Schipplein and Andriacchi, 1991; Zhao et al., 2007b). This moment is often expressed as an external adduction moment with two peaks during the early and late stance phase of gait. During stance, the ground reaction force vector generally passes medial to the knee joint center, creating a positive adduction torque on the knee joint (Hunt et al., 2006). This external torque acts to adduct the knee into a more varus position, which in turn is countered by an internal knee abduction moment (KAbM) (Cerejo et al., 2002; Schipplein and Andriacchi, 1991). Given the relationship of knee osteoarthritis as a predecessor to TKA, study of the knee OA literature is important, yet can villainize KAbM as the culprit responsible for disease progress. It is important to consider that an increased KAbM is a product of joint degeneration, not the root cause. It has been demonstrated that the interaction between muscles, bones, and soft tissues is what provides dynamic stability during stance

(Schipplein and Andriacchi, 1991). With the development of knee OA, anatomical changes are introduced to the knee joint such as joint space narrowing (Andriacchi et al., 2009), increased bone mineral density (Miyazaki et al., 2002), increased joint laxity (Lewek et al., 2004). The end result of these anatomic changes is that compressive forces of the medial compartment can become higher than non-pathological knee joints. During adduction of the knee, the lateral compartment is off loaded, while at the same time, the medial compartment is compressed. The result of this increased medial compartment compression is a joint space narrowing resulting from cartilage degradation, which increases the joint laxity of the knee joint (Lewek et al., 2004). As it pertains to the TKA population, increased KAbM may likely contribute to, or even accelerate prosthesis degradation. This is particularly important as we see the incidence of TKA increase rapidly, and the age of first time TKA patients decreasing (Kurtz et al., 2007).

The primary goals of TKA are to alleviate knee pain and restore the loss of knee joint function (Andriacchi et al., 1999; Andriacchi et al., 2009). Qualitative analysis of the waveform of KAbM during gait indicates a bimodal waveform with a peak occurring in the first 50% of stance for loading-response and a second peak towards the latter part of stance for push-off. Understanding of the behavior of KAbM following TKA is inconclusive. It has been shown by some that loading-response peak KAbM decreases in the replaced limb relative to non-replaced and healthy control limbs. In an investigation of 15 patients following TKA, Orishimo et al. (2012) reported that 6 months post-TKA, KAbM was reduced to 85% of the preoperative level, also noting, that at the 1 year post-TKA follow-up that KAbM had increased an additional 10%. They speculate that although successful at restring frontal plane static knee alignment, the TKA operation did

not maintain this restoration of alignment for more than a year. It was the opinion of the authors that the post-TKA KAbM was a likely contributor to the wearing down of the implant. The findings of Orishimo et al. were echoed by Shimada et al. (2016) who also reported decreased KAbM at the 3 week post-TKA (-0.24 Nm/kg decrease), 3 month post-TKA (-0.21 Nm/kg decrease), and 6 month post-TKA (-0.19 Nm/kg decrease), yet at the 1 year post-TKA mark found no difference from pre-TKA KAbM (0.67 ± 0.14 Nm/kg vs. 0.80 ± 0.25 Nm/kg). On the other hand, there have been other studies that have shown no significant changes in peak KAbM between the replaced and non-replaced limb following TKA. Wen et al. (2019), for example, reported no differences in the replaced vs. non-replaced limbs of patients with TKA during any inclinations. They did, however, report that as slope increased, peak KAbM decreased for all limbs, and was significantly different between 0° and 10° as well as 0° and 15° inclinations (Wen et al., 2019). Though no inter-limb comparisons were made, Haggerty et al. (2014) reported similar trends of decreasing KAbM with increasing slope in young healthy individuals.

Although there is a fair amount of evidence that suggest TKA can decrease medial compartment joint loading, as represented by KAbM, there have also been those who have reported no significant differences. Yoshida et al. (2008), for example, reported no significant difference for KAbM or KEM between the replaced and non-replaced limbs at both the 3-month and 12-month post-TAK follow-up. Milner et al. (2008) reported no difference in loading-response peak KAbM for patients after TKA compared to healthy controls.

Uphill Walking

Although over 1.5 million TKA are performed globally on an annual basis, biomechanical investigation of the behavior of the knee joint during downhill walking is scant (Gallo et al., 2013; Simon et al., 2018; Wen et al., 2019; Wiik et al., 2015). The following sections will discuss the most current, up to date research presented on the biomechanics of the knee joint during uphill and downhill walking.

Walking on an inclined surface presents a challenge for an individual who is in pain or lacks the physical ability to negotiate the task. Walking uphill requires a different arrangement of muscle activation and force production and also demands increased metabolic cost to raise the body's center of mass while also providing the necessary forward propulsion (Silder et al., 2012). Analysis of the behavior of gait on inclined surfaces has been recently introduced in the literature with the aims to better understand effects on rehabilitation (Lange et al., 1996; Leroux et al., 2006; Meier et al., 2008), and TKA prosthesis design (Stansfield and Nicol, 2002). The effects of inclination on lower extremity gait biomechanics have been studied using both instrumented ramp systems and treadmills. In that there is relatively little literature which discusses the biomechanics of the knee joint when walking up inclined or declined surfaces, the following sections will individually discuss the gait biomechanics of uphill and downhill walking, first, briefly in healthy adults, and then in TKA populations.

Kinematics

During uphill walking in healthy individuals, the knee flexion angle at heel strike appears to increase as slope increases (Franz and Kram, 2014; Lay et al., 2006; McIntosh et al., 2006). In one of the first studies examining knee joint biomechanics during uphill

walking, Lay et al. (2006) reported kinematics of 9 healthy adults as they negotiated grades of 0°, 8.5°, and 21° while walking at a self-selected speed. At initial contact, the knee flexion angle skyrocketed from 3.6° during level walking to 21.3° at 8.5° and then to 48.4° at 21°. As stance phase continued, they reported an increased stance phase knee flexion from 7.0° during level walking to 4.8° at 8.5° and then to 48.41° at 21°, to lift the body up the inclination.

Similarly, McIntosh et al. (2006) measured the gait of 11 adult males during uphill walking at 0°, 5°, 8°, and 10° inclination. They reported mean knee flexion angle at heel strike of 7° during level walking, which increased to 33° during uphill walking at 10°. Knee flexion during mid stance also increased from 19° to 41° over the same inclination interval. In assessing the effects of uphill walking on older adults, Franz et al. (2014) compared the gait of old (72 ± 5 years) and young (27 ± 5 years) adults walking at a 9° incline. Aside from a reduced step-length for older adults (-10%), the authors found no differences in the kinematics of older and younger adults. Knee flexion angle at initial contact increased to close to 30° with increased slope and peak knee extension ROM was similar for all conditions.

Very few studies have examined knee joint kinematics during uphill walking in the TKA population (Tarnita et al., 2020; Wen et al., 2019). Some studies have looked at the effects of different prosthesis design on certain kinematic variables and bone movement using dual fluoroscopy (Grieco et al., 2016; Khasian et al., 2020). However, the limited scope of investigation of these studies makes comparison with traditional biomechanics literature difficult.

Using a system that incorporated electro-goniometers, accelerometers, and force platforms, Tarnita et al. (2020) reported sagittal plane kinematics on 5 patients prior to, and three months post-TKA as they walked on an inclined treadmill at slopes 0°, 3°, 7°, 11°, and 15°. For the TKA patients, knee flexion angle at heel strike increased, as did peak knee flexion angle. The authors suggest that the increased knee flexion angles are indicative of gait improvement following TKA.

In a more recent study of 25 patients with TKA, Wen et al. (2019) reported the knee joint biomechanics during uphill walking at 0°, 5°, 10°, and 15° slopes while walking at a self-selected pace. The TKA and control groups of this study ascended an adjustable instrumented ramp system within a motion capture volume. As ramp inclination increased from 5° to 15°, both knee flexion ROM (defined as the sagittal plane joint excursion from initial heel strike to peak flexion/extension angle) decreased while knee extension ROM increased. There was no significant difference between replaced and non-replaced limbs for knee flexion ROM as inclination was raised from 5° (-34.5 ± 5.4° for the replaced limb, -36.8°± 5.4° for the non-replaced limb) to 15° (-28.9 ± 4.7° for the replaced limb, -28.6 ± 6.8° for the non-replaced limb). A significant limb × slope interaction was reported, however, for knee extension ROM suggesting that demonstrated a greater increase in knee extension ROM from 5° (4.4 ± 6.6° for the replaced limb, 3.9 ± 6.1° for the non-replaced limb) to 15° (29.8 ± 6.8° for the replaced limb, 31.5 ± 7.6° for the non-replaced limb).

As it pertains to the TKA population during uphill walking, examination of knee joint biomechanics in the frontal plane during uphill walking is a newly emerging topic (Komnik et al., 2016; Wen et al., 2019). With only two studies reporting frontal plane

kinematics of patients with TKA during uphill walking, reported results are heterogeneous and must be considered against the small sample sizes.

Komnik et al. (2016) investigated non-sagittal plane biomechanics in total (TKA) and uni-compartmental arthroplasty patients and compared their results against an age matched control group. The TKA cohort of this study ultimately consisted of 11 participants, while the uni-compartmental TKA and control groups both included 13 participants. All participants walked at a controlled pace (1.25 m/s) down a flat walkway that led to a three-step ramp instrumented with one force platform and set to an inclination grade of 21%. Komnick et al. (2016) reported no significant differences in peak knee adduction angles between the TKA (6.2 ± 2.7°), uni-compartmental (5.8 ± 2.5), and control groups (6.5 ± 4.0). Inter-limb comparison of the TKA group specifically indicated a significant difference in knee adduction angle during incline walking with the replaced limb achieving peak adduction angle of 6.2 ± 2.7° while the non-replaced limb achieving peak adduction angle of 8.4 ± 3.1° ($p = 0.021$).

In the frontal plane, Wen et al. (2019) reported that as slope increased, the frontal plane knee abduction ROM increased as well for both the replaced and non-replaced limb, however, there was no significant difference between the limbs for the knee abduction ROM with increased slope (-3.5 ± 1.6° vs. -3.6 ± 1.5° at 5° to -8.1 ± 4.6° vs. -8.1 ± 4.2° at 15°).

Kinetics

Given the necessity to propel the body upward and forward during uphill walking, vertical and anteroposterior GRF are commonly reported in uphill walking. A review of the literature suggests that the shape, with two primary peaks related to loading-response

and push-off, and temporal spacing of the vertical GRF in ramp walking are similar, however, results regarding the magnitudes of GRF and their peak values are inconsistent (Lay et al., 2006; McIntosh et al., 2006).

Lay et al. (2006) recorded GRF as 9 healthy adults walking up ramped surfaces at grades of 15% and 39%. Peak push-off GRF (10.79 N/kg) was generally slightly higher than the loading-response peak GRF (10.45 N/kg) at 0% grade yet did not change significantly with increased slope [e.g., 10.61 N/kg at 15% grade and 11.24 N (non-significant) at 15% for peak loading-response GRF]. Based on this reported data, it appears that the trend of increase peak push-off GRF being just slightly larger than loading-response peak GRF is consistent as the grade of inclination increases. McIntosh et al. (2006) on the other hand recorded GRF of 11 healthy males while walking up inclines of 5°, 8°, and 10°. They demonstrated that the magnitude of the loading-response vertical GRF increased as the participants walked up the increasing slopes. Loading-response peak GRF increased from approximately 9 N/kg during level walking to nearly 12 N/kg at 8° and 10° inclinations.

Wen et al. (2019) reported peak loading-response and peak push-off vertical GRF of both the replaced and non-replaced limbs of patients following TKA. They reported peak loading-response vertical GRF decreased by nearly 6% for the replaced limb and 5% for the non-replaced limb. Decreased loading-response peak vertical GRF with increasing slope has been previously shown in studies with healthy participants (Franz and Kram, 2014; Hong et al., 2014; Lay et al., 2006). In a trade off, peak push-off vertical GRF increased from level walking to an inclination of 10° by 4% for the replaced limb

and 5% for the non-replaced limb, indicating increased demands for propulsive power generation as slope increases.

Sagittal Plane

Knee joint kinetics have been reported during uphill walking to provide a better understanding of the demands of the task on the lower extremity. Counter-intuitively, it has been reported that although peak vertical GRF decreases slightly, peak KEM increases with increased slope. Franz et al. (2013) suggested that older adults employ a compensation strategy when walking uphill by performing greater center of mass work during the single support phase of stance as opposed to greater lower limb muscular work. They specifically showed that older adults demonstrate smaller increases in ankle plantarflexion musculature EMG activation with increased slope, but greater recruitment of gluteal hip extensor muscle EMG activation (Franz and Kram, 2013). They postulated that as task demand increases and walking performance decreases, a disproportionate recruitment of proximal leg musculature relative to distal leg musculature is adopted, and thus, as peak vertical GRF decreases, increases in the knee (as well as the hip) joint moment is observed. Compared to level walking, it appears that a greater amount of force and power is produced at the hip when walking uphill. As might be expected, all lower extremity joint moments increase during stance in order to elevate the body up the incline (Franz and Kram, 2014; Hong et al., 2014; Lay et al., 2006). Hong et al. (2014) calculated lower extremity joint moments for 15 adults as they walked up increasing slopes of 0°, 5°, 10°, and 15°. They reported an increase in loading-response peak knee extension moment of over 168% between level walking (4.1 ± 2.3 %BW × leg length) and their 15° condition (11.0 ± 2.8 %BW × leg length). In further support, and using a

sample of older healthy adults, Wen et al. (2019) reported an increase of peak knee extension moment of 49% from level walking (0.49 ± 0.12 Nm/kg) to their 15° condition (0.73 ± 0.43 Nm/kg). Sample demographics need to be considered when comparing these two studies together, as Hong et al. (2014) reported a sample of 15 younger adults (age: 32 ± 5.2 years) who walked with a self-selected gait velocity (1.0 m/s for level walking, 0.9 m/s for 15°), whereas Wen et al. (2019) reported a sample of 10 older adults (69.1 ± 4.6 years) who walked at a self-selected pace of 1.17 m/s for level walking at 0.95 m/s for 15° (Hong et al., 2014; Wen et al., 2019).

For patients following TKA, the knee extension moment (KEM) has been shown to be decreased in the replaced limb vs. the non-replaced limb during uphill walking at steeper inclines of 10° and 15° (Wen et al., 2019). While walking at 10° uphill, Wen et al. (2019) reported decreased peak KEM for the replaced limb (0.39 ± 0.27 Nm/kg) vs. the non-replaced limb (0.52 ± 0.32 Nm/kg). Similarly, at 15° uphill, Wen et al. reported peak KEM for the replaced limb (0.45 ± 0.28 Nm/kg) vs. the non-replaced limb (0.61 ± 0.33 Nm/kg). These results suggest that asymmetries in knee joint loading appear to be exacerbated when walking demand is increased. Uphill walking requires greater muscular contribution to power generation which may require greater reliance on the strength of the non-replaced limb. Reduced KEM in the replaced limb compared to the non-replaced limb has also been shown in other instances where walking demand is greater, such as stair ascent (Standifird et al., 2016).

Frontal Plane

In the frontal plane, there appears to be a general trend in the decrease of the KAbM. Both Wen et al. (2019) and Haggerty et al. (2014) reported decreases in peak

KAbM as the slope increased. In their sample of 15 healthy males, Haggerty reported a 46% decrease in peak KAbM during level walking (0.54 ± 0.15 Nm/kg) compared to their 15° condition (0.37 ± 0.18 Nm/kg) (Haggerty et al., 2014). In addition to a 16% decrease of peak loading-response KAbM between level walking (-0.36 ± 0.12 Nm/kg) and 15° incline (-0.31 ± 0.11 Nm/kg), Wen also reported a 68% decrease in peak push-off KAbM between level walking (-0.27 ± 0.18 Nm/kg) and their 15° incline (-0.16 ± 0.29 Nm/kg) (Wen et al., 2019).

Downhill Walking

In one the most complete studies performed, Wen et al. (2021) recorded motion and GRF data for 25 TKA patients and 10 control participants as they walked at self-selected pace on declines of -5°, -10°, and -15°. Knee flexion ROM in both the replaced and non-replaced limbs increased as the slope increased from 0° (-41.3 ± 5.3° for the replaced limb and -43.1 ± 6.3° in the non-replaced limb) to -15° (-65.8 ± 6.0° in the replaced limb and -66.7 ± 6.3° in the non-replaced limb). No significant changes were reported between limbs or across the different slopes for knee flexion ROM.

A significant difference between the replaced and non-replaced limbs was reported for peak loading-response vertical GRF at the 10° and 15° decline angles. At level walking, peak loading-response vertical GRF was similar for the replaced (1.03 ± 0.08 BW) limb and non-replaced limb (1.05 ± 0.07 BW). At the 10° decline, the replaced limb (1.17 ± 0.13 BW) demonstrated significantly smaller loading-response vertical GRF than the non-replaced limb (1.23 ± 0.13 BW). At the 15° decline, the replaced limb (1.23 ± 0.18 BW) also demonstrated significantly smaller loading-response peak vertical GRF than the non-replaced limb (1.30 ± 0.17). At the 15° decline, the replaced limb

experienced 19% greater peak loading-response vertical GRF compared to level walking while the non-replaced limb experienced an increase of 24%. This asymmetry in vertical GRF also translated to a between-limb asymmetry of KEM, with the replaced limb demonstrating an increase of KEM of 115% from level walking to the 15° decline while the non-replaced limb saw an increase of KEM of 150%. Although Wen et al. (2021) did not report frontal plane knee kinematics during any downhill walking conditions, however, they did report that peak KAbM did not change significantly between the replaced (-0.36 ± 0.12 Nm/kg) and non-replaced (-0.41 ± 0.20) limb during level walking or any of the decline conditions [e.g., KAbM at the 15° decline condition for replaced (-0.38 ± 0.14 Nm/kg) and non-replaced limb (-0.44 ± 0.23 Nm/kg) were not statistically different].

In an investigation between the stability of two different types of knee implant styles (posterior cruciate retaining (PCR), and bicruciate retaining (BiCR) implants), Simon et al. (2018) reported peak sagittal and frontal plane kinematics and kinetics of 27 patients following TKA while walking on a decline grade of 12.5% (~7°). Although comparisons were made between implant styles using t-tests, no statistical tests of the effect of slope, nor the interaction between slope and implant style were made. Furthermore, statistical results for downhill walking revealed that there were no significant differences between implant styles for knee flexion ROM (PCR: 67.4 ± 12.5°, BiCR: 66.7 ± 8.1°), KEM (PCR: -1.82 ± 0.59 %BW × height, BiCR: -1.63 ± 0.73 %BW × height) or KAbM (PCR: 0.51 ± 0.27 %BW × height,
BiCR: -0.37 ± 0.37 %BW × height).

Instrumented Knee Joint Compressive Forces

Previous research has shown that joint loading variables such as KEM and KAbM have been highly correlated to and used in predictions of medial compartment tibiofemoral compressive force (MCF) in level walking (Walter et al., 2010). However, these variables alone do not directly indicate the magnitude or behavior of tibiofemoral compressive forces. Understandably, knee joint prostheses instrumented with force measurement capacity are expensive and impractical for wide-scale clinical use. They do, however, provide the capability to accurately measure the loading environment of the knee joint. Many studies have reported *in-vivo* tibiofemoral contact forces in a variety of settings, including walking, stair ascent and descent, and various activities of daily living such as deep knee flexion and standing up from a chair (Bergmann et al., 2014; D'Lima et al., 2007; D'Lima et al., 2006; D'Lima et al., 2008; Heinlein et al., 2009; Kutzner et al., 2010; Kutzner et al., 2013; Mundermann et al., 2008; Zhao et al., 2007a). The following section will discuss the design and construction of instrumented tibiofemoral implants as well as tibiofemoral compressive forces obtained from these implants during level walking and stair ascent and descent.

During TKA, an orthopedic surgeon resurfaces the distal surface of the femur and proximal surface of the tibia. The damaged and decayed bone tissue of the femur and tibia are removed and replaced with tibial and femoral prosthesis components. These components are secured to the native bone by drilling into the bone and securing the components with screws or adhesives such as bone cement (Varacallo et al., 2020). Often times during TKA, the ligaments responsible for limiting anterior and posterior translation of the tibia with relation to the femur (anterior and posterior cruciate

ligaments) are removed entirely. As such, high impact, dynamic movements such as running are often discouraged following TKA. Implants may also be instrumented with force transducers, capable of measuring 3-Dimensional forces (i.e. vertical tibiofemoral contact force, or, compressive force (TCF), anteroposterior tibiofemoral contact force, or, shear force, and transverse plane rotational force, or, torsional force) and computing contact moments between the tibia and femur (D'Lima et al., 2006). In these cases, transducers are embedded in the tibial component and report forces acting upon the tibia by the femur.

The waveforms of TCF during level walking has been shown to be bimodal with peaks corresponding to loading-response and push-off of the stance phase of gait, similar to that of vertical GRF. Peak TCFs have been reported to be over two BW. In an early study, Zhao et al. (2007a) reported tibiofemoral contact forces in a single patients who was 80 years of age and who received a knee joint implant that consisted of 4 uniaxial force transducers. Peak TCF during the stance phase was reported at 2.2 BW, with 53.4% of TCF accounted for by the compressive force specifically from the medial compartment of the knee joint. In another hallmark study, Heinlein et al. (2009) reported knee joint kinematics, GRF, and tibiofemoral contact forces in two participants (ages 63 and 71 years). Ten-months following TKA the peak stance phase TCF was reported to be 2.76 BW and 2.08 BW for the two participants, respectively. The data obtained from these two participants were among the first to be published on the freely available public database (www.orthoload.com). Since the first studies reported tibiofemoral compressive forces, several others have followed, utilizing different implant designs (Bergmann et al., 2014), different footwear (Kutzner et al., 2013), and larger sample sizes (Bergmann et al., 2014;

D'Lima et al., 2008), all reporting peak TCF during stance phase between 2.25 and 2.75 BW during walking.

Tibiofemoral contact forces that occur during the negotiation of stairs in patients with instrumented knee implants have often been reported in addition to those experienced during level walking. Stair ascent and descent generally require greater muscular efforts to elevate or lower the body mass and therefore are accompanied by greater TCF (Bergmann et al., 2014; D'Lima et al., 2007; Heinlein et al., 2009; Kutzner et al., 2010; Zhao et al., 2007a). Similar to the waveform patterns of level walking, the waveform of TCF during stair ascent is bimodal with the first (larger peak, loading-response) peak and second (push-off) peak, occurring in the first and second half of stance, respectively, and achieving peak loading-response values around 3.5 BW and peak push-off values around 3.0 BW (Heinlein et al., 2009; Zhao et al., 2007a). In a sample of 5 older adults who received an instrumented knee implant, Kutzner et al. (2010) also reported that peak loading-response TCF during stair descent was, on average, greater than stair ascent by nearly 0.3 BW, or between an 8-10% increase in TCF. From their sample, peak push-off TCF during stair ascent was reported as 3.45 BW, while during stair descent it was reported as 3.75 BW. Likewise, in comparison of 8 participants with instrumented knee implants, Bergmann et al. (2014) reported non-normalized TCF increase of nearly 12% during stair descent compared to stair ascent (4787 N vs. 4209 N). Surprisingly, Bergmann et al. (2014) also asked three willing participants to jog at a pace of 1.6 m/s while tibiofemoral compressive forces were measured. Although the authors did not perform any statistical analysis on the jogging data, it does serve as a baseline for qualitative assessment between other conditions. Peak

TCF while jogging was 5551 N, representing an increase of TCF of 13% over stair descent, 25% over stair ascent, and 44% over level walking (Bergmann et al., 2014).

In an effort to examine the correlation between the knee abduction moment, a common surrogate variable for MCF, and MCF, Walter et al. (2010) compared *in vivo* tibiofemoral compressive forces (both TCF and MCF) with the external knee adduction moment obtained through an inverse dynamics calculation during normal walking, medial hip thrust walking, and walking with Nordic poles. Linear regression analysis was performed to assess the ability of KAM and the external knee flexion moment to predict changes in MCF. The results of their regression analysis showed a combination of KAM and knee flexion moment could predict both first and second peak MCF with an R^2 value of 0.92. Using the regression equation of Walter et al. (Walter et al., 2010), Wen et al. (2019) predicted peak MCF for the replaced and non-replaced limbs of patients with TKA during level and uphill walking. During level walking, peak loading-response MCF was reported at 1.52 ± 0.30 BW for the replaced limb compared to 1.61 ± 0.46 BW for the non-replaced limb. There was a significant interaction for peak loading-response MCF between limb and slope as well as a significant main effect of limb. Thus, at 15° incline, peak loading-response MCF was reported at 1.51 ± 0.34 BW for the replaced limb compared to 1.72 ± 0.46 BW for the non-replaced limb, suggesting compensatory, protective gait mechanism that inherently reduce joint loading of the replaced limb.

In summary, recent developments in technology have allowed for knee joint implants to be instrumented with transducers capable of measuring contact forces between the tibia and femur. This allows for researchers for better understanding and quantifying the joint loading environment of the knee during a multitude of activities. During level walking,

TCF exhibits a bimodal waveform with peak loading-response TCF in the range of 2.25 – 2.75 BW. During stair ascent, this peak TCF increases to approximately 3.5 BW and increases closer to 3.75 BW during stair descent. Given scarcity of the patient population who have been fit with knee joint implants capable of measuring forces, the depth of data that has been obtained from these implants is still in the earlier stages of collection. As such, at the time of the writing of this document, it does not appear that there have been any studies that have published tibiofemoral joint contact forces during ramp incline or decline walking.

Simulation Techniques for Determining Knee Joint Compressive Forces

Over the last three decades computational musculoskeletal modeling has afforded clinicians and researchers the ability improve surgical and rehabilitation treatment plans informed by models based on principles of physics and physiology (Fregly et al., 2012). Simulations of human movement that utilize these musculoskeletal models offer practical solutions to the impossibility of measuring *in vivo* forces, such as joint contact forces, muscle forces, and tendonous forces (Lai et al., 2017). The following section will focus on the brief history and recent methodology of estimating tibiofemoral compressive forces.

Knee joint compressive forces can be estimated mathematically by modeling the lower extremity as multiple rigid bodies that are connected through joints or other constraints to form kinematic chains. Using these rigid body models, multibody dynamics are used to solve the equations of motion for the entire system. One commonly used software that has this capability is OpenSim, a freely-available open source platform designed for the musculoskeletal simulation of biological systems and movements (Delp

et al., 2007). To determine joint compressive forces, the equations of motion first need to be solved in terms of generalized coordinates (joint angles) and generalized forces (external loads). Solving these generalized equations of motion does not require the determination of internal muscle or compressive forces, and as such, the Joint reaction analysis (JRA) tool in OpenSim is a post-processing tool that implements muscle forces determined from either static optimization or computed muscle control (CMC), generalized joint coordinates, and external loads to calculate, in this specific context, three-dimensional reaction forces at the ankle, knee, and hip joints (Demers et al., 2014; Steele et al., 2012). In short, the resultant forces and moments at the knee joint solved for using JRA are expressed as the sum the forces produced from the mass and acceleration of the segment (i.e., the tibia) and the sum of all external loads, muscle forces, and joint reaction forces contributed from the distal segment (Steele et al., 2012).

Knee joint prostheses instrumented with force measurement capacity are expensive and impractical for normal clinical use. Additionally, *in vivo* measurements only report forces from the instrumented knee prostheses, and not the contralateral non-replaced knee, and compartment-specific compressive forces are not typically reported. The first methodological studies that explored tibiofemoral contact force estimation were first published in the 1970s (Morrison, 1970; Seireg and Arvikar, 1973). Since then, advancements have been made in both simulation and modelling techniques that have improved accessibility to the tools needed for contact force estimation. Many of these techniques utilize one of three techniques to determine intersegmental, muscle and contact forces; optimization, EMG-driven models, and reduction models (Fregly et al.,

2012). For the sake of this chapter, only optimization and EMG-driven algorithms will be explored.

EMG-driven musculoskeletal models use experimentally collected EMG as inputs to help solve the muscle redundancy problem inherent with musculoskeletal modeling (Fregly et al., 2012). These EMG-driven models use experimentally collected EMG to serve as neural commands in forward dynamics simulations (Buchanan et al., 2004). The *forward* component of 'forward-dynamics', from a nomenclature perspective, refers to the direction Newton's second law of motion is solved. In a forward dynamics solution, EMG signals are first transformed in to muscle activations, which are mathematically represented as a time varying scalar variable with a magnitude between 0 and 1. Using these muscle activations, muscle forces can be determined from *a priori* muscle parameters such as isometric strength, length, and contraction velocity. These muscle forces are then multiplied by their respective moment arms for the joint(s) they cross to generate a muscle moment about that joint which contributes toward the total moment about the joint (Buchanan et al., 2004). After having determined the joint moments, the resulting accelerations, velocities, and angles for each joint can be determined. In this context, Newton's second law of motion is solved from left to right by determining force from EMG and then computing position, velocity, and acceleration, or, in other words, solving the equation forwards.

Using an EMG-driven model, Winby et al. (2009) solved for lower limb muscle forces, and then joint contact forces and moments generated at the medial and lateral articular surfaces of the knee. Experimental data were collected on 11 participants while walking at a self-selected pace, walking at a faster pace, and jogging slowly. EMG was

collected on 10 muscles surrounding the knee joint: semitendinosus, long head of the biceps femoris, sartorius, rectus femoris, tensor fascia late, gracilis, vastus medialis, vastus lateralis, and medial and lateral gastrocnemius. In their determination of joint contact forces, three simplifying assumptions were made. First, it was assumed that only compressive forces, and resultant forces from the frontal plane rotational moment contribute to articular loading (i.e., torsional force between the femur and tibia does not contribute to joint loading). Second, that the loads distributed through the knee act only through a singular point in each respective condyle (e.g., medial, and lateral condyles of the knee). Finally, it was assumed that ligaments do not contribute to joint loading. Reported compressive force for the medial and lateral compartments, as well as the total compressive force (the sum of the two medial and lateral compressive forces) indicate that the model predicted forces in similar wave forms, yet the model overestimated all three forces when compared to previous reports of *in vivo* compressive forces (Hurwitz et al., 1998; Shelburne et al., 2006; Zhao et al., 2007a). The model also appropriately predicted the absence of the unloading of the lateral compartment, which the authors suggest, is a result of muscular stabilization of the knee joint against the external frontal plane ab/adduction moments (Winby et al., 2009).

Saxby et al. (2016) also used an EMG-driven model to explore the association between MCF and the frontal plane adduction moment during more dynamic movements such as side-stepping. They hypothesized that side stepping would have larger TCF than straight walking or straight running, and that using traditional regression equations to estimate MCF from the external adduction moment might be insufficient during dynamic tasks. Kinematic, kinetic, and EMG data were collected for a larger sample of 60 healthy

adults while they performed level walking, running, and sidestepping at a 45° angle. Model predictions for peak TCF during level walking were 2.83 ± 0.64 BW, consistent with the literature. Total compressive force was lower in walking than those in running (7.83 ± 1.48 BW) and sidestepping (8.47 ± 1.57 BW).

The authors also determined the relative contribution of external loads (i.e., frontal plane joint moments) and muscle forces about the medial and lateral femoral contact points. The contribution of these components was reported as a percentage of MCF and LCF. For both the medial and lateral compartment, contact force contribution was relatively balanced between external loads and muscle forces, with contributing approximately 50% of the load. Divergent patterns were observed for both medial and lateral compartments of the knee for running and sidestepping tasks as the muscle contribution to MCF and LCF dominated the contribution of the external loads such that the muscle forces accounted for 83% and 91% of MCF and 88% and 79% of LCF.

Finally, Saxby et al, (2016) used three types of linear predictive models to determine the relationship between external loads and tibiofemoral compressive forces. They first regressed peak TCF on to the corresponding peak external adduction moment. In subsequent models, they then added a categorical variable that represented each different gait task. Finally, they utilized several other external measures to include in a stepwise regression, external adduction moment, knee flexion moment, vertical ground reaction force, body mass, gait velocity, and the activation of the gastrocnemius muscle. The relationships between the external measures (knee adduction moment, knee flexion moment, vertical ground reaction force, and gait velocity) and TCF were weak-to-moderate, with all reported R^2 less than or equal to 0.36. Using the stepwise regression

revealed that the peak vertical ground reaction force, external adduction moment, body mass, and knee flexion moment were the most important external measures, yielding a stronger R^2 value of 0.78.

Optimization approaches determine a specific solution of muscle activations which produce muscle forces and subsequently contribute to, alongside external loads, joint contact forces. In these solutions, activations are determined by minimizing a cost function, or, in other words, minimizing the total 'cost' of a pre-specific parameter. One frequently used cost function is the squared sum of all muscle activations, which serves to represent physiological endurance of skeletal muscle (Crowninshield and Brand, 1981). The optimization criteria, however, is also subject to operating within pre-determined control constraints. In musculoskeletal modeling this frequently requires that the net joint torques produced by the combination of the optimized muscle forces and external loads matches the external joint torques determined from either an inverse or forwards dynamic simulation (Fregly et al., 2012). Static optimization determines the optimized solutions by treating each frame of data as a static, non-moving point in time. At each time step, an optimized set of muscle activations and forces is found. Dynamic optimization, on the other hand, uses numerical integration throughout the time interval to find the optimal solutions of activations and forces. While still requiring experimentally input data, dynamic optimization allows for dynamic consistency to be achieved throughout a motion, rather than treating each individual frame as a solution that is independent from adjacent frames of data.

Steele et al. (2012) used a static optimization approach to solve for muscle forces in nine children with cerebral palsy who walked with characteristically greater knee

flexion, often referred to as ‘crouch gait’ (Steele et al., 2012). These muscle forces, along with external loads served as inputs for a Joint reaction analysis in OpenSim. The cerebral palsy patient sample was also compared against a small sample of healthy children, as well as an older adult with an instrumented TKA, against whom they could validate predicted TCF results. Results indicated that those with milder crouch gait walked with similar peak TCF compared to unimpaired walking. Those with severe crouch gait produced peak TCF greater than 6 BW, primarily due to increased quadriceps forces from increased knee flexion. The authors concluded that patients walking with crouch gait did indeed experience greater TCF that contributes to increased joint pain and cartilage damage (Steele et al., 2012).

Lerner et al. (2015) used a static optimization approach in association with a musculoskeletal model that was capable of resolving TCF into the compartment-specific compressive forces (MCF and LCF). Results of his model were compared against *in vivo* tibiofemoral compressive forces (Fregly et al., 2012). Although this model is a revised version of the generic OpenSim model, it accounted for patient-specific frontal plane alignment of the lower extremity as well as for patient specific condylar contact points. At the knee joint specifically, two revolute joints which work only in the frontal plane connect the femur to the tibia. These revolute joints alone cannot allow frontal plane rotation of the knee joint, but, acting in parallel, work to share all loads that are transmitted through the joint thus allowing for the resolution of TCF into MCF and LCF. These resolute joints are placed specifically at the pre-determined, subject specific condylar contact points and thus can accurately determine compressive forces as well as moments of force.

With the complexity of the model, Lerner et al. tested four variations of the model. A uniformed model, which did not incorporate subject specific alignment or contact points. In this uninformed model, contact points were evenly distributed 0.02 m medial and lateral from the knee joint center. An alignment-informed model, which accounted for subject specific frontal plane alignment but did not account for condylar contact points. A contact-point-informed model, which accounted for condylar contact points but not frontal plane alignment, and, finally, a fully informed model which incorporated subject specific frontal plane alignment of the knee joint as well as subject specific condylar contact points. As one might be expected, the fully informed model performed the best. All 4 models over estimated both first and second peak MCF and LCF during level walking when compared against the *in vivo* TCF. However, the fully informed model only over estimated compressive forces ~10%. The alignment-informed model performed second best, with MCF and LCF errors of approximately 20% for MCF and LCF. Error rates were substantially greater for estimation of MCF with the contact point model (>40%) and the uninformed model (>60%). These results highlight the importance of including all pertinent parameters that might affect load distribution through the knee joint for any accuracy of model prediction. They further support the idea that frontal plane knee joint alignment and knee joint angle are greater contributors to increased MCF, and subsequent implications for knee osteoarthritis, than the frontal plane knee moment KAbM (Marouane and Shirazi-Adl, 2019).

In vivo tibiofemoral compressive forces measured with an instrumented knee replacement during level walking suggest that the knee can experience joint loads that exceed two times body weight (BW) during stance. Previous research has shown that

joint loading variables such as KEM and KAbM have been correlated to medial compartment tibiofemoral compressive force in level walking (Walter et al., 2010). However, these variables do not directly indicate the magnitude or behavior of compressive forces. In light of the limitations of instrumented knee joint prostheses, musculoskeletal modeling and simulation provide tools that allow for the estimation of tibiofemoral compressive forces and related muscle forces without in vivo measurements (Delp et al., 2007; Lerner et al., 2015; Steele et al., 2012). Recent developments of musculoskeletal modeling have provided the ability to estimate TCF, with estimation of MCF and LCF (Lerner et al., 2015).

Statistical Parametric Mapping

Discrete point analysis has been a common form of data analyses in biomechanics. With discrete point analyses, the dimensionality of a time-series, or the plot of a primary dependent variable against an independent variable (i.e., a join angle plotted across time), is reduced to a single point (e.g., local minima or maxima) that is used to describe the entirety of the biological movement (Warmenhoven et al., 2018). The ability, though, to examine a biomechanical variable throughout the entirety of a specified movement is of particular interest and has led to the introduction of three emerging statistical methodologies, Principal Component Analysis (PCA) (Deluzio et al., 1997), Functional Data Analysis (FDA) (Ramsay, 2004) and Statistical Parametric Mapping (SPM) (Friston, 2003), to assess the time-series of biomechanical variables throughout the entirety of a movement. In short, PCA provides an objective characterization of how waveforms differ between subjects by determining important waveform features, called principal components, which can express the original data

using only a few important components (Brandon et al., 2013). FDA expresses individual observations within a time series in the form of a function. Then, each function is treated as an individual observation for statistical analysis (Warmenhoven et al., 2018). In a likely manner, SPM considers entire time-series as a single observation.

SPM relies upon Random Field Theory (Adler and Taylor, 2009), which maps the conventional Gaussian distribution to smoothed n-dimensional continua for hypothesis testing. For application of SPM within the field of biomechanics, variables are frequently mapped as a one-dimensional (1D) continuum, with the dimension of the variable being time. Todd Pataky and colleagues have pioneering the implementation of SPM in the biomechanical work. It is from their work that different SPM statistical tests have been validated and that the source code for both Python and MATLAB have been created and shared for free at www.spm1d.org (Pataky, 2010; Pataky et al., 2013, 2016a; Pataky et al., 2015, 2016b; Vanrenterghem et al., 2012; Warmenhoven et al., 2018).

For simplicity in this review, the theory and arithmetic of the *t*-statistic will be discussed. First, it is important to remember that all statistical models require a model of randomness. Conventional statistical tests determine the probability that the results occurred randomly (Pataky et al., 2015). In traditional discrete point analysis, a time-series of a biomechanical variable is distilled down to single zero-dimensional (0D) scalar values (e.g., local minima or maxima) that are used to describe the entirety of the biological movement. In these traditional cases, 0D models of randomness, generally based on the Gaussian distribution for normally distributed data or on non-parametric distributions derived from experimentally collected data, are wholly sufficient. If, though,

analysis of a 1D time-series is conducted, a 1D model of randomness is imperative (Good, 2006).

Definition of the 1D *t* statistic is similar to that of the 0D *t* statistic and is presented in equation (1). The equations presented here have been derived from Pataky et al. (2015).

$$t(q) = \frac{\bar{y}(q)}{s(q) \,/\, \sqrt{J}} \tag{1}$$

Where *t(q)*, $\bar{y}$, *s(q)*, and *J* are the 1D *t* statistic at the dimension interval *(q)*, the sample mean, sample standard deviation, and sample size, respectively. When *t(q)* is computed at each time point, a continuous trajectory of *t* can be formed. Then, the probability that the computed 1D *t* statistic will exceed the t-critical value threshold, will be determined using Random Field Theory (Adler and Taylor, 2009) as follows:

$$P(t(q)_{Max} > t^*_{1\mathrm{D}}) = 1 - exp\left(-\int_{t^*_{1\mathrm{D}}}^{\infty} f_{0D}(x)\, dx - ED\right) = a \tag{2}$$

where $t(q)_{max}$ represents the maximum value that the *t* statistic can take, $f_{0D}(x)$ is the zero-dimensional t-statistic probability density function, and *ED* is the Euler density function. Similar to 0D probability estimation, equation (2) represents the probability that $t(q)_{max}$ exceeds $t_{1\mathrm{D}}$ * (Pataky et al., 2015). Just as in conventional hypothesis testing, the null hypothesis is rejected if $t(q)_{max}$ exceeds $t_{1\mathrm{D}}$ *.

SPM has been applied in numerous avenues of human movement including analysis of kinematic, kinetic and EMG profiles (Pataky et al., 2013; Pataky et al., 2016b), running (Vanrenterghem et al., 2012), interval training (Whyte et al., 2018), ACL

injury risk (Fox et al., 2017) and the association between foot progression angles and joint contact forces (Bennett et al., 2021).

CHAPTER III

MATERIALS AND METHODS

Abstract

The purpose of the studies within this dissertation were to examine differences in tibiofemoral joint compressive forces between different limbs (replaced, non-replaced, and control), and different slopes, and their interactions during uphill and downhill walking. We also explored differences in total tibiofemoral compressive force (TCF) impulse and muscle forces between different limbs and slopes. This chapter details the participants and data set utilized in this study, the methodology of data collection, processing, and statistical analysis.

Data of 9 patients with total knee arthroplasty (TKA) and 9 healthy control participants walking uphill and downhill on an instrumented ramp system were collected. Kinematic data were recorded with a motion capture system, ground reaction force data (GRF) were recorded with force platforms, and electromyography (EMG) data were recorded with a wireless EMG system. A musculoskeletal model was used to perform inverse dynamics, static optimization, and joint reaction analysis. Tibiofemoral compressive forces and muscle forces for the entire stance phase of the gait cycle were statistically examined using 3×3 two-way repeated measures Statistical Parametric Mapping (SPM) ANOVA (SMP{F}). Significant interactions and main effects were tested with *post-hoc* SPM{t} tests. The impulse of the total compressive force was also calculated and evaluated using a mixed-model ANOVA and *post hoc* pairwise t-tests.

Participants

Nine patients with TKA (5 male 4 female,67.5 ± 5.5 years, 1.74 ± 0.10 m, 84.3 ± 15.6 kg, 27.8 ± 3.2 months since surgery) were recruited from a local orthopedic clinic to attend one laboratory session. All patients with TKA had received Cruciate Retaining

knee joint prostheses from a primary TKA. Inclusion/exclusion criteria, and full data collection methods have been previously reported (Wen et al., 2019). In short, potential patients were excluded if they had any additional lower extremity joint replacement, any diagnosed osteoarthritis of the hip or ankle, or more than 75% radiographic joint space narrowing and chronic pain of the contralateral, non-replaced knee, BMI greater than 38 kg/m^2, or any neurological diseases. Additionally, 9 healthy adults between the ages of 50-75 (5 male 4 female, 69.5 ± 4.3 years, 1.77 ± 0.12 m, 76.5 ± 25.4 kg) were recruited to serve in a control group. Control group participants were excluded from the study if they reported knee pain during daily activities, had been diagnosed with any type of osteoarthritis, had undergone any lower extremity joint replacement, arthroscopic surgery, or had received an intra-articular injection.

Experimental Protocol

All participants were asked to complete five trials of walking at self-selected pace so that each limb cleanly contacted the first force platform at 0° (level walking) 5°, 10°, and 15° incline on a customized adjustable ramp system which was instrumented with two force platforms. To minimize the duration of the data collection session, ramp incline conditions (5°, 10°, 15°) were performed first, followed by the level walking conditions. Ramp conditions were performed in a randomized order, with inclination angle first randomized, followed by randomization of leading limb (replaced vs. non-replaced). Level walking conditions were also randomized by the leading limb (replaced vs. non-replaced). Three-dimensional (3D) kinematics (240 Hz, Vicon Motional Analysis Inc., Oxford, UK) and GRF (1200 Hz, BP600600 and OR-6-7, American Mechanical Technology Inc. Watertown, MA, USA) were recorded during testing. A handrail was

provided on the right side for balance; however, participants were not encouraged to use it.

Lower limb alignment was determined as the mechanical axis angle (Bennett et al., 2016; Bennett et al., 2018; Vanwanseele et al., 2009). This mechanical axis was determined from the standing static trial obtained during motion capture as the angle between a line connecting the hip joint center to the knee joint center, and a line connecting the knee joint center to the ankle joint center. In this alignment, 0° indicated neutral alignment.

Instrumentation

A 16-channel surface electromyography (EMG) system (1200 Hz, Trigno™ Wireless EMG System, Delsys, INC, Natick MA, USA) was used to monitor the muscle EMG activities on following muscles on both sides of the body: vastus lateralis, vastus medialis, medial head of the gastrocnemius, semitendinosus, and biceps femoris. The skin of the electrode attachment sites was shaved and cleaned with alcohol swab before the application of the electrodes. The placement of the EMG electrodes on the selected muscles were based on the recommendations of SENIAM (Surface ElectroMyoGraphy for the Non-Invasive Assessment of Muscles) (Hermens et al., 2000). Both GRF and EMG data were sampled simultaneously with the 3D kinematic data using the VICON system and Nexus software package (2.5, Vicon Motion Analysis Inc., Oxford, UK).

Data Analyses

The EMG data were analyzed using the Visual3D. Raw EMG signals were filtered with a band-pass filter with a high and low pass cutoff frequencies 10 Hz and 450 Hz and full wave rectified. A moving root-mean-square (RMS) filter was used to filter

the rectified EMG signals using a 60-millisecond moving window. The maximum value of the RMS EMG signals of three functional test trials was used to normalize the filtered EMG signals of the testing movement trials.

Musculoskeletal Primary variables of interest include peak loading-response and push-off TCF, MCF, and LCF. Secondary variables of interest include TCF impulse, as well as forces of the knee flexors: biceps femoris long and short heads, semimembranosus, semitendinosus, sartorius, gracilis, and both medial and lateral head of the gastrocnemius, knee extensors: rectus femoris, vastus lateralis, vastus intermedius, and vastus medialis, medial knee extensor: vastus medialis, lateral knee extensor: vastus lateralis, medial knee flexor: semimembranosus, semitendinosus, sartorius, gracilis, and lateral knee flexor: biceps femoris long and short heads muscle groups. The left and right limbs of healthy controls were randomly selected to match the replaced and non-replaced limbs of TKR patients.

Modeling and Simulation

An open-source musculoskeletal model [18 segments, 23 degrees-of-freedom (DOF), 92 muscle-tendon actuators] capable of resolving knee TCF, MCF, and LCF was used to perform the musculoskeletal simulations (Lerner et al., 2015). The knee joint of this model consists of 1 DOF (flexion/extension) supplemented with added medial and lateral compartments. The model was first scaled to each participant's height and mass and the subtalar and metatarsal-phalangeal joints were locked for the analysis.

Generalized joint coordinates derived from inverse kinematics calculations were exported from Visual3D (Version 6, C-Motion, Inc., Germantown, MD, USA) and imported into OpenSim for simulations (3.3 OpenSim, SimTK, Stanford University). The

generalized joint coordinates were applied to each subject-specific scaled musculoskeletal model. Inverse dynamics calculations were performed in OpenSim to compute lower extremity joint moments. Next, muscle activations and forces during level and up- and downhill walking were calculated using static optimization (Steele et al., 2012). The static optimization calculations included muscle physiology (force-length-velocity relationships) and an objective function to minimize the sum of squared muscle activations (Crowninshield and Brand, 1981). Maximum reserve torque actuator values for all lower extremity joints were checked and found to be within suggested guidelines (Hicks et al., 2015). Joint compressive forces (MCF, LCF, TCF) were calculated using joint reaction analysis in OpenSim and expressed in the tibia reference frame (Steele et al., 2012).

Statistical Analyses

To assess differences between joint compressive forces and muscle forces between groups, one-dimensional statistical parametric mapping using Random Field Theory to correct for Type I error inflation (Pataky et al., 2013, 2016a) was implemented using MATLAB R2019B (MATLAB, MathWorks, Natick, MA, USA) with the source code made available by Pataky et al. (Pataky et al., 2016a).

Study One: Uphill Walking

To assess differences between limb and slope, a 3×3 [Limb (replaced, non-replaced, control] × Slope (0°, 10°, 15°)] SPM{F} repeated measures ANOVA was conducted on selected variables. Limb and Slope main effects were deemed significant when the SPM{F} trajectory crossed the critical threshold boundary (Pataky et al., 2013).

Main effects of Limb and Slope were tested with one-way SMP{F} tests. If a significant Limb × Slope interaction was found, *post hoc* SPM{t} tests were conducted on each pairwise comparison.

A 3×3 (Limb [replaced, non-replaced, control] × Slope [0°, 10° , 15°]) mixed model ANOVA was used to detect differences between limb and group conditions and their interaction for TCF impulse (25.0 IBM SPSS, Armonk, NY, USA). An α level of 0.05 was set a priori. If an interaction was present, pairwise *t*-tests were performed in the *post hoc* analysis with Bonferroni adjustments to determine the location of the statistical differences between slope and limb. The alpha level adjusted for post hoc comparisons for interaction were adjusted to be such that the interaction $\alpha < 0.006$ (9 comparisons), and main effect $\alpha < 0.017$ (3 comparisons). Effect size for all significant main effects and interactions will be reported using partial eta squared (η_p^2) effect size defined as small >0.02, medium >0.13, and large >0.26 (Cohen, 2013).

Study Two: Downhill Walking

To assess differences between limb and slope, a 3×3 (Limb [replaced, non-replaced, control] × Slope [0°, 10°, 15°] SPM{F} repeated measures ANOVA was conducted on selected variables. Limb and Slope main effects were deemed significant when the SPM{F} trajectory crossed the critical threshold boundary (Pataky et al., 2013). Main effects of Limb and Slope were tested with one-way SMP{F} tests. If a significant Limb × Slope interaction was found, *post-hoc* If a significant interaction was found, *pot-hoc* SPM{t} tests were conducted on each pairwise comparison.

A 3×3 (Limb [replaced, non-replaced, control] × Slope [0°, 10°, 15°] mixed model ANOVA was used to detect differences between limb and group conditions and

their interaction for TCF impulse (25.0 IBM SPSS, Armonk, NY, USA). An α level of 0.05 was set a priori. If an interaction was present, a pairwise *t*-test were performed in the *post hoc* analysis with Bonferroni adjustments to determine the location of the statistical differences between slope and limb. The alpha level for post hoc comparisons for interaction were adjusted to be $\alpha < 0.0125$. The alpha level for post-hoc comparisons for main effects were adjusted to 0.017. The Bonferroni adjusted alpha levels were determined as the quotient of the original alpha level (0.05) and the number of comparisons made. Effect size for all significant main effects and interactions will be reported using partial eta squared (η_p^2) effect size defined as small >0.02, medium >0.13, and large >0.26 (Cohen, 2013).

CHAPTER IV

EXAMINATION OF TIBIOFEMORAL COMPRESSIVE FORCES DURING UPHILL WALKING IN PATIENTS WITH PRIMARY TOTAL KNEE ARTHOPLASTY

Abstract

The purpose of this study was to determine differences in total (TCF), medial compartment (MCF) and lateral compartment (LCF) tibiofemoral joint compressive forces and related muscle forces between different limbs (replaced, non-replaced, and control), and different slopes [0° (level), and 5° and 10° (uphill)] during level and uphill walking using SPM. A musculoskeletal modeling and simulation approach using static optimization was used to determine muscle and TCF, MCF and LCF for 9 patients with primary TKA and 9 healthy control participants during the level and uphill walking trials. Total stance phase, loading response, and push off TCF impulse were also calculated. A 3×3 [Limb (replaced, non-replaced, control] × Slope (0°, 10°, 15°)] SPM{F} repeated measures ANOVA was conducted on knee compressive forces and muscle forces. A 3×3 (Limb [replaced, non-replaced, control] × Slope [0°, 10° , 15°]) mixed model ANOVA was used to detect differences between limb and group conditions and their interaction for TCF. Significant between-limb differences were observed for MCF during 23-30% stance between the replaced and control limbs. Significant differences between slopes were observed for all variables, except knee flexor muscle force. TCF impulse also indicates that the cumulative joint load is greater for all limbs as slope increases. A small sample size with high variability between patients with TKA who utilize different gait strategies may have rendered difference between limbs insignificant.

Keywords: total knee arthroplasty, musculoskeletal modeling, knee compressive force, uphill walking

Introduction

It is projected that over the next decade the incidence of total knee arthroplasty (TKA) will grow over 600% to nearly 3.5 million procedures performed annually in the U.S. alone (Kurtz et al., 2007). The primary goals of TKA are to alleviate knee pain and restore the loss of knee joint functions (Andriacchi et al., 1999; Andriacchi et al., 2009). With an aging population, and increase in the prevalence of TKA in those under 50 years old, the necessity for understanding biomechanical impacts of TKA for postoperative care is essential (Meier et al., 2008). Evidence suggests that muscle weakness and postoperative pain reduce functional ability nearly three-times more for patients after TKA than for their healthy age-matched counterparts (Wylde et al., 2007). Patients with TKA have reported great difficulty during daily tasks such as getting out of bed, stairs ascent, shopping, and walking (Boutron et al., 2003; Hawker et al., 1998).

Although it has been incorporated in exercise and rehabilitative routines, one daily task those with TKA may encounter is uphill ramp walking (Meier et al., 2008). Wen et al. (2019) conducted one of the first biomechanical studies of uphill walking in which patients with TKA and heathy controls performed walking trials on slopes of 0° (level), 5°, 10°, and 15°. Patients with TKA reported greater knee pain during all walking conditions compared to the healthy control participants. They also exhibited lower knee extension moment (KEM) in both the replaced and non-replaced limbs than did healthy controls. More importantly, there was a significant limb × slope interaction, showing that the non-replaced limb demonstrated greater increases in peak KEM from 0° to 15° than the replaced limb. However, Wen et al. (2019) did not investigate tibiofemoral compressive forces. A more comprehensive understanding of tibiofemoral joint loading

during uphill walking in people with TKA may help to inform rehabilitation protocol and prosthesis design.

Obtaining true tibiofemoral compressive forces *in vivo* requires the use of a specialized instrumented prosthesis which is very costly and not practical for large-scale use. Furthermore, these instrumented prostheses only report forces in the replaced limb, and not in the contralateral, non-replaced limb, making intra-limb comparisons impossible. Musculoskeletal modeling and simulations provide tools that allow for the estimation of tibiofemoral compressive forces and related muscle forces without need of *in vivo* measurements (Delp et al., 2007; Lerner et al., 2015; Steele et al., 2012). Lerner et al. (2015) implemented a static optimization approach in OpenSim with a novel musculoskeletal knee model using two revolute joints which was capable of resolving total tibiofemoral compressive force (TCF) into medial (MCF) and lateral (LCF) compartment-specific compressive forces. These tools allow researchers the ability to examine tibiofemoral compressive forces in limbs that do not have instrumented prostheses. In an effort to describe and compare the behavior of tibiofemoral compressive forces, peak compressive force (i.e. minimum or maximum) and stance phase joint contact force impulse are two variables that have previously been reported in the literature which quantify and describe the cumulative joint loading during movements (Correa et al., 2010; Lerner et al., 2015; Stensgaard Stoltze et al., 2018; Walter et al., 2010). Given the nature of increased medial compartment joint loading (i.e., increased MCF) that was likely a contributing factor to knee osteoarthritis (OA) preceding TKA, investigation of the response of TCF, MCF, and LCF and stance phase TCF impulse in uphill walking can provide insight not only to overall joint loading but also changes in

medial compartment joint loading consequential of TKA in both replaced and contralateral non-replaced knees.

Discrete point analysis has long been the most common form of data analysis in the field of biomechanics Examining biomechanical variables, however, throughout the entirety of a movement phase is of particular interest. Statistical Parametric Mapping (SPM) has gained recent popularity in assessing time-series of biomechanical variables throughout the entire movement phase (Pataky et al., 2015). One strength of SPM is that a time-normalized dependent variable can be evaluated over a specific time continuum, rather than discrete values (i.e., maximum or minimum value). In SPM, a time series of the statistical test-specific critical value is determined from the smoothness of the residuals of the data (Penny et al., 2011).

Therefore, the purpose of this study was to determine differences in TCF, MCF and LCF and related muscle forces between different limbs (replaced, non-replaced, and control), and different slopes [0° (level), and 5° and 10° (uphill)] during stance phase using SPM. We also sought to explore differences in TCF impulse between different limbs and slopes. We hypothesized that tibiofemoral compressive forces, TCF impulse, and knee joint-spanning muscle forces during uphill walking would be greater in the control limb, followed by the non-replaced limb of the TKA group, and lowest in the replaced limb of the TKA group, at each slope during the entirety of stance. We also hypothesized an interaction would be present between limbs and slopes for tibiofemoral compressive forces and muscle forces.

Methods

Participants

Nine patients with TKA (5 male and 4 female, 67.5 ± 5.5 years, 1.74 ± 0.10 m, 84.3 ± 15.6 kg, 27.8 ± 3.2 months since surgery) were recruited from a local orthopedic clinic to attend one laboratory session. All nine patients had received cruciate retaining knee joint prosthesis from a primary TKA. Inclusion/exclusion criteria, and full data collection methods have been previously reported (Wen et al., 2019). In short, potential patients were excluded if they had any additional lower extremity joint replacement, any diagnosed osteoarthritis of the hip or ankle, more than 75% radiographic joint space narrowing and chronic pain of the contralateral, non-replaced knee, BMI greater than 38 kg/m^2, or any neurological diseases. Furthermore, participants for an age-matched control group (5 male and 4 female, 69.5 ± 4.3 years, 1.77 ± 0.12 m, 76.5 ± 25.4 kg) were recruited from the local community. Exclusion criteria for the control group participants included any self-reported knee pain during typical every-day activities, any diagnosis or osteoarthritis, any lower limb joint arthroplasty, arthroscopic surgery, or inter-articular injection.

Experimental Protocol

The detail of experimental protocol and equipment are described elsewhere, and a brief account is provided here (Wen et al., 2019). All participants completed five trials of uphill walking at self-selected pace on 0° (level walking) 5°, and 10° incline on a customized adjustable ramp system which was instrumented with two force platforms. A trial was deemed successfully if contact was made only with the first force plate during the ramp ascent, or level walking. To minimize the duration of the data collection

session, ramp incline conditions (5°, 10°) were performed first, followed by the level walking conditions. Ramp conditions were performed in a randomized order, with inclination angle first randomized, followed by randomization of leading limb (replaced vs. non-replaced). Level walking conditions were also randomized by the leading limb (replaced vs. non-replaced).

Instrumentation

Three-dimensional (3D) kinematics (240 Hz, Vicon Motional Analysis Inc., Oxford, UK) and ground reaction force (GRF, 1200 Hz, BP600600 and OR-6-7, American Mechanical Technology Inc. Watertown, MA, USA) were recorded during testing. A handrail was provided on the right side for balance; however, participants were not encouraged to use it (Wen et al., 2019).

A 16-channel surface electromyography (EMG) system (1200 Hz, Trigno™ Wireless EMG System, Delsys, INC, Natick MA, USA) was used to monitor the muscle EMG activities on following muscles on both sides of the body: vastus lateralis, vastus medialis, medial head of the gastrocnemius, semitendinosus, and biceps femoris. The skin of the electrode attachment sites was shaved and cleaned with alcohol swab before the application of the electrodes. The placement of the EMG electrodes on the selected muscles were based on the recommendations of SENIAM (Surface ElectroMyoGraphy for the Non-Invasive Assessment of Muscles) (Hermens et al., 2000). Both GRF and EMG data were sampled simultaneously with the 3D kinematic data using the VICON system and Nexus software package (2.5, Vicon Motion Analysis Inc., Oxford, UK).

Data analysis

The EMG data were analyzed using the Visual3D. Raw EMG signals were band-pass filtered at cutoff frequencies of 10 Hz and 450 Hz and then full wave rectified. A moving root-mean-square (RMS) filter was used to filter the rectified EMG signals using a 60-millisecond moving window. The maximum value of the RMS EMG signals of three functional test trials was used to normalize the filtered EMG signals of the testing movement trials.

Musculoskeletal Modeling and Simulation

An open-source musculoskeletal model [18 segments, 23 degrees-of-freedom (DOF), 92 muscle-tendon actuators] was used to perform the simulations (Lerner et al., 2015). The knee joint of this model consists of 1 DOF (flexion/extension) supplemented with added medial and lateral compartments. The model was first scaled to each participant's height and mass and the subtalar and metatarsal-phalangeal joints were locked for the analysis.

Generalized joint coordinates derived from inverse kinematics calculations were exported from Visual3D (Version 6, C-Motion, Inc., Germantown, MD, USA) and imported into OpenSim for simulations (3.3 OpenSim, SimTK, Stanford University). The generalized joint coordinates were applied to each subject-specific scaled musculoskeletal model. Inverse dynamics calculations were performed in OpenSim to compute lower extremity joint moments. Next, muscle activations and forces during level and uphill walking were calculated using static optimization (Anderson and Pandy, 2001; Crowninshield and Brand, 1981). The static optimization calculations included muscle physiology (force-length-velocity relationships) and an objective function to minimize

the sum of squared muscle activations (Crowninshield and Brand, 1981). Maximum reserve torque actuator values for all lower extremity joints were checked and found to be within suggested guidelines (Hicks et al., 2015). Joint compressive forces (MCF, LCF, TCF) were calculated using joint reaction analysis in OpenSim and expressed in the tibia reference frame (Steele et al., 2012).

Primary variables of interest included TCF, MCF, and LCF. Secondary variables of interest included TCF impulse, demarcated as total TCF impulse (over the entire stance phase), loading-response TCF impulse (the first 50% of stance), and push-off impulse (the last 50% stance). TCF impulse was found with numerical integration of the TCF curves of the respective phases of stance by means of the trapezoidal method with unit spacing. Muscle forces of the knee flexors were also included as secondary variables, specifically, the biceps femoris long and short heads, semimembranosus, semitendinosus, sartorius, gracilis, and both medial and lateral head of the gastrocnemius. The knee extensors group was defined by the rectus femoris, vastus lateralis, vastus intermedius, and vastus medialis. The left or right limbs of healthy controls were randomly selected for use in the control group for the replaced and non-replaced limbs of TKR patients.

Statistical analysis

To assess differences between joint compressive forces and muscle forces between groups, one-dimensional statistical parametric mapping using Random Field Theory to correct for Type I error inflation (Pataky et al., 2013, 2016a) was implemented using MATLAB R2019B (MATLAB, MathWorks, Natick, MA, USA) with the source code made available by Pataky et al. (2016a). The data were first checked for normality using D'Agostino-Pearson K^2 test (D'agostino et al., 1990).

To assess differences between limb and slope, a 3×3 [Limb (replaced, non-replaced, control] × Slope (0°, 10°, 15°)] SPM{F} repeated measures ANOVA was conducted on selected variables. Limb and Slope main effects were deemed significant when the SPM{F} trajectory crossed the critical threshold (Pataky et al., 2013). Main effects of Limb and Slope were tested with one-way SMP{F} tests. If a significant Limb × Slope interaction was found, *post hoc* SPM{t} tests were conducted on each pairwise comparison. Effect size for all significant *post-hoc* comparisons were computed from the mean difference between the two waveforms throughout the duration of a supra-threshold cluster and were reported using Cohen's d (Cohen, 2013; Schroeder et al., 2021).

A 3×3 (Limb [replaced, non-replaced, control] × Slope [0°, 10°, 15°]) mixed model ANOVA was used to detect differences between limb and group conditions and their interaction for TCF impulse (25.0 IBM SPSS, Armonk, NY, USA). An α level of 0.05 was set a priori. If an interaction was present, pairwise *t*-tests were performed in the *post hoc* analysis with Bonferroni adjustments to determine the location of the statistical differences between slope and limb. The alpha level adjusted for post hoc comparisons for interaction were adjusted to be such that the interaction $\alpha < 0.006$ (9 comparisons), main effect $\alpha < 0.017$ (3 comparisons). Effect size for all significant main effects and interactions were reported using partial eta squared (η^2_p) effect size defined as small >0.02, medium >0.13, and large >0.26 (Cohen, 2013).

Results

There were no differences of age, height, mass, or BMI between patients with TKA and control participants (Table 1). Frontal-plane lower limb alignment between the replaced limb, non-replaced limb, and control limb were also similar (Table 1).

Magnitudes of reserve torque actuator moments for all lower extremity joints were checked and found to be within suggested levels (Appendix G) (Hicks et al., 2015). Qualitative analysis the model predicted muscle activations (biceps femoris long head, semitendinosus, vastus medialis, vastus lateralis, and medial head of the gastrocnemius) generally agree with our experimentally collected EMG (Figure 1).

The SPM{F} test for TCF revealed a significant main effect of slope ($p < 0.001$, Figure 2A). *Post-hoc* SPM{t} analysis found 3 significant regions between level and 10° uphill walking that exceeded the critical threshold ($t_{critical} = 3.44$, Table 2, Figure 2C) indicating TCF during 10° uphill walking was greater at the beginning of stance (1-5%), during loading-response (12-33% stance) and at the end of stance (89-97%). Two significant regions were also found between 5° and 10° ($t_{critical} = 3.45$, Table 2, Figure 2D), as TCF in 10° was greater than 5° uphill walking (1-4% and 12-35%).

For MCF, both main effect of slope ($p < 0.001$, Figure 3A) and limb ($p = 0.022$, Figure 3A) were found significant with SPM{F} test. *Post-hoc* SPM{t} analysis revealed one significant region between the replaced limb and the control limb ($t_{critical} = 3.15$, Table 2, Figure 3C), suggesting greater MCF experienced by the control limb between 23-30% stance. Two significant regions were found between level and 10° uphill walking between 14-26% and 41-46% stance ($t_{critical} = 3.39$, Table 2, Figure 3F).

SPM{F} test for LCF revealed two significant regions for the interaction between slope and limb ($F_{critical} = 7.50$, $p = 0.004$, and $p < 0.01$, Figure 4A). *Post-hoc* SPM{t} revealed one significantly different region between level and 10° during 15-28% stance ($t_{critical} = 4.5665$, Figure 4C) for the replaced limb, and between 5° and 10° during 15-28% stance ($t_{critical} = 4.3959$, Figure 4D). One significant region was found between level

and 10° walking for the non-replaced limb during 17-31% stance ($t_{critical}$ = 4.6787, Figure 4F). Finally, one significant region was found during 15-33% stance between level and 10° ($t_{critical}$ = 4.9022, Figure 4I) and at 11-34% stance between 5° and 10° ($t_{critical}$ = 5.1770, Figure 4J). For the control limb, one significant region indicated greater LCF in during 10° than both level walking between 15-33% stance ($t_{critical}$ = 4.9022, Table 2, Figure 4I), and 5° between 11-34% stance ($t_{critical}$ = 5.1770, Table 2, Figure 4J).

For the knee extensor muscle force, significant main effects of both slope ($p < 0.001$, Figure 5A) and limb ($p = 0.010$, Figure 5A) were found with the SPM{F} test. *Post-hoc* tests showed that the knee extensor muscle group generated more force during push-off in level walking than during 5° uphill walking (61-98% stance, $t_{critical}$ = 3.44, Table 2, Figure 5E). In the 10°, greater loading-response knee extensor muscle forces (6-38% stance for both 5° and 10°) were seen compared to both level ($t_{critical}$ = 3.44, Table 2, Figure 5F) and 5° ($t_{critical}$ = 3.43, Table 2, Figure 5G) conditions. Interestingly, push-off phase knee extensor muscle force was greater during level walking than during 5° or 10° uphill walking conditions (Figure 5E-F). There were no significant interactions or main effects discovered for knee flexor muscle force between any limb or slope conditions.

There was a main effect of slope for TCF impulse in stance phase ($p = 0.021$), loading-response ($p = 0.028$), and push-off ($p = 0.004$, Table 3). *Post-hoc* tests indicated that cumulative TCF during stance, loading-response and push-off was greater during 10° than level ($p \leq 0.002$ for all comparisons) and 5° ($p \leq 0.013$ for all comparisons).

Discussion

The purpose of this study was to determine differences in tibiofemoral joint compressive forces (TCF, MCF, LCF) between different limbs (replaced, non-replaced, and control), and different slopes (0°, 5° and 10°). We also sought to explore differences in TCF impulse and muscle forces between different limbs and slopes. Our first hypothesis, that tibiofemoral compressive forces, TCF impulse, and knee joint-spanning muscle forces during uphill walking would be greater in the control limb, followed by the non-replaced limb of the TKA group, and lowest in the replaced limb of the TKA group, at each slope during the entirety of stance, was partially supported.

There was one significantly different region for MCF between the replaced limb and the control limb indicating lower MCF in the replaced limb during 23-30% stance across all slopes (Figure 3C). The replaced limb experienced, on average, 0.41 BW less MCF. These findings align with previous literature that has shown decreased peak MCF in the replaced limb following TKA. Using regression equations first determined by Walter et al. (2010), Wen et. al (2019) estimated peak MCF of replaced and non-replaced limbs by using a combination of KEM and peak knee abduction moment. Though statistical comparisons were not made between the replaced and control limbs, qualitative assessment of the difference in peak MCF between the healthy control limbs and the replaced limb is between 0.3-0.4 BW (Wen et al., 2019). Though the significant region of MCF in this study was short in overall duration of stance, a large effect size (1.68, Table 2) suggests meaningful separation between the two limbs.

The TCF results showed no differences between the replaced, non-replaced and control limbs. Inverse dynamics-based studies have frequently used KEM as an

indication of overall loading at the knee joint (Astephen et al., 2008; Benedetti et al., 2003; Kuster et al., 1997; McClelland et al., 2014; Ngai and Wimmer, 2015; Ro et al., 2018). For the TKA population specifically, overall joint loading is of particular interest as it has been related to increased wear and degradation of the prosthesis and joint loading asymmetry (Benedetti et al., 2003; Ro et al., 2018). Previous studies have demonstrated a deficit of KEM in the replaced limb compared to the non-replaced limbs of patients with TKA in various activities such as level walking, stair ascent, and ramp ascent (Standifird et al., 2016; Wen et al., 2019; Yoshida et al., 2008). Yoshida et al. (2008) reported smaller KEM of 19.9 ± 15.5 Nm in the replaced limb, compared to the non-replaced limb of 35.6 ± 18.4 Nm during level walking. Standifird et al. (2016) also reported smaller peak loading-response KEM for the replaced limb (0.98 Nm/kg), compared to the control limb (1.3 Nm/kg) and the non-replaced limb (1.18 Nm/kg) and during stair ascent. Wen et al. (2019) similarly reported reduced peak loading-response KEM in the replaced limb during uphill walking at 10° and 15°, compared to the replaced and control limbs. The lack of between limb difference in the TCF found in this current study may be due to lack of differences in knee-joint-spanning muscle forces. The magnitude of TCF is contributed from three sources: GRF, muscle forces, and the inertial characteristics of the segment (Steele et al., 2012). During level walking, peak vertical GRF has been reported about 1.08 BW for healthy limbs, 1.04 BW for the non-replaced limb, and 1.03 BW for replaced limbs and decreased with increasing slope (Wen et al., 2019). While inertial characteristics of the limb contribute minimally to the compressive forces, muscle forces are the primary contributor to TCF. In this current study, knee extensor muscle forces are between 1.5-2.0 BW, and knee flexor muscle forces range

between 1.0-2.0 BW (Figure 6). Although not statistically significant between limbs, the knee flexor muscle forces produced over 1.0 BW of force (Figure 6). Given the lack of between-limb significance in this study, it is possible that different gait strategies have been adopted by individual patients that occlude significant between-limb differences in this small sample. Some patients with better post-operative recovery may exert greater or equal amounts of knee extensor and flexor muscle forces in the replaced limb during walking. Others may rely more heavily on muscle forces from the non-replaced limb. Thus, a small sample size with high variability between patients with TKA who utilize different gait strategies may have rendered difference between limbs insignificant.

Our second hypothesis, that an interaction would be present between limbs and slopes for tibiofemoral compressive forces and muscle forces was also partially supported as an interaction was found for LCF. P*ost-hoc* comparisons, however, did not reveal any between-limb differences. This study utilized a simulation-based static optimization approach to determine tibiofemoral compressive forces, whereas Wen et al. (2019) predicted MCF using regression equations based on inverse dynamics calculation of sagittal and frontal plane joint moments. Differences in compressive force determination between this current study and Wen et a. (2019) and a small sample size here may be attributable for lack of additional between-limb differences in the compressive forces.

A secondary finding of this study is that changes to tibiofemoral joint compressive forces between slopes occur specifically during loading-response. TCF were significantly different for 10° compared to level and 5° between approximately 12-35% stance. Significant differences around 25% of stance were observed for MCF, LCF, and knee extensor muscle force (Figure 3-5). Similar trends were observed for TCF impulse.

There was a main effect of slope for total, loading-response, and push-off TCF impulse (Table 2). Increasing loading-response impulse is consistent with TCF, which increases with slope. Although no significant differences were observed for push-off TCF amongst different limbs or slopes, qualitatively, second peak TCF (push-off) is greater in magnitude and duration than first peak TCF (loading-response), and therefore a significant effect of slope is observed.

Significant differences in knee extensor muscle force were present during both loading-response and push-off between slopes (Figure 5). Significant differences between loading-response knee extensor muscle force are a logical expectation which are in line with the significant differences seen with TCF. Differences of loading-response knee extensor muscle force between level and 10° and 5° and 10° both occur between 6-38% stance and are consistent with similar increases in TCF - 12-33% stance between level and 10° and 12-35% between 5° and 10°. Knee extensor muscle force is one of the dominant contributors to TCF in addition to GRF and segment inertial properties. Thus, consistent patterns between the two variables suggest that increased knee extensor muscle force may be the primarily responsible for increased TCF.

Increased knee extensor muscle force in push-off without increased contact force, however, is an interesting finding of this study. During loading-response, the knee extensors must produce eccentric force to absorb loading to the knee joint and maintain posture during the first part of stance. As slope increases, the required demand of the knee extensor muscle is increased to propel the body forward and upward on the incline. In uphill walking, the knee compressive force increased with the increased slopes during

loading-response, (specifically 12-35% of stance) and provides meaningful information to clinicians involved with postoperative TKA rehabilitation.

Wen et al. (2019) recommended against the use of 10° and 15° uphill walking during TKA rehabilitation due to increased KEM experienced by the replaced limb, and the association between KEM, increased TCF, and damage to the knee prosthesis (D'Lima et al., 2001; D'Lima et al., 2012). Deficits in quadriceps strength and KEM in the replaced limb have been demonstrated immediately following TKA operation up to several years post-TKA (Huang et al., 1996; Mizner et al., 2005). Recent recommendations, however, have suggested that, despite deficits of replaced limb KEM, early high intensity rehabilitation following TKA leads to improved short-term and long-term functional outcomes compared to a lower intensity rehabilitation program (Bade and Stevens-Lapsley, 2011; Bade et al., 2017; Zaghlol et al., 2020). As part of both high and low intensity rehabilitation programs, quadriceps strengthening exercises such as quadriceps setting, weight bearing lunges, body-weight squatting, and stair ambulation have been incorporated into rehabilitation plans for patients with TKA to improve muscle strength asymmetries between the replaced and non-replaced limbs (Bade et al., 2017). However, quadriceps strengthening has been shown to have no effect on KEM or KAbM in patients with knee osteoarthritis in gait (DeVita et al., 2018; Foroughi et al., 2011). In this context, uphill walking may be an effective exercise for high intensity early and long-term rehabilitation programs, with lower peak GRF than stair ambulation. Additionally, uphill walking facilitates increased muscular demand and quadriceps strengthening with increased slope while promoting the reacquisition of normal gait

patterns following TKA, which may not be achieved in traditional quadriceps strengthening exercises.

There are certain limitations to this work that need to be acknowledged. Although, all data met the assumptions of normality from the D'Agostino-Pearson K^2 test (D'agostino et al., 1990; Pataky et al., 2015), the small sample size within each limb group may result in increased variability of the variables examined, and manifest as large standard deviations (Table 3, for example). This small sample of cruciate-retaining patients with TKA was selected intentionally from a subset of the data examined by Wen et al. (2018). SPM{F} two-way ANOVA requires that the equal number of observations in each group (e.g., replaced limb, non-replaced limb, and control limb), which dictated that we could only analyze one sub-set of the three different implant styles from Wen et al. (2019). Due to tracking errors of the trunk, one control participant was excluded from simulation and analysis. Due to this reduction in sample size of the control group, the TKA group size was also reduced. Additionally, SPM analysis between groups or conditions mandates temporal synchrony for comparisons over time to be made. In order to meet these requirements, time-normalization (to 101 data points) was performed on compressive and muscle force waveforms. With such reductions in resolution, it is possible that true peak values may be reduced (or smoothed out) as a result of the time normalization which may also contribute to the lack of difference of TCF between limbs.

Lerner et al. (2015) reported contact force estimations using three variations of this model. The fully informed model using both alignment and condylar contact points produced the best estimation of compressive force. Participant-specific condylar contact locations for these data of the current study were unknown. We estimated lower limb

alignment using the mechanical axis angle from motion capture data of static trial (Bennett et al., 2018; Vanwanseele et al., 2009). There was no difference for mechanical axis angle between the replaced, non-replaced, and control limbs (Table 1). With the similarities between frontal plane alignment between the participants of this study, we feel confident that differences that may arise from implementing participant-specific frontal plane lower limb alignment were minimized.

In conclusion, joint loading appears to be similar for the majority of stance between replaced, non-replaced, and control limbs, with significant differences of TCF and MCF occurring between 12-35% of stance between slopes. TCF impulse also indicates that the cumulative joint load is greater for all limbs as slope increases.

Appendix A – Chapter IV Tables and Figures

Table 1. Descriptive statistics and tibiofemoral joint frontal-plane alignment.

	TKR	Healthy	p-value	
Age (years)	67 ± 5.8	70 ± 4.2	0.406	
Height (cm)	174.0 ± 9.4	176.1 ± 11.5	0.464	
Mass (kg)	84.3 ± 13.4	76.5 ± 23.8	0.125	
BMI (kg/m^2)	27.8 ± 3.4	24.1 ± 4.7	0.428	
	Replaced	Non-Replaced	Control	p-value
Mechanical Axis Angle (°)	176.8 ± 3.9	175.7 ± 5.6	177.1 ± 3.1	0.843

Table 2. SPM summary for uphill walking. Significant region ranges (% stance), significant region p-values, mean difference between conditions within each region (BW) and Cohen's d effect size c for knee compressive forces and knee extensor muscle force

		Region	p	Mean Difference (BW)	Cohen's d
TCF	Level vs. 10°	1-5%	0.019	0.39	1.77
		12-33%	< 0.001	0.81	1.96
		89-97%	0.002	0.16	1.85
	5° vs. 10°	1-4%	0.026	0.20	1.55
		12-35%	< 0.001	0.64	1.53
MCF	Replaced vs. Control limb	23-30%	0.012	0.41	1.68
	Level vs. 10°	14-26%	< 0.001	0.29	1.33
		41-46%	0.018	0.18	1.69
LCF	Replaced: Level vs. 10°	15-28%	<0.001	0.55	1.48
	Replaced: 5° vs. 10°	15-28%	< 0.001	0.59	1.29
	Non-Replaced: Level vs. 10°	17-31%	< 0.001	0.05	0.18
	Control: Level vs. 10°	15-33%	< 0.001	0.78	2.53
	Control: 5° vs. 10°	11-34%	< 0.001	0.55	1.69
Knee Extensor Muscle Force	Level vs. 5°	61-98%	< 0.001	0.15	2.68
	Level vs. 10°	6-38%	< 0.001	0.46	1.58
		57-98%	< 0.001	0.22	4.00
	5° vs. 10°	6-38%	< 0.001	0.54	2.39
		69-94%	< 0.001	0.09	1.33

Table 3. TCF impulse during uphill walking. Total, loading-response, and push-off phase TCF impulse (BW·s, mean ± standard deviation) during level, 5° uphill, and 10° uphill walking conditions. Bold values indicate statistical significance.

Variable	Limb	Level Walking	5° Uphill	10° Uphill	Slope (η^2_p)	Limb (η^2_p)	Interaction (η^2_p)
Stance Impulse*#	Replaced	0.84 ± 0.64	0.91 ± 0.68	1.06 ±0.81	**0.021** (0.284)	0.960 (0.004)	0.261 (0.106)
	Non-Replaced	0.99 ± 0.82	0.94 ± 0.76	1.21 ± 1.16			
	Control	0.85 ± 0.64	0.97 ± 0.73	1.08 ± 0.75			
Loading-Response Impulse*#	Replaced	0.29 ± 0.32	0.32 ± 0.35	0.39 ± 0.43	**0.028** (0.267)	0.928 (0.006)	0.364 (0.084)
	Non-Replaced	0.39 ± 0.46	0.35 ± 0.41	0.47 ± 0.55			
	Control	0.29 ± 0.32	0.37 ± 0.44	0.38 ± 0.42			
Push-off Impulse*#	Replaced	0.55 ± 0.33	0.59 ± 0.36	0.68 ± 0.40	**0.004** (0.381)	0.290 (0.002)	0.665 (0.050)
	Non-Replaced	0.60 ± 0.42	0.58 ± 0.38	0.74 ± 0.66			
	Control	0.57 ± 0.33	0.60 ± 0.34	0.69 ± 0.36			

Different between level and 10°

* Different between 5° and 10°.

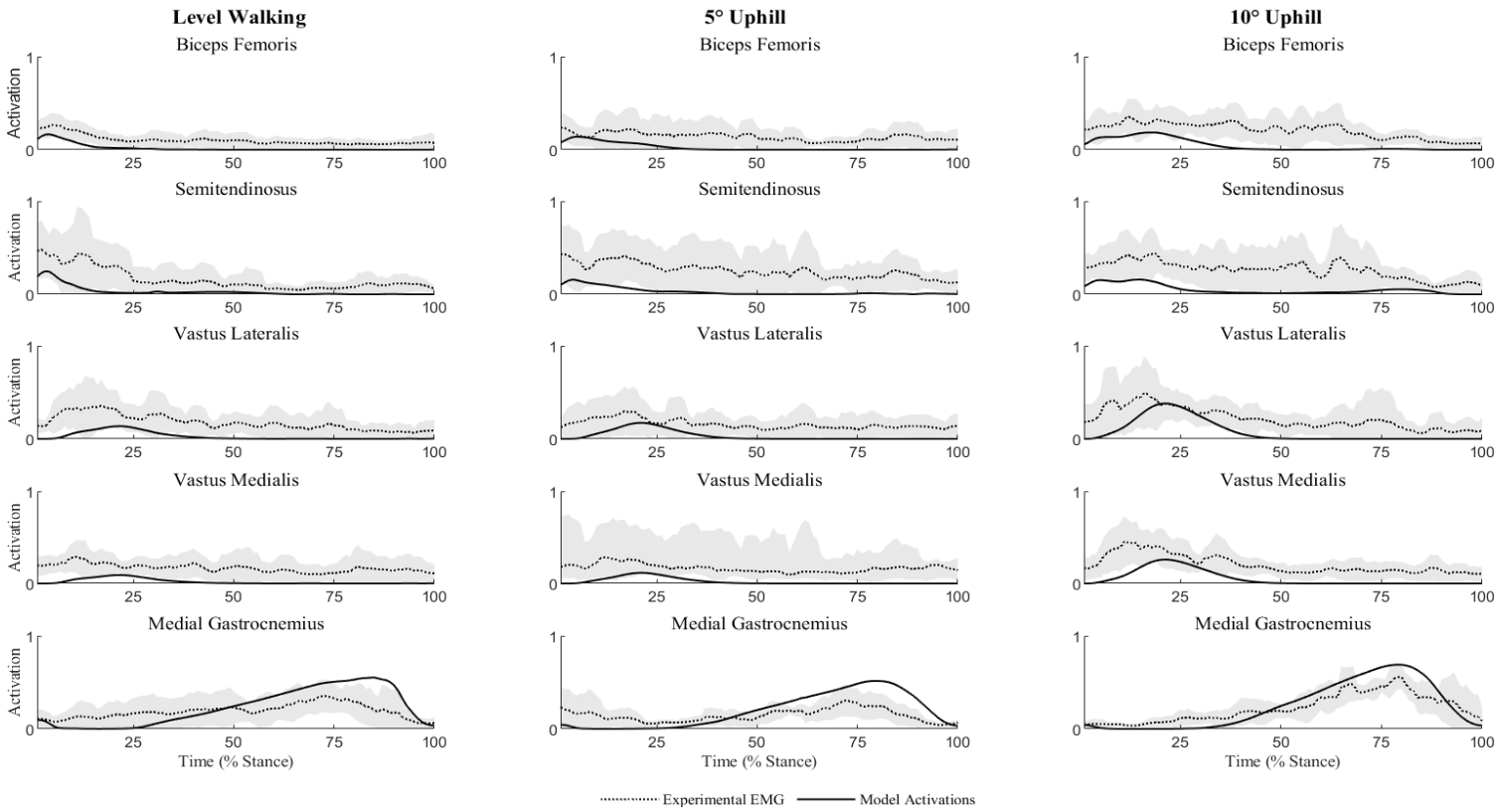

Figure 1. Muscle activations of the replaced limb during uphill walking. The solid line represents the mean activation level obtained from static optimization while the dashed line represents the mean activation level obtained from EMG with the shaded region representing ± 1 standard deviation of EMG activation.

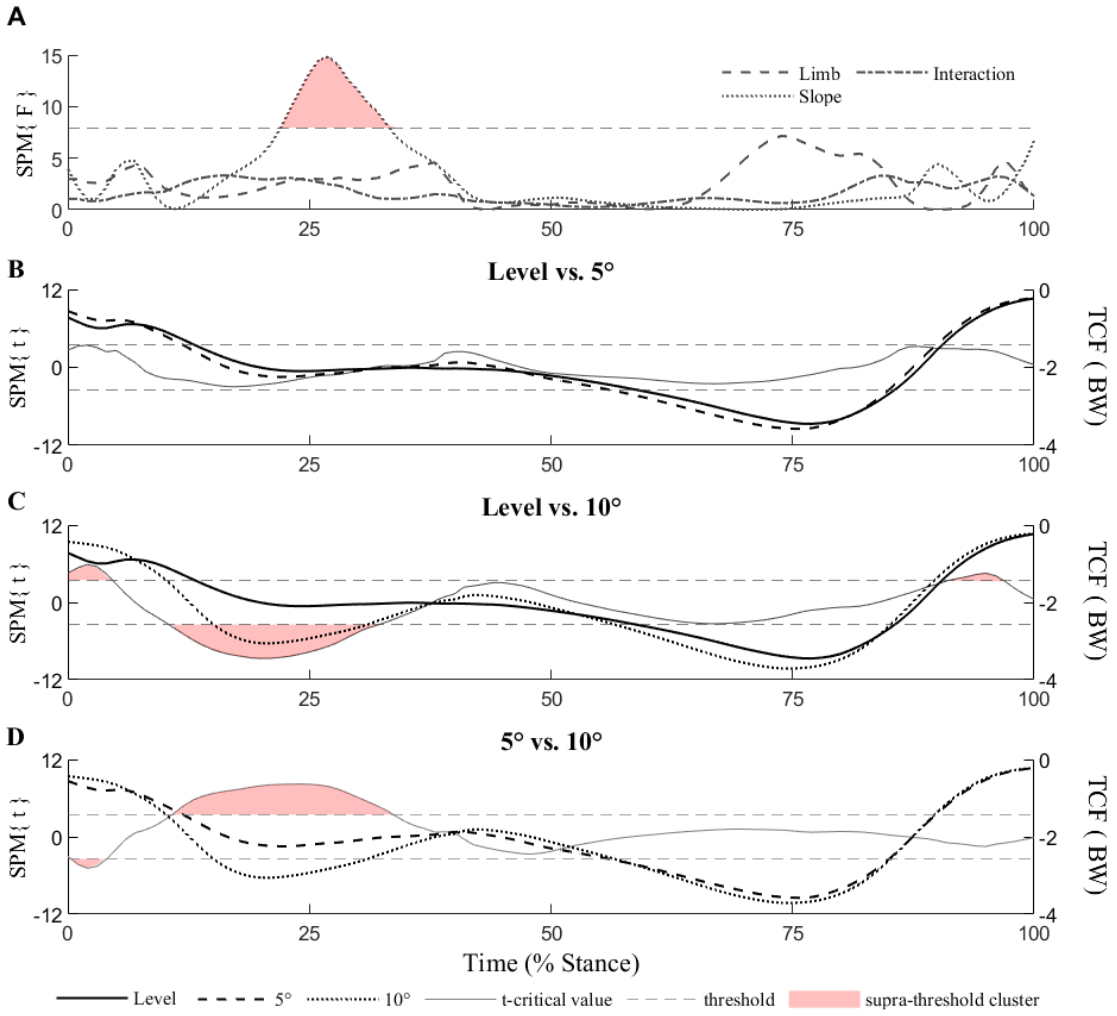

Figure 2. SPM results for TCF during uphill walking. **A)** Results of the SMP{F} test. **B-D)** *Post-hoc* SPM{t} test results plotted on the left y-axis. Shaded regions indicate the ranges the *t*-critical value time series crossed above or below the critical threshold (i.e., supra-threshold cluster). Mean time series waveforms for *post-hoc* TCF comparisons are also plotted on the same graph against the right y-axis. With *post-hoc* SPM{t} and TCF overlaid together, significantly different ranges of TCF can more easily be determined between comparisons. For Figure 2A, refer to the legend in panel A. For Figure 2B-D, refer to legend beneath panel D.

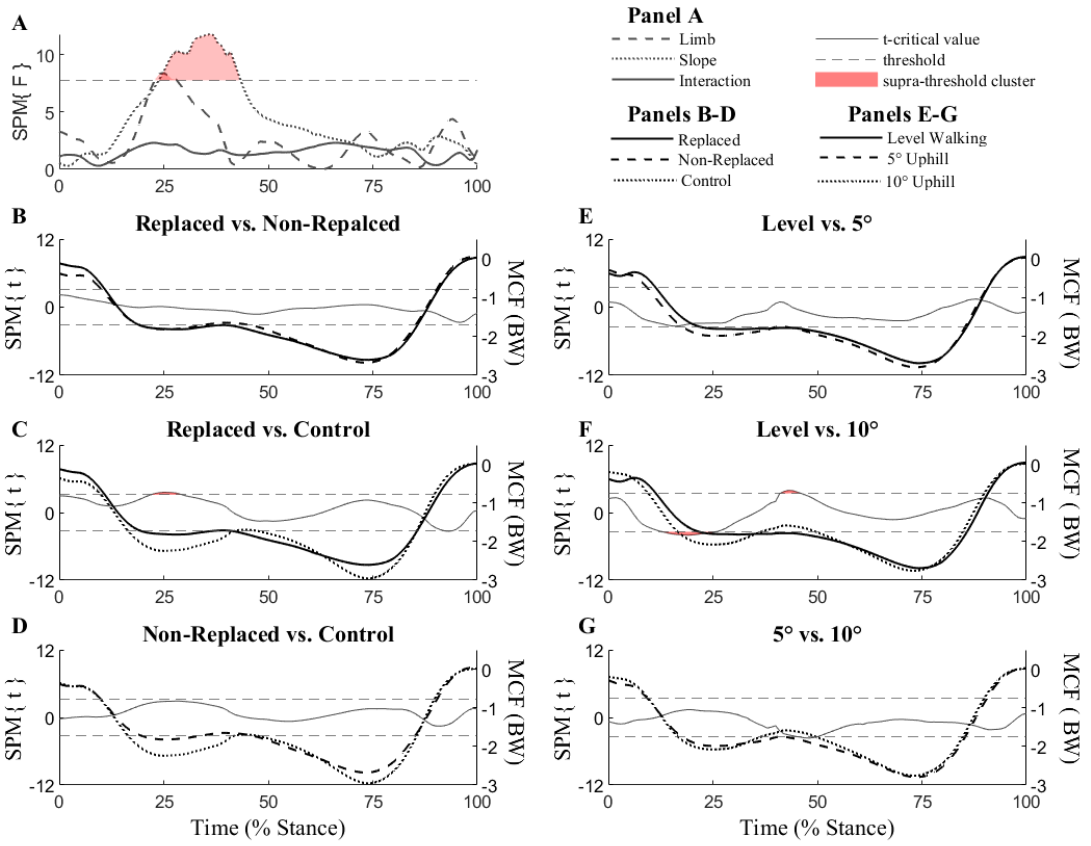

Figure 3. SPM results for MCF during uphill walking. **A)** Results of the SPM{F} test. **B-G)** *Post-hoc* SPM{t} test results plotted on the left y-axis. Shaded regions indicate the ranges the *t*-critical value time series crossed above or below the critical threshold (i.e., supra-threshold cluster). Mean time series waveforms for *post-hoc* MCF comparisons are also plotted on the same graph against the right y-axis. With *post-hoc* SPM{t} and MCF overlaid together, significantly different ranges of MCF can more easily be determined between comparisons.

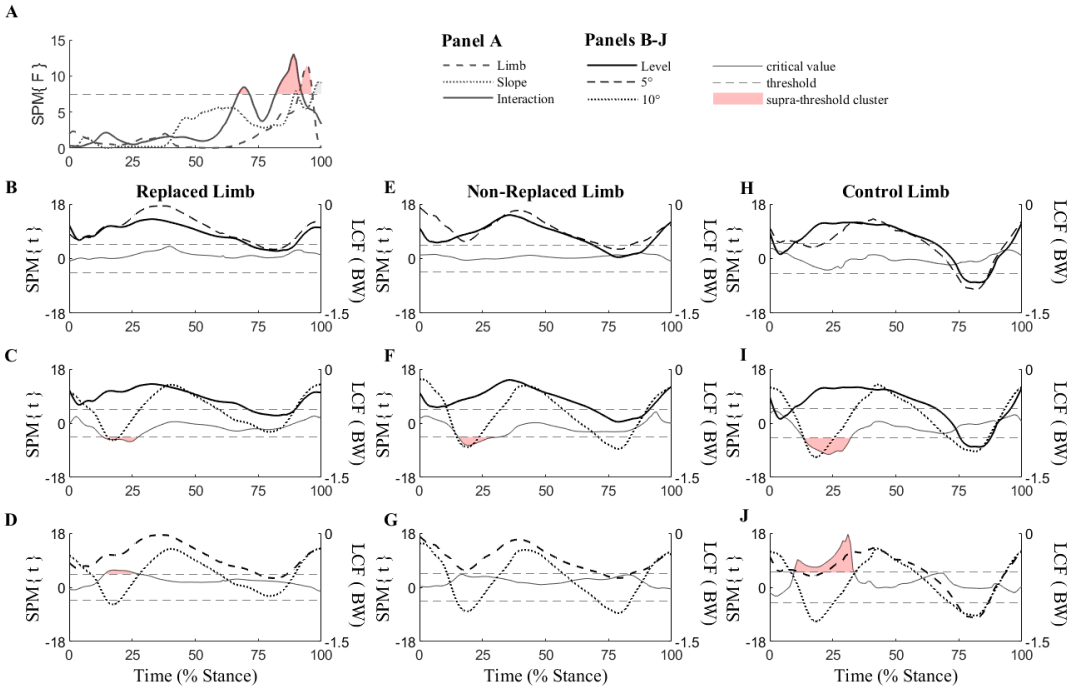

Figure 4. SPM results for LCF during uphill walking. **A)** SPM{F} test results for LCF. **B-D)** *Post-hoc* SPM{t} test results for the replaced limb, **E-G)** the non-replaced limb, and **H-J)** the control limb. For panels B-J, SPM{t} results are plotted on the left y-axis. Shaded regions indicate the ranges the *t*-critical value time series crossed above or below the critical threshold (i.e., supra-threshold cluster). Mean time series waveforms for *post-hoc* LCF comparisons are also plotted on the same graph against the right y-axis. With *post-hoc* SPM{t} and LCF overlaid together, significantly different ranges of LCF can more easily be determined between comparisons.

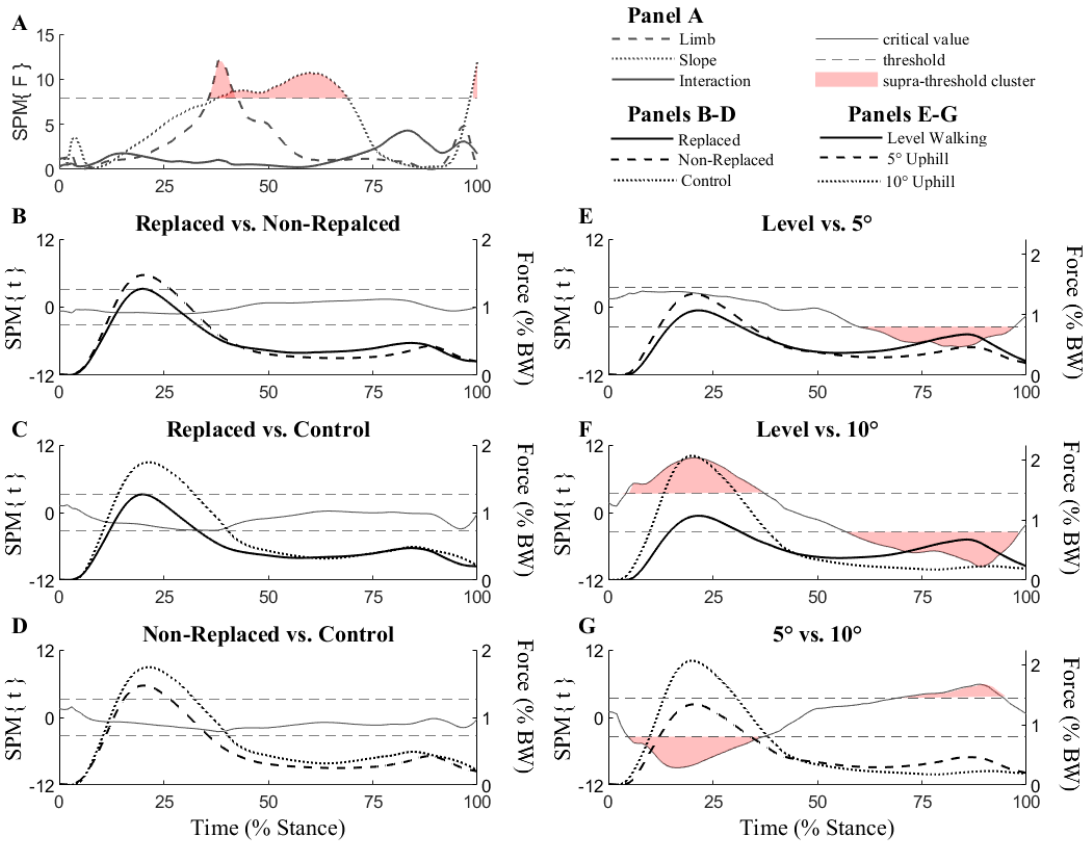

Figure 5. SPM results of knee extensor muscle forces during uphill walking.**A)** SPM{F} test results for knee extensor muscle force. **B-G)** *Post-hoc* SPM{t} test results plotted on the left y-axis. Shaded regions indicate the ranges the *t*-critical value time series crossed above or below the critical threshold (i.e., supra-threshold cluster). Mean time series waveforms for *post-hoc* knee extensor muscle force comparisons are also plotted on the same graph against the right y-axis. With *post-hoc* SPM{t} and knee extensor muscle force overlaid together, significantly different ranges of knee extensor muscle force can more easily be determined between comparisons.

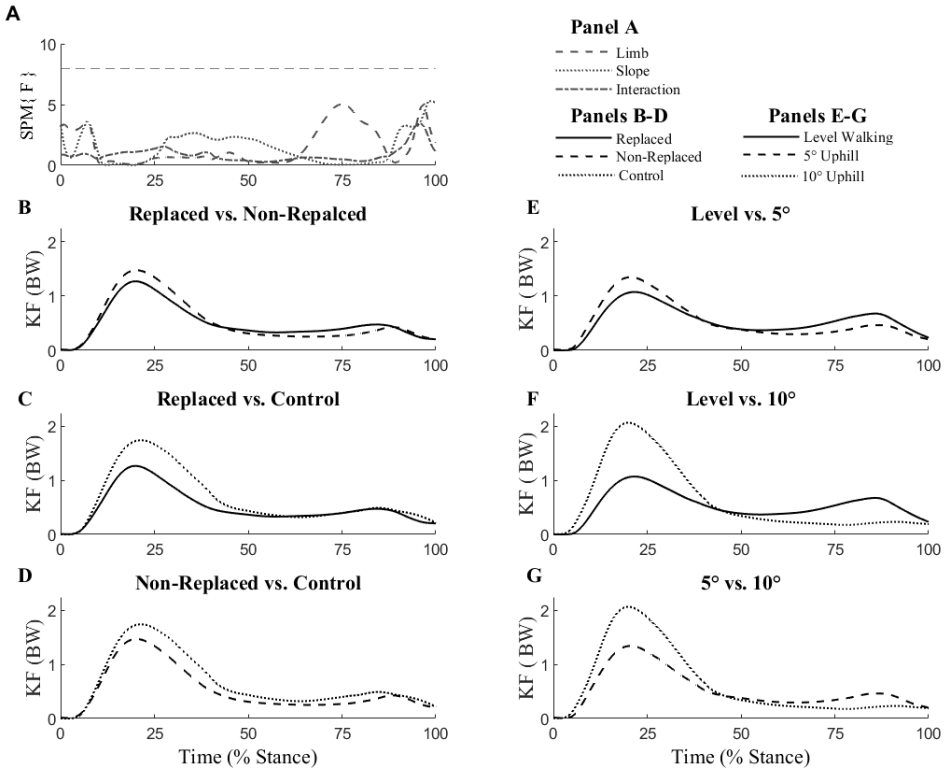

Figure 6. SPM results for knee flexion muscle forces during uphill walking.**A)** SPM{F} test results for knee flexor muscle force. **B-G)** Mean time series waveforms for *post-hoc* knee extensor muscle force comparisons.

CHAPTER V

EXAMINATION OF TIBIOFEMORAL COMPRESSIVE FORCES DURING DOWNHILL WALKING IN PARTIENTS WITH PRIMARY TOTAL KNEE ARTHOPLASTY

Abstract

The purpose of this study was to determine differences in the behavior of total (TCF), medial (MCF), and lateral (LCF) tibiofemoral compressive forces as well as knee extensor and flexor muscle forces and TCF impulse between different limbs of patients with TKA (replaced, non-replaced, and control), and different downhill slopes [0° (level), and 5° and 10°] during downhill walking. Musculoskeletal modeling was implemented to determine muscle forces as well as tibiofemoral compressive forces in 9 patients with TKA and 9 control participants. Total stance phase, loading response, and push off TCF impulse were also calculated. A 3×3 [Limb (replaced, non-replaced, control] × Slope (0°, 10°, 15°)] SPM{F} repeated measures ANOVA was conducted on selected variables. A 3×3 mixed model ANOVA was used to detect differences between limb and group conditions and their interaction for TCF. There were significant differences in TCF, MCF, and knee flexor muscle forces between the replaced and control limbs during early loading-response (1-5% stance). Following TKA, patients adopt an altered gait pattern whereby they rely on increased knee flexor muscle force for stability and posture as they walk downhill. No significant differences were found between limbs for MCF or LCF, suggesting that TKA may have been reasonably successful in correcting errant frontal plane alignment for these patients. Loading-response TCF impulse increased with increasing decline slope yet push-off TCF impulse decreased with increasing slope suggesting decreased knee joint loading during push off while not having to overcome the effects of gravity.

Introduction

Total knee arthroplasty is an increasingly common surgical procedure that has been shown to be effective at reducing pain and correcting frontal plane malalignment from end stage knee osteoarthritis (Andriacchi et al., 1999; Andriacchi et al., 2009). As surrogates for tibiofemoral joint loading, the internal knee extension moment (KEM) and internal knee abduction moment (KAbM) have been reported during various activities for both the replaced and non-replaced limbs of patients following TKA including level walking, stair ascent, and cycling (Hummer et al., 2021; Standifird et al., 2016; Wen et al., 2021). During level walking, the replaced limb of patients with TKA has shown reduced KEM and KAbM compared to the non-replaced limb, which suggests that although TKA may have been successful in correcting alignment, inter-limb joint loading asymmetries still exist.

Few studies have reported knee joint biomechanics of downhill walking of patients with TKA. Simon et al. (2018) compared knee joint kinematics and kinetics between posterior cruciate retaining and bi-cruciate retaining knee prostheses during level and downhill walking at a 12.5% slope. Though between-slope comparisons were not made statistically, sagittal plane range of motion (ROM) was qualitatively greater during downhill walking, while KEM and KAbM were all qualitatively lower during downhill walking. Reynolds et al. (2013), reported kinematics and kinetics of 17 patients with TKA and 17 control participants while walking down hill at 12.5°. They reported that the replaced limb demonstrated decreased knee joint ROM, decreased peak knee flexion angle, and peak loading-response KEM, compared to a control limb. They also reported that peak knee flexion peak KEM were lower in the replaced limb than the non-replaced limb. Wen et al. (2021) provided the most robust examination of knee joint

biomechanics in patients with TKA walking downhill at 0°, 5°, 10°, and 15°. At every decline slope, replaced limb peak KEM was lower than that of the control limb, but were not different than the non-replaced limb. They also reported a significant interaction between groups, suggesting that as decline increased, control limb KEM increased by a greater amount than both the replaced and non-replaced limbs.

Previous research has shown that joint loading variables such as KEM and KAbM have been highly correlated to and used in predictions of medial compartment tibiofemoral compressive force (MCF) in level walking (Walter et al., 2010). However, these variables alone do not directly indicate the magnitude or behavior of tibiofemoral compressive forces. Understanding the true behavior of knee compressive forces is necessary for researchers for better understanding of joint loading environment of the knee during a multitude of activities for TKA population. Obtaining *in vivo* tibiofemoral compressive forces requires the use of specialized knee joint prostheses instrumented with force transducers. Many studies have reported *in-vivo* tibiofemoral contact forces in a variety of gait, including level, stair ascent and descent walking, and various activities of daily living such as deep knee flexion and standing up from a chair (Bergmann et al., 2014; D'Lima et al., 2007; D'Lima et al., 2006; D'Lima et al., 2008; Heinlein et al., 2009; Kutzner et al., 2010; Kutzner et al., 2013; Mundermann et al., 2008; Zhao et al., 2007a). Peak TCFs have been reported to be over two body weight (BW) in level walking. In an early study, Zhao et al. (2007a) reported tibiofemoral contact forces of 2.2 BW, with 53.4% of TCF accounted for by the medial compartment compressive force (MCF). In another study, Heinlein et al. (2009) reported peak stance phase TCF to be 2.76 BW and 2.08 BW for the two participants of TKA. Since the first studies reported tibiofemoral compressive forces, several others have followed, utilizing different implant designs (Bergmann et al., 2014),

different footwear (Kutzner et al., 2013), and larger sample sizes (Bergmann et al., 2014; D'Lima et al., 2008), all reporting peak TCF during stance phase between 2.25 and 2.75 BW during level walking.

Computational musculoskeletal modeling and simulation provide a toolset that overcomes the limitations of using *in vivo* knee implants (Delp et al., 2007; Shu et al., 2020). Musculoskeletal simulations have been previously used in the estimation of muscle and knee joint compressive forces in patients with TKA in a variety of tasks including level walking, (Lerner et al., 2015; Piazza and Delp, 2001), stair ascent (Rasnick et al., 2016), and cycling (Hummer et al., 2021).

Despite of relatively rich literature on knee joint contract forces in other types of gait, the magnitude and behavior of knee joint compressive forces throughout the entirety of stance in response to changes in slope during downhill walking in people with TKA remains mostly unexplored. The purpose of this study was, therefore, to determine differences in tibiofemoral joint compressive forces (TCF, MCF, LCF) between the replaced, non-replaced, and control group limbs at different slopes ([0° (level), -5° and -10° (downhill)]. We also explored differences in TCF impulse and muscle forces between different limbs and slopes. It was hypothesized that tibiofemoral compressive forces, TCF impulse, and knee joint-spanning muscle forces during downhill walking would be greater in the control group, followed by the non-replaced limb of the TKA group, and lowest in the replaced limb of the TKA group, at each slope. We also hypothesized an interaction between limbs and decline slopes would be present for tibiofemoral compressive forces and muscle forces.

Methods

Participants

Nine patients with TKA (5 male and 4 female,67.5 ± 5.5 years, 1.74 ± 0.10 m, 84.3 ± 15.6 kg, 27.8 ± 3.2 months since surgery) were recruited from a local orthopedic clinic (Table 1). All nine patients had received cruciate retaining knee joint prosthesis from a primary TKA. Inclusion/exclusion criteria, and full data collection methods have been previously reported (Wen et al., 2019). In short, potential patients were excluded if they had any additional lower extremity joint replacement, any diagnosed osteoarthritis of the hip or ankle, or more than 75% radiographic joint space narrowing and chronic pain of the contralateral, non-replaced knee, BMI greater than 38 kg/m^2, or any neurological diseases. Furthermore, healthy participants for an age-matched control group (5 male 4 female, 69.5 ± 4.3 years, 1.77 ± 0.12 m, 76.5 ± 25.4 kg) were recruited from the local community. Exclusion criteria for the control group participants included any self-reported knee pain during typical every-day activities, any diagnosis or osteoarthritis, any lower limb joint arthroplasty, arthroscopic surgery, or inter-articular injection.

Experimental Protocol

The details of experimental protocol and equipment are described elsewhere and a brief account is provided here (Wen et al., 2021). All participants performed five successful trials of walking at three different decline slopes: 0° (level), 5°, and 10°. Participants walked down on a customized adjustable instrumented ramp system. Walking conditions were performed in a randomized fashion, with decline angle randomized first, followed by leading limb. A successful trial required that the participant cleanly strike the first force platform in the ramp system with the designated leading foot.

Instrumentation

Kinematic data were obtained by placing the instrumented ramp within a motion capture volume (240 Hz, Vicon Motional Analysis Inc., Oxford, UK). Ground reaction force data (GRF) were collected from two force platforms embedded in the ground and secured to the ramp system (1200 Hz, BP600600 and OR-6-7, American Mechanical Technology Inc. Watertown, MA, USA). Electromyography (EMG) were recorded bilaterally from five lower extremity muscles: vastus lateralis, vastus medialis, biceps femoris, semitendinosus, and the medial head of the gastrocnemius (1200 Hz, Trigno™ Wireless EMG System, Delsys, INC, Natick MA, USA). The skin of the electrode attachment sites was shaved and cleaned with alcohol swab before the application of the electrodes. The placement of the EMG electrodes on the selected muscles were based on the recommendations of SENIAM (Surface ElectroMyoGraphy for the Non-Invasive Assessment of Muscles) (Hermens et al., 2000). Both GRF and EMG data were sampled simultaneously with the 3D kinematic data using the VICON system and Nexus software package (2.5, Vicon Motion Analysis Inc., Oxford, UK).

Data Analysis

The EMG data were analyzed using the Visual3D. Raw EMG signals were processed with a band-pass filter at cutoff frequencies of 10 Hz and 450 Hz. They were then full wave rectified and a moving root-mean-square (RMS) filter was used to filter the rectified EMG signals using a 60-millisecond moving window. The maximum value of the RMS EMG signals of three functional test trials was used to normalize the filtered EMG signals of the testing movement trials.

Musculoskeletal Modeling and Simulation

An open-source musculoskeletal model [18 segments, 23 degrees-of-freedom, 92 muscle-tendon actuators] was used to perform the simulations (Lerner et al., 2015). The knee joint of this model consists of 1 DOF (flexion/extension) and was supplemented with added medial and lateral compartments. The model was first scaled to each participant's height and mass and the subtalar and metatarsal-phalangeal joints were locked for the analysis.

Generalized joint coordinates derived from inverse kinematics calculations were exported from Visual3D (Version 6, C-Motion, Inc., Germantown, MD, USA) and imported into OpenSim for simulations (3.3 OpenSim, SimTK, Stanford University). The generalized joint coordinates were applied to each subject-specific scaled musculoskeletal model. Inverse dynamics calculations were performed in OpenSim to compute lower extremity joint moments. Next, muscle activations and forces during level and up- and downhill walking were calculated using static optimization (Steele et al., 2012). The static optimization calculations included muscle mechanics (force-length-velocity relationships) and an objective function to minimize the sum of squared muscle activations (Crowninshield and Brand, 1981). Maximum reserve torque actuator values for all lower extremity joints were checked and found to be within suggested guidelines (Hicks et al., 2015). Joint compressive forces (MCF, LCF, TCF) were calculated using joint reaction analysis in OpenSim and expressed in the tibia reference frame (Steele et al., 2012).

Primary variables of interest included TCF, MCF, and LCF. Secondary variables of interest included TCF impulse, demarcated as total TCF impulse (over the entire stance phase), loading-response TCF impulse (the first 50% of stance), and push-off impulse (the last 50% stance). TCF impulse was found with numerical integration of the TCF curves of the respective

phases of stance by means of the trapezoidal method with unit spacing. Muscle forces of the knee extensor and knee flexor muscle groups were also included as secondary variables. The knee extensors group was defined by the rectus femoris, vastus lateralis, vastus intermedius, and vastus medialis. The knee flexor muscle group was defined with the biceps femoris long and short heads, semimembranosus, semitendinosus, sartorius, gracilis, and both medial and lateral head of the gastrocnemius. The left or right limbs of healthy controls were randomly selected for use in the control group for comparisons with the replaced and non-replaced limbs of TKR patients.

Statistical Analysis

To assess differences between joint compressive forces and muscle forces between groups, one-dimensional statistical parametric mapping using Random Field Theory to correct for Type I error inflation (Pataky et al., 2013, 2016a) was implemented using MATLAB R2019B (MATLAB, MathWorks, Natick, MA, USA) with the open source code made available by Pataky et al. (2016a). The data were first checked for normality using D'Agostino-Pearson K^2 test (D'agostino et al., 1990).

To assess differences between limb and slope, a 3×3 [Limb (replaced, non-replaced, control] × Slope (0°, 10°, 15°)] SPM{F} repeated measures ANOVA was conducted on selected variables. An α level was set at 0.05 a priori. Limb, Slope main effects and their interaction were deemed significant when the SPM{F} trajectory crossed the critical threshold (Pataky et al., 2013). If a significant Limb × Slope interaction, limb, or slope main effect was found, *post hoc* SPM{t} tests were conducted on each pairwise comparison. Effect size for all significant *post-hoc* comparisons were computed from the mean difference between the two waveforms throughout the duration of a supra-threshold cluster and were reported using Cohen's d (Cohen,

2013; Schroeder et al., 2021).

A 3×3 [Limb (replaced, non-replaced, control) × Slope (0°, 10°, 15°)] mixed model ANOVA was used to detect differences between limb and group conditions and their interaction for TCF impulse (25.0 IBM SPSS, Armonk, NY, USA). An α level of 0.05 was set a priori. If an interaction was present, pairwise *t*-tests were performed in the *post hoc* analysis with Bonferroni adjustments to determine the location of the statistical differences between slope and limb. The alpha level adjusted for post hoc comparisons for interaction were adjusted to be such that the interaction $\alpha < 0.006$ (0.05/9 comparisons), main effect $\alpha < 0.017$ (0.05/3 comparisons). Effect size for all significant main effects and interactions were reported using partial eta squared (η^2_p) effect size defined as small >0.02, medium >0.13, and large >0.26 (Cohen, 2013).

Results

There were no differences of age, height, mass, or BMI between patients with TKA and control participants (Appendix B – Chapter V Tables and Figures). Frontal-plane lower limb alignment between the replaced limb, non-replaced limb, and control limb were also similar (Table 1). Magnitudes of reserve torque actuator moments for all lower extremity joints were checked and found to be within suggested levels (Appendix G) (Hicks et al., 2015). The model predicted muscle activations (biceps femoris long head, semitendinosus, vastus medialis, vastus lateralis, and medial head of the gastrocnemius) generally agreed with our experimentally collected EMG activation profiles (Figure 7).

The SPM{F} test for TCF revealed a significant main effect of limb ($p < 0.036$, Figure **8**A). *Post-hoc* SPM{t} analysis found the replaced limb experienced lower TCF during the first 4% of stance ($t_{critical} = 3.13$, Table 4, Figure 8C). There was also a main effect of slope ($p = 0.42$, Figure 8A). Between slopes, one significantly different region was found between level and 5°

downhill walking ($t_{critical}$ = 3.40, Table **4** 4, Figure 8E) indicating TCF during 5° uphill walking was greater during loading-response (27-35%) than level walking. Two significant regions were found between level and 10° ($t_{critical}$ = 3.29, Table 4, Figure 8F), as TCF in 10° was greater than level walking during loading response (15-36% stance) and during push-off (90-100% stance). Finally, two significant regions were found between 5° and 10° ($t_{critical}$ = 3.30, Table 4, Figure 8G), as TCF in 10° was greater than 5° walking during loading response (13-32% stance) and during push-off (88-95% stance).

For SPM{F} test of MCF, both main effect of slope ($p < 0.001$, Figure 9A) and limb ($p = 0.030$, Figure 9A) were found significant. *Post-hoc* SPM{t} analysis revealed one significant region between the replaced limb and the control limb ($t_{critical}$ = 3.13, Table 4, Figure **9**C), showing greater MCF experienced by the control limb over the first 5% of stance. Between level and 10° uphill walking, greater MCF was experienced during 10° between 18-29%, however, greater MCF was experienced during level walking during 55-73% stance ($t_{critical}$= 3.30, Table 4, Figure 9). There were no significant interactions or main effects observed for LCF (Figure 10).

For the knee extensor muscle force, a significant main effect of slope ($p < 0.001$, Figure **11**A) was found with the SPM{F} test. *Post-hoc* tests showed that the knee extensor muscle group generated more force during push-off in level walking than during 5° uphill walking (34-99% stance, $t_{critical}$ = 3.34, Table **4** 4, Figure 11B). Significantly different knee extensor muscle forces were seen for 10° compared to both level (16-100% stance, $t_{critical}$ = 3.38, Table 4, Figure 11C) and 5° (13-97% stance, $t_{critical}$ = 3.27, Table 4, Figure 11D) conditions. Interestingly, push-off phase knee extensor muscle force was greater during level walking than during 5° or 10° uphill walking conditions (Figure 11B-D). It appears that during the first 50% of stance, knee

extensor muscle force increases with slope. During the last 50% of stance however, knee extensor muscle force is lowest in 10°, followed by 5° and level.

For the knee flexor muscle force, a significant main effect of limb ($p < 0.001$, Figure **12**A) was found with the SPM{F} test. *Post-hoc* tests showed that the knee flexor muscle group forces were greater for the control limb during the first 4% of stance ($t_{critical} = 3.10$, Table 4, Figure 12C).

For TCF impulse, there was a main effect of slope in loading-response ($p=0.002$), and push-off ($p < 0.001$, Table 5). *Post-hoc* tests indicated that loading-response TCF during loading-response and push-off was greater during 10° than level ($p \leq 0.001$) and 5° ($p \leq 0.017$). *Post-hoc* tests also indicated that loading-response TCF during push-off was greater during 10° than level ($p \leq 0.001$).

Discussion

The purpose of this study was, therefore, to determine differences in tibiofemoral joint compressive forces (TCF, MCF, LCF) between the replaced, non-replaced, and control group limbs at different downhill slopes [0° (level), 5°, and 10°]. We also explored differences in TCF impulse and muscle forces between different limbs and slopes. Our first hypothesis, that TCF, MCF, LCF, muscle forces would be greater in the control limb, followed by the non-replaced limb, and lowest in the replaced limb, at each slope during the entirety of stance, was partially supported.

There were significant differences in TCF, MCF, and knee flexor muscle forces between the replaced and control limbs. These compressive and muscle forces were greater for the replaced limb, all during early loading-response (1-5% stance). This may suggest that following TKA, patients adopt an altered gait pattern whereby they rely on increased knee flexor muscle

force for stability and posture during initial heel-strike as they walk downhill. Both Wen et al. (2021) and Reynolds et al. (2013) reported decreased peak KEM for the replaced limb compared to the control limb. Peak loading-response KEM has been shown to occur around 25% of stance (Wen et al., 2021), similar to TCF (Figure 8). However, SPM analysis revealed significant differences much earlier in stance. Our results showed not difference between limbs near peak loading-response TCF. Focusing part of post-operative rehabilitation on muscular control of the replaced limb, especially right near heel strike, through lower extremity strengthening, may improve ramp negotiation in patients following TKA.

The lack of significant differences of peak TCF between limbs in this current study merits attention. As previously mentioned, using inverse-dynamics based approaches, both Wen et al. (2021) and Reynolds et al. (2013) reported decreased peak KEM for the replaced limb compared to both the non-replaced limb and the control limb. With the inherent difficulties obtaining *in vivo* TCF, KEM has often been used to represent overall knee joint loading (Astephen et al., 2008; Benedetti et al., 2003; Kuster et al., 1997; McClelland et al., 2014; Ngai and Wimmer, 2015; Ro et al., 2018). Numerous studies in addition to those previously mentioned have shown that KEM is reduced in the replaced limb compared to the non-replaced limb in patients with TKA in a variety of tasks including ramp ascent (Wen et al., 2019), stair ascent (Standifird et al., 2016), and cycling (Hummer et al., 2021). Though there were no statistically significant regions between limbs for TCF outside of the first 5% of stance, Figure **8**C-D suggests a trend of increased TCF for the control limb relative to the replaced and non-replaced limbs. With a greater sample size, between-limb differences for TCF may have a chance to reach the threshold for significance in the region around peak TCF.

The primary goals of TKA are to alleviate knee pain and restore the loss of knee joint function for patients with knee osteoarthritis (Andriacchi et al., 1999; Andriacchi et al., 2009). Increased medial compartment loading has been identified as a contributor to joint degradation prior to primary TKA (Schipplein and Andriacchi, 1991). Degradation of medial compartment articular cartilage can alter the mechanical alignment of the knee joint through joint-space narrowing (Andriacchi et al., 2009). As such, a secondary goal of TKA is to restore neutral knee joint alignment. In this study, there were no significant regions between limbs for MCF and LCF near the loading-response or push-off peak compressive forces. Additionally, frontal plane alignment of the replaced limb, non-replaced limb, and control limb of this study were similar (Table 1). Wen et al. (2021) also reported no differences of KAbM between replaced, non-replaced and control limbs during level and downhill walking. Collectively, this evidence may suggest that the TKA procedures may have been reasonably successful in correcting errant frontal plane alignment , manifest through the similar medial compartment loading between limbs.

Our second hypothesis, that there would be an interaction between limbs and slopes for tibiofemoral compressive forces and muscle forces was not supported as no significant interactions were found for any variables. The most predominant statistical significance observed from this current study was the effect of slope on TCF and muscle forces. At every comparison of slope, TCF and its accompanying knee extensor muscle force demonstrated significant increases. Greater changes with regard to increased decline slope were observed during loading-response as TCF was greater in 5° downhill walking compared to level walking between 27-35% of stance and TCF was greater in 10° downhill walking compared to level walking between 15-35% stance and 5° between 12-32% stance. The SPM results are also supported by the changes

in the TCF impulse during loading-response. However, the TCF changes during push-off are smaller in magnitude and in opposite directions (Figure 8A, E-F).

During push-off, no significant differences were observed for TCF between any slopes. These results are not consistent with push-off peak KEM results reported by Wen et al. (2021), which showed significant increases in KEM with increased slope from level to 15°. Furthermore, Wen et al. (2021) reported decreased or constant peak vertical GRF with increasing downhill slope. Since the GRF was reported in the global reference system, the magnitude of the vertical component of GRF is reduced by the increased slope. Consequentially, although unreported by Wen et al. (2021), it is likely that the anteroposterior (AP) component of GRF increased with increased slope, thus potentially increasing the magnitude of the resultant force vector and moving the orientation of the GRF vector further posterior to the knee joint center and therefore increasing KEM. In the context of this current study, small knee flexor and knee extensor muscle forces during push-off as well as diminished vertical GRF do not contribute substantially to any changes in TCF between slopes. Although we did not examine tibiofemoral shear force, it is likely that significant increases would be observed with increasing slope, similar to anteroposterior GRF. Additionally, these changes may be consequential from the lowering of the center of mass as the decline slope is negotiated while not having to overcome the effects of gravity to the same extent as level or uphill walking. During push-off, the effects of gravity does not need to be overcome, rather, just enough muscle force needs to be produced to maintain a controlled descent. Thus, loading response TCF increases as decline slope increases, but push off TCF which is a product of diminished vertical GRF and muscle forces but increased anteroposterior GRF, remains similar. These differing trends may also help explain why no slope main effect was observed for total stance phase TCF impulse. As decline slope increased,

loading-response impulse increased as well. This suggest that greater loading is experienced during the first 50% of stance as decline slope is increased, which is also observed in the trends of TCF (Figure 8). During push-off, however, TCF impulse decreased between level and 5°, but then increased again between 5° and 10°. Thus, these conflicting trends between loading-response and push-off TCF impulse, also demonstrated by the trends of TCF in Figure 8, may diminish significant differences of total stance phase TCF impulse.

Wen et al. (2021) recommended against the implementation of downhill walking in the early stages rehabilitation procedures following TKA. These recommendations suggest that increased KEM with increasing decline slope may propagate increased compressive forces on the prosthesis (D'Lima et al., 2001; D'Lima et al., 2012). Following TKA, deficits of quadriceps strength are manifest from immediately following surgery to several years post TKA (Huang et al., 1996; Mizner et al., 2005). High-intensity rehabilitation protocols have led to improved function and outcomes after TKA procedures (Bade and Stevens-Lapsley, 2011; Bade et al., 2017). As part of both high and low intensity rehabilitation programs, quadriceps strengthening exercises have been suggested for clinicians to incorporate into their rehabilitation plans to improve muscle strength and reduce asymmetries between replaced and non-replaced limbs (Bade et al., 2017). Though these exercises may improve muscle strength and post-operative functional outcomes, quadriceps strengthening has been shown to have no effect on KEM or KAbM in patients with knee osteoarthritis (DeVita et al., 2018; Foroughi et al., 2011). Our simulation results seem to support downhill walking as an effective exercise for high intensity early and long-term rehabilitation. Downhill walking facilitates increased muscular demand and quadriceps strengthening via eccentric contractions with increased slope while regaining normal gait patterns following TKA, which may not be readily transferable from traditional quadriceps

strengthening exercises. During the early stages of rehabilitation, gradually increasing the decline slope may provide an effective modality whereby quadriceps muscles can be strengthened during a gait-specific task.

Results of this study need to be considered in the context of notable limitations. First, SPM analysis requires that all waveforms are time-normalized to 101 data points. Thus, inverse kinematic and static optimization algorithms were executed on 'raw' kinematic and kinetic data which were "sampled" at 240 Hz. It has been shown that the stance phase of gait lasts for approximately 60% of the gait cycle (Sutherland et al., 1980). Patients in this current study were reported to walk with an average velocity of about 1.08 m/s. During level walking trials, participants were in contact with the ground, on average, for 0.66 seconds. With the given sampling rate, the average stance phase included 50% more data points (156 frames of data) than the 101 points used in SPM. With such reductions in resolution, it is possible that true peak values may be reduced (or smoothed out) as a result of the time normalization which may also contribute to the lack of difference of TCF between limbs.

This study used a small sample size of 9 replaced, non-replaced, and control limbs. These data were specifically identified as a subset of participants from previously examined data (Wen et al., 2021) in order to fulfill the requirement of equal group sizes for SPM analysis. Though these data did not violate the assumptions of normality (D'agostino et al., 1990; Pataky et al., 2015), these data did contain relatively large variability. The SPM requirement of equal observations in each group dictated that we analyze one sub-set of the three different implant styles from Wen et al. (2019). Due to due to tracking errors of trunk, one control participant was excluded from simulation and analysis, and therefore one patient from the TKA group was excluded as well so that all groups had 9 participants.

Finally, in predicting MCF from *in vivo* TCF, Lerner et al. (2015) tested the predictive strength of the knee model with varying parameters including participant-specific contact locations between the femur and the tibia, as well as the inclusion of frontal plane alignment in the model. Participant-specific condylar contact locations for these data of the current study were unknown. We estimated lower limb alignment using the mechanical axis angle from motion capture data of static trial (Bennett et al., 2018; Vanwanseele et al., 2009). There was no difference for mechanical axis angle between the replaced, non-replaced, and control limbs (Table 1). With the similarities between frontal plane alignment between the participants of this study, we feel confident that differences that may arise from implementing participant-specific frontal plane lower limb alignment were minimized.

In conclusion, during downhill walking the replaced limb appears to experience greater TCF and MCF during the first 5% of stance, that likely is a product of increased knee flexor force at heel strike. Joint loading appears to be similar for the majority of stance between replaced, non-replaced, and control limbs. Significant differences of TCF were observed between 12-35% of stance during 10° compared to level and 5°. Smaller differences in TCF were found between 27-35% stance.

Appendix B – Chapter V Tables and Figures

Table 4. SPM summary during downhill walking. Significant supra-threshold cluster ranges (% stance), supra-threshold cluster p-values, mean difference between conditions within each cluster (BW) and Cohen's d effect size c for knee compressive forces and knee extensor muscle force.

		Region	p	Mean Difference	Cohen's d
TCF	Replaced vs. Control limb	1-5%	0.036	0.42	1.77
	Level vs. 5°	27-35%	0.003	0.25	1.26
	Level vs. 10°	15-36%	< 0.001	0.55	3.24
		90-100%	0.004	0.46	6.87
	5° vs. 10°	12-32%	< 0.001	0.53	4.76
MCF	Replaced vs. Control limb	1-5%	0.034	0.28	1.17
	Level vs. 10°	18-29%	0.002	0.26	1.22
		55-73%	< 0.001	0.32	1.47
Knee Extensor Muscle Force	Level vs. 5°	34-99%	< 0.001	0.34	4.71
	Level vs. 10°	16-100%	< 0.001	0.29	3.30
	5° vs. 10°	13-97%	< 0.001	0.28	3.21
Knee Flexor Muscle Force	Replaced vs. Control limb	1-4%	0.048	0.03	0.79

Table 5. TCF impulse during downhill walking. Total, loading-response, and push-off phase TCF impulse (BW·s, mean ± standard deviation) during level, 5° uphill, and 10° uphill walking conditions. Bold values indicate statistical significance.

Variable	Limb	Level Walking	5° Downhill	10° Downhill	Slope (η^2_p)	Limb (η^2_p)	Interaction (η^2_p)
Stance Impulse	Replaced	0.84 ± 0.64	0.87 ± 0.66	1.05 ±0.86	0.072 (0.205)	0.960 (0.003)	0.626 (0.054)
	Non-Replaced	0.99 ± 0.82	0.92 ± 0.62	1.10 ± 0.85			
	Control	0.85 ± 0.64	0.92 ± 0.61	1.00 ± 0.77			
Loading-Response*# Impulse	Replaced	0.29 ± 0.32	0.40 ± 0.29	0.54 ± 0.32	**0.002** (0.407)	0.928 (0.010)	0.787 (0.036)
	Non-Replaced	0.39 ± 0.46	0.50 ± 0.23	0.54 ± 0.26			
	Control	0.29 ± 0.32	0.47 ± 0.25	0.55 ± 0.25			
Push-off # Impulse	Replaced	0.55 ± 0.33	0.47 ± 0.39	0.51 ± 0.57	**<0.001** (0.496)	0.981 (0.002)	0.368 (0.087)
	Non-Replaced	0.60 ± 0.42	0.43 ± 0.41	0.56 ± 0.62			
	Control	0.57 ± 0.33	0.45 ± 0.41	0.44 ± 0.48			

[#] Different from level walking
[*] Different from 5°
[α] Different from non-replaced limb at the same slope

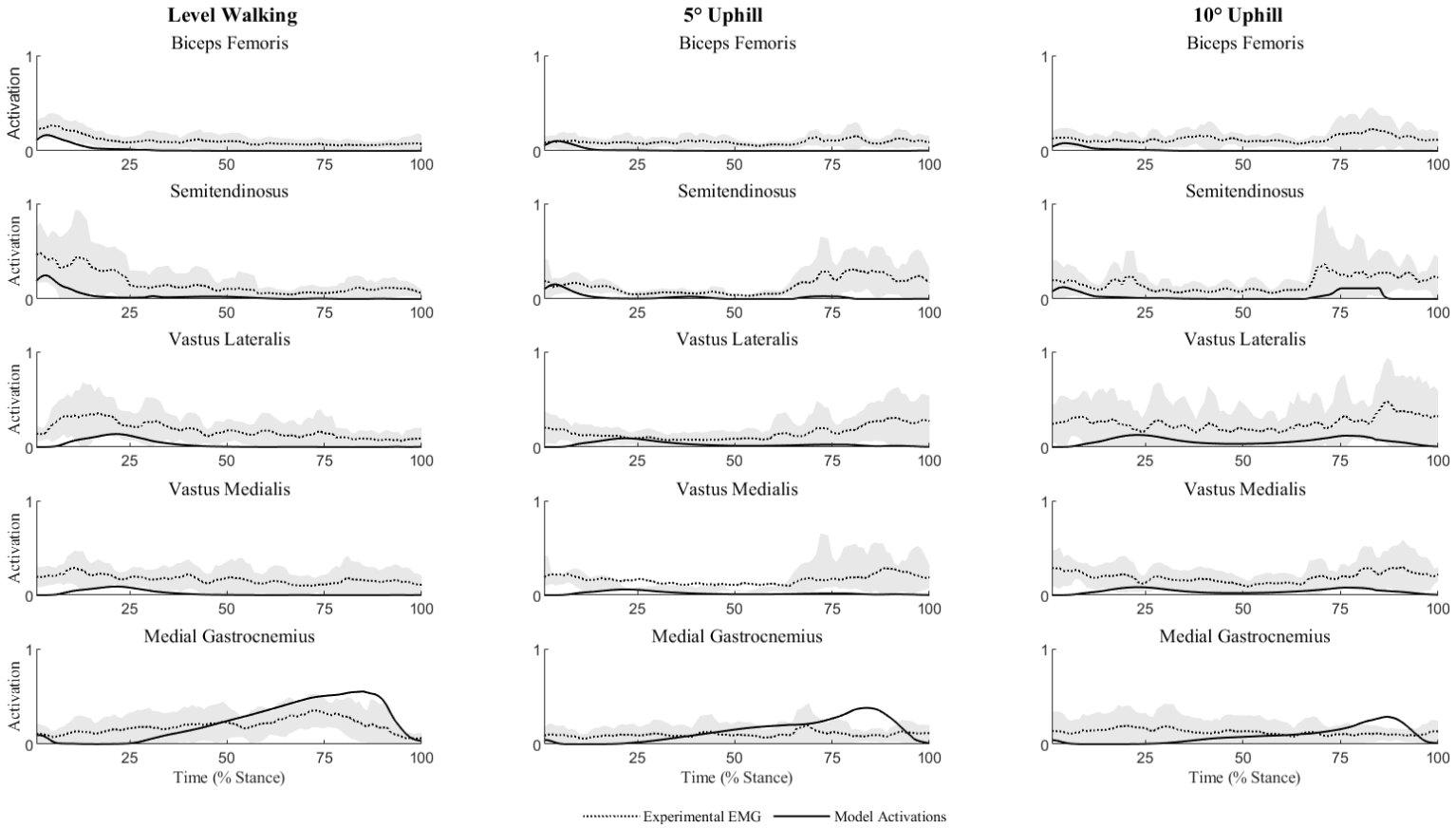

Figure 7. Muscle activations of the replaced limb during downhill walking.The solid line represents the mean activation level obtained from static optimization while the dashed line represents the mean activation level obtained from EMG with the shaded region representing ± 1 standard deviation of EMG activation.

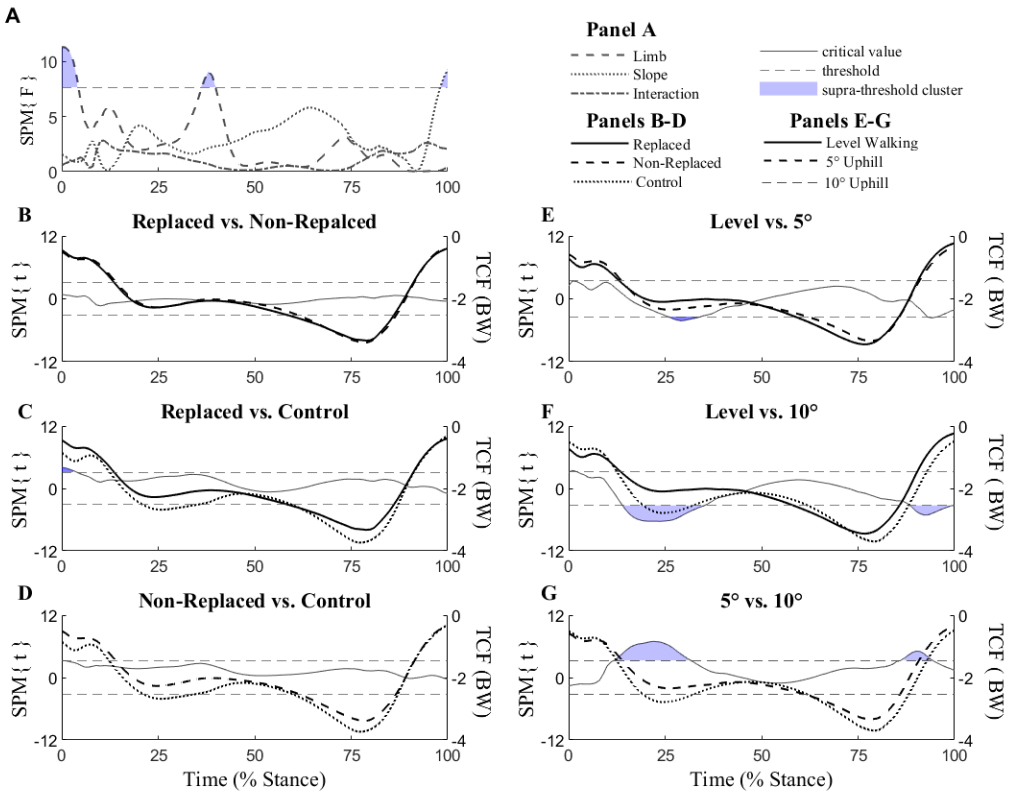

Figure 8. SPM results for TCF during downhill walking.**A)** SPM{F} test results for TCF. **B-G)** *Post-hoc* SPM{t} test results plotted on the left y-axis. Shaded regions indicate the ranges the *t*-critical value time series crossed above or below the critical threshold (i.e., supra-threshold cluster). Mean time series waveforms for *post-hoc* TCF comparisons are also plotted on the same graph against the right y-axis. With *post-hoc* SPM{t} and TCF overlaid together, significantly different ranges of TCF can more easily be determined between comparisons.

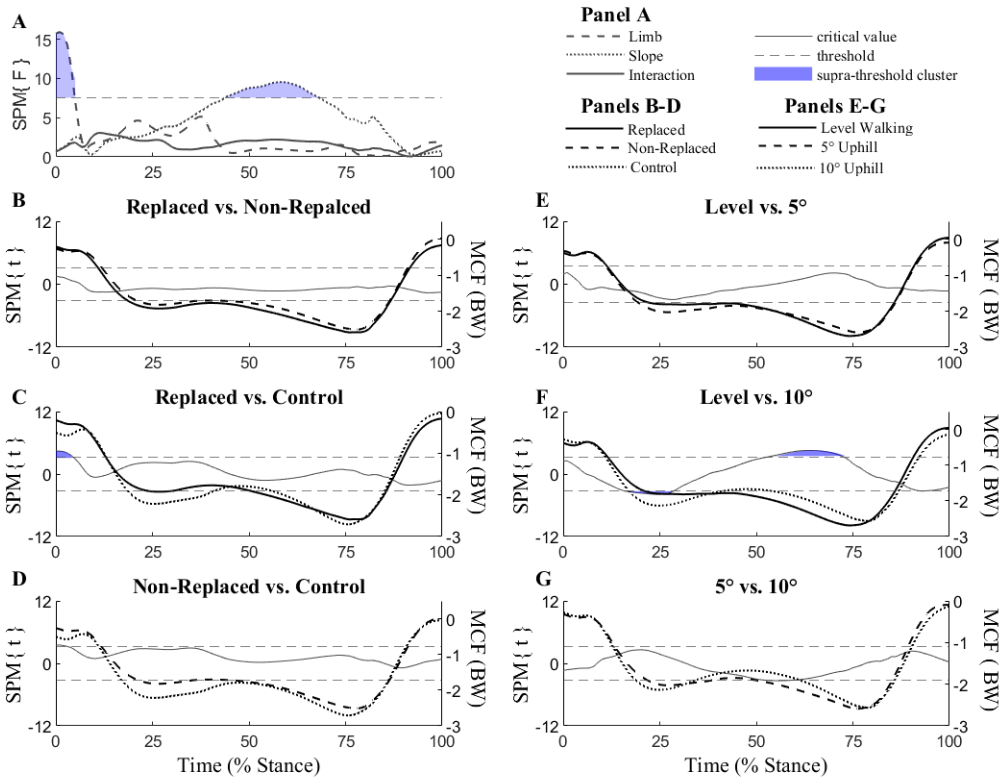

Figure 9. SPM results for MCF during downhill walking. **A)** SPM{F} test results for MCF. **B-G)** *Post-hoc* SPM{t} test results plotted on the left y-axis. Shaded regions indicate the ranges the *t*-critical value time series crossed above or below the critical threshold (i.e., supra-threshold cluster). Mean time series waveforms for *post-hoc* MCF comparisons are also plotted on the same graph against the right y-axis. With *post-hoc* SPM{t} and TCF overlaid together, significantly different ranges of TCF can more easily be determined between comparisons.

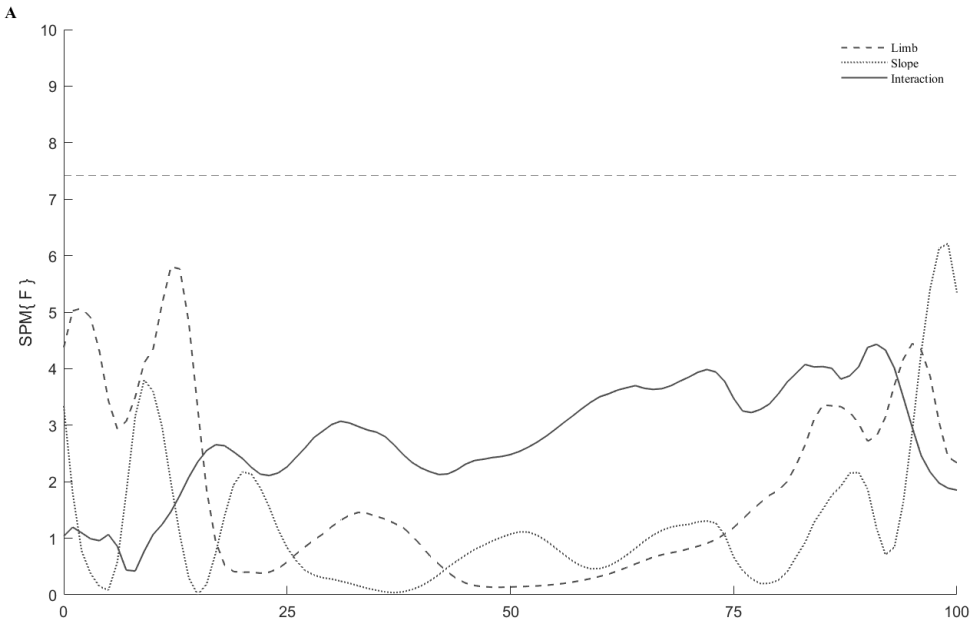

Figure 10. SPM results for LCF during downhill walking. Dotted horizontal line represents SPM{F} critical threshold value.

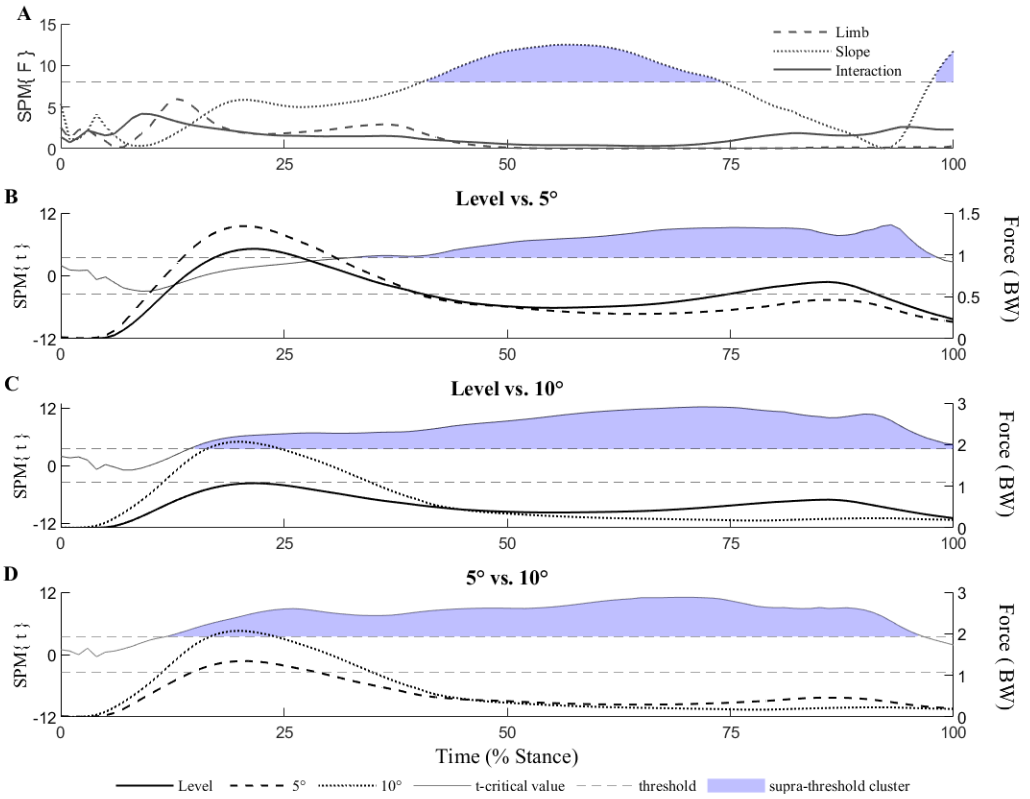

Figure 11. SPM results for knee extensor muscle force during downhill walking. **A)** SPM{F} test results for knee extensor muscle force. **B-D)** *Post-hoc* SPM{t} test results plotted on the left y-axis. Shaded regions indicate the ranges the *t*-critical value time series crossed above or below the critical threshold (i.e., supra-threshold cluster). Mean time series waveforms for *post-hoc* knee extensor muscle force comparisons are also plotted on the same graph against the right y-axis. With *post-hoc* SPM{t} and knee extensor muscle force overlaid together, significantly different ranges of knee extensor muscle force can more easily be determined between comparisons.

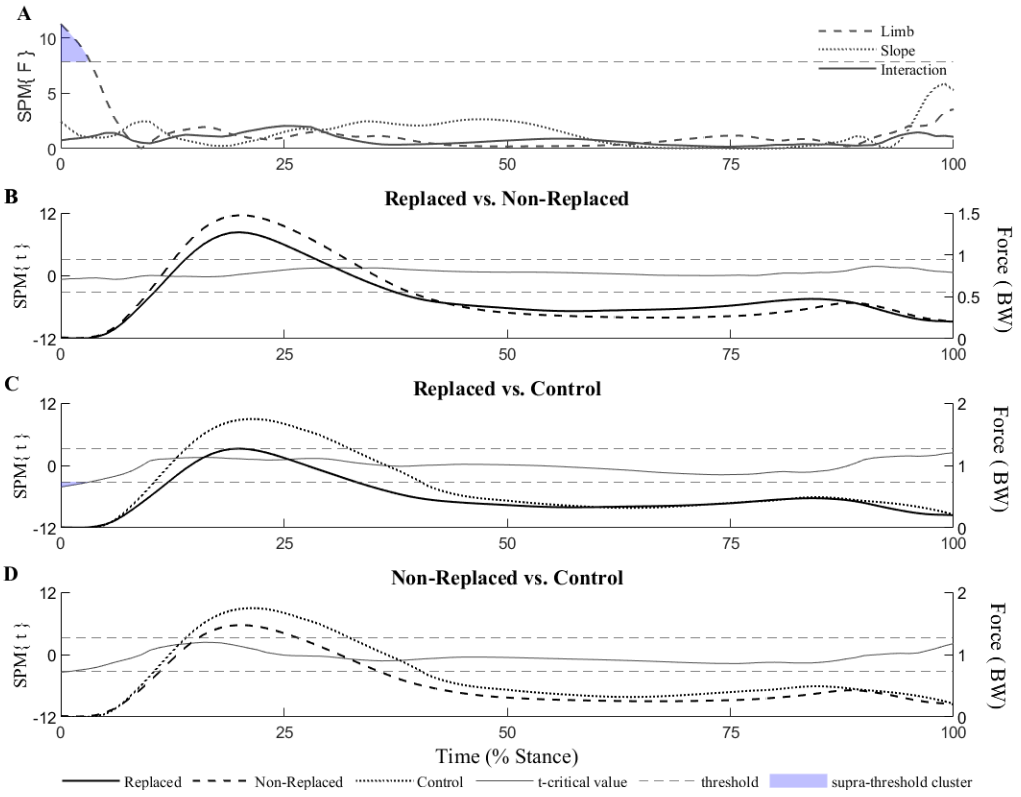

Figure 12. SPM results for knee flexor muscle forces during downhill walking. **A)** SPM{F} test results for knee flexor muscle force. **B-D)** *Post-hoc* SPM{t} test results plotted on the left y-axis. Shaded regions indicate the ranges the *t*-critical value time series crossed above or below the critical threshold (i.e., supra-threshold cluster). Mean time series waveforms for *post-hoc* knee flexor muscle force comparisons are also plotted on the same graph against the right y-axis. With *post-hoc* SPM{t} and knee flexor muscle force overlaid together, significantly different ranges of knee extensor muscle force can more easily be determined between comparisons.

CHAPTER VI

CONCLUSION

The purposes of these studies were to determine differences in total (TCF), medial compartment (MCF) and lateral compartment (LCF) and related muscle forces between different limbs and between slopes during uphill and downhill walking.

Chapter 4 showed significant between-limb differences for MCF during 23-30% stance between the replaced and control limbs. Significant differences between slopes were observed for all variables, except knee flexor muscle force. TCF impulse also indicates that the cumulative joint load is greater for all limbs as slope increases. A small sample size with high variability between patients with TKA who utilize different gait strategies may have rendered difference between limbs insignificant. Uphill walking may be an effective exercise for high intensity early and long-term rehabilitation programs, with lower peak GRF than stair ambulation. Additionally, uphill walking facilitates increased muscular demand and quadriceps strengthening with increased slope while promoting the reacquisition of normal gait patterns following TKA, which may not be achieved in traditional quadriceps strengthening exercises.

Chapter 5 showed significant differences were found for TCF, MCF, and knee flexor muscle forces between the replaced and control limbs during early loading-response (1-5% stance). Following TKA, patients adopt an altered gait pattern whereby they rely on increased knee flexor muscle force for stability and posture as they walk downhill. No significant differences were found between limbs for MCF or LCF,

suggesting that TKA may have been reasonably successful in correcting errant frontal plane alignment for these patients. Loading-response TCF impulse increased with increasing decline slope yet push-off TCF impulse decreased with increasing decline slope suggesting decreased knee joint loading during push-off while not having to overcome the effects of gravity. Our simulation results seem to support downhill walking as an effective exercise for high intensity early and long-term rehabilitation. Downhill walking facilitates increased muscular demand and quadriceps strengthening via eccentric contractions with increased slope while regaining normal gait patterns following TKA, which may not be readily transferable from traditional quadriceps strengthening exercises. During the early stages of rehabilitation, gradually increasing the decline slope may provide an effective modality whereby quadriceps muscles can be strengthened during a gait-specific task.

REFERENCES

Adler, R.J., Taylor, J.E., 2009. Random fields and geometry. Springer Science & Business Media.

Alexander, N., Schwameder, H., 2016. Effect of sloped walking on lower limb muscle forces. Gait Posture 47, 62-67.10.1016/j.gaitpost.2016.03.022

Aljehani, M., Madara, K., Snyder-Mackler, L., Christiansen, C., Zeni Jr, J.A., 2019. The contralateral knee may not be a valid control for biomechanical outcomes after unilateral total knee arthroplasty. Gait & posture 70, 179-184

Alnahdi, A.H., Zeni, J.A., Snyder-Mackler, L., 2011. Gait after unilateral total knee arthroplasty: frontal plane analysis. Journal of orthopaedic research : official publication of the Orthopaedic Research Society 29, 647-652.10.1002/jor.21323

Anderson, F.C., Pandy, M.G., 2001. Static and dynamic optimization solutions for gait are practically equivalent. J Biomech 34, 153-161.10.1016/s0021-9290(00)00155-x

Andriacchi, T., Alexander, E., Goodman, S., Year Understanding the role of functional adaptations in patients with total knee replacements. In International conference on knee replacement.

Andriacchi, T.P., Koo, S., Scanlan, S.F., 2009. Gait mechanics influence healthy cartilage morphology and osteoarthritis of the knee. The Journal of bone and joint surgery. American volume 91 Suppl 1, 95-101.10.2106/JBJS.H.01408

Astephen, J.L., Deluzio, K.J., Caldwell, G.E., Dunbar, M.J., 2008. Biomechanical changes at the hip, knee, and ankle joints during gait are associated with knee osteoarthritis severity. Journal of orthopaedic research : official publication of the Orthopaedic Research Society 26, 332-341.10.1002/jor.20496

Bade, M.J., Stevens-Lapsley, J.E., 2011. Early high-intensity rehabilitation following total knee arthroplasty improves outcomes. The Journal of orthopaedic and sports physical therapy 41, 932-941.10.2519/jospt.2011.3734

Bade, M.J., Struessel, T., Dayton, M., Foran, J., Kim, R.H., Miner, T., Wolfe, P., Kohrt, W.M., Dennis, D., Stevens-Lapsley, J.E., 2017. Early High-Intensity Versus Low-Intensity Rehabilitation After Total Knee Arthroplasty: A Randomized Controlled Trial. Arthritis care & research 69, 1360-1368.10.1002/acr.23139

Benedetti, M.G., Catani, F., Bilotta, T.W., Marcacci, M., Mariani, E., Giannini, S., 2003. Muscle activation pattern and gait biomechanics after total knee replacement. Clin Biomech (Bristol, Avon) 18, 871-876.10.1016/s0268-0033(03)00146-3

Bennett, H.J., Shen, G., Weinhandl, J.T., Zhang, S., 2016. Validation of the greater trochanter method with radiographic measurements of frontal plane hip joint centers and knee mechanical axis angles and two other hip joint center methods. J Biomech 49, 3047-3051.10.1016/j.jbiomech.2016.06.013

Bennett, H.J., Valenzuela, K.A., Lynn, S.K., Weinhandl, J.T., 2021. Foot Rotation Gait Modifications Affect Hip and Ankle, But Not Knee, Stance Phase Joint Reaction Forces During Running. Journal of Biomechanical Engineering 143, 021001

Bennett, H.J., Weinhandl, J.T., Fleenor, K., Zhang, S., 2018. Frontal Plane Tibiofemoral Alignment is Strongly Related to Compartmental Knee Joint Contact Forces and Muscle Control Strategies during Stair Ascent. J Biomech Eng 140, 061011.10.1115/1.4039578

Bergmann, G., Bender, A., Graichen, F., Dymke, J., Rohlmann, A., Trepczynski, A., Heller, M.O., Kutzner, I., 2014. Standardized loads acting in knee implants. PLoS One 9, e86035.10.1371/journal.pone.0086035

Boutron, I., Poiraudeau, S., Ravaud, J.F., Baron, G., Revel, M., Nizard, R., Dougados, M., Ravaud, P., 2003. Disability in adults with hip and knee arthroplasty: a French national community based survey. Annals of the rheumatic diseases 62, 748-754.10.1136/ard.62.8.748

Brandon, S.C., Graham, R.B., Almosnino, S., Sadler, E.M., Stevenson, J.M., Deluzio, K.J., 2013. Interpreting principal components in biomechanics: representative extremes and single component reconstruction. J Electromyogr Kinesiol 23, 1304-1310.10.1016/j.jelekin.2013.09.010

Buchanan, T.S., Lloyd, D.G., Manal, K., Besier, T.F., 2004. Neuromusculoskeletal modeling: estimation of muscle forces and joint moments and movements from measurements of neural command. Journal of applied biomechanics 20, 367-395.10.1123/jab.20.4.367

Burnett, D.R., Campbell-Kyureghyan, N.H., Topp, R.V., Quesada, P.M., 2015. Biomechanics of Lower Limbs during Walking among Candidates for Total Knee Arthroplasty with and without Low Back Pain. Biomed Res Int 2015, 142562.10.1155/2015/142562

Cao, J., Worsley, K.J., 1999. The detection of local shape changes via the geometry of Hotelling's T-2 fields. Annals of Statistics 27, 925-942

Cerejo, R., Dunlop, D.D., Cahue, S., Channin, D., Song, J., Sharma, L., 2002. The influence of alignment on risk of knee osteoarthritis progression according to baseline stage of disease. Arthritis and rheumatism 46, 2632-2636.10.1002/art.10530

Cohen, J., 2013. Statistical power analysis for the behavioral sciences. Academic press.

Correa, T.A., Crossley, K.M., Kim, H.J., Pandy, M.G., 2010. Contributions of individual muscles to hip joint contact force in normal walking. J Biomech 43, 1618-1622.10.1016/j.jbiomech.2010.02.008

Crowninshield, R.D., Brand, R.A., 1981. A physiologically based criterion of muscle force prediction in locomotion. J Biomech 14, 793-801.10.1016/0021-9290(81)90035-x

D'agostino, R.B., Belanger, A., D'Agostino Jr, R.B., 1990. A suggestion for using powerful and informative tests of normality. The American Statistician 44, 316-321

D'Lima, D.D., Chen, P.C., Colwell, C.W., Jr., 2001. Polyethylene contact stresses, articular congruity, and knee alignment. Clin Orthop Relat Res 392, 232-238.10.1097/00003086-200111000-00029

D'Lima, D.D., Fregly, B.J., Patil, S., Steklov, N., Colwell, C.W., Jr., 2012. Knee joint forces: prediction, measurement, and significance. Proc Inst Mech Eng H 226, 95-102.10.1177/0954411911433372

D'Lima, D.D., Patil, S., Steklov, N., Chien, S., Colwell, C.W., Jr., 2007. In vivo knee moments and shear after total knee arthroplasty. J Biomech 40 Suppl 1, S11-17.10.1016/j.jbiomech.2007.03.004

D'Lima, D.D., Patil, S., Steklov, N., Slamin, J.E., Colwell, C.W., Jr., 2006. Tibial forces measured in vivo after total knee arthroplasty. J Arthroplasty 21, 255-262.10.1016/j.arth.2005.07.011

D'Lima, D.D., Steklov, N., Patil, S., Colwell, C.W., Jr., 2008. The Mark Coventry Award: in vivo knee forces during recreation and exercise after knee arthroplasty. Clin Orthop Relat Res 466, 2605-2611.10.1007/s11999-008-0345-x

Delp, S.L., Anderson, F.C., Arnold, A.S., Loan, P., Habib, A., John, C.T., Guendelman, E., Thelen, D.G., 2007. OpenSim: open-source software to create and analyze dynamic simulations of movement. IEEE Trans Biomed Eng 54, 1940-1950.10.1109/TBME.2007.901024

Deluzio, K.J., Wyss, U.P., Zee, B., Costigan, P.A., Serbie, C., 1997. Principal component models of knee kinematics and kinetics: Normal vs. pathological gait patterns. Human Movement Science 16, 201-217.10.1016/s0167-9457(96)00051-6

Demers, M.S., Pal, S., Delp, S.L., 2014. Changes in tibiofemoral forces due to variations in muscle activity during walking. Journal of orthopaedic research : official publication of the Orthopaedic Research Society 32, 769-776.10.1002/jor.22601

DeVita, P., Aaboe, J., Bartholdy, C., Leonardis, J.M., Bliddal, H., Henriksen, M., 2018. Quadriceps-strengthening exercise and quadriceps and knee biomechanics during walking in knee osteoarthritis: A two-centre randomized controlled trial. Clin Biomech (Bristol, Avon) 59, 199-206.10.1016/j.clinbiomech.2018.09.016

Ehlen, K.A., Reiser, R.F., 2nd, Browning, R.C., 2011. Energetics and biomechanics of inclined treadmill walking in obese adults. Medicine and science in sports and exercise 43, 1251-1259.10.1249/MSS.0b013e3182098a6c

Foroughi, N., Smith, R.M., Lange, A.K., Baker, M.K., Singh, M.A.F., Vanwanseele, B., 2011. Lower limb muscle strengthening does not change frontal plane moments in women with knee osteoarthritis: a randomized controlled trial. Clinical biomechanics 26, 167-174

Fox, A.S., Bonacci, J., McLean, S.G., Saunders, N., 2017. Efficacy of ACL injury risk screening methods in identifying high-risk landing patterns during a sport-specific task. Scand J Med Sci Sports 27, 525-534.10.1111/sms.12715

Franz, J.R., Kram, R., 2013. How does age affect leg muscle activity/coactivity during uphill and downhill walking? Gait & posture 37, 378-384

Franz, J.R., Kram, R., 2014. Advanced age and the mechanics of uphill walking: a joint-level, inverse dynamic analysis. Gait Posture 39, 135-140.10.1016/j.gaitpost.2013.06.012

Fregly, B.J., Besier, T.F., Lloyd, D.G., Delp, S.L., Banks, S.A., Pandy, M.G., D'Lima, D.D., 2012. Grand challenge competition to predict in vivo knee loads. Journal of orthopaedic research : official publication of the Orthopaedic Research Society 30, 503-513.10.1002/jor.22023

Friston, K.J., 2003. Statistical parametric mapping, Neuroscience databases. Springer, pp. 237-250.

Gallo, J., Goodman, S.B., Konttinen, Y.T., Wimmer, M.A., Holinka, M., 2013. Osteolysis around total knee arthroplasty: a review of pathogenetic mechanisms. Acta Biomater 9, 8046-8058.10.1016/j.actbio.2013.05.005

Gerus, P., Sartori, M., Besier, T.F., Fregly, B.J., Delp, S.L., Banks, S.A., Pandy, M.G., D'Lima, D.D., Lloyd, D.G., 2013. Subject-specific knee joint geometry improves predictions of medial tibiofemoral contact forces. J Biomech 46, 2778-2786.10.1016/j.jbiomech.2013.09.005

Good, P.I., 2006. Permutation, parametric, and bootstrap tests of hypotheses. Springer Science & Business Media.

Grieco, T.F., Sharma, A., Komistek, R.D., Cates, H.E., 2016. Single Versus Multiple-Radii Cruciate-Retaining Total Knee Arthroplasty: An In Vivo Mobile Fluoroscopy Study. J Arthroplasty 31, 694-701.10.1016/j.arth.2015.10.029

Haggerty, M., Dickin, D.C., Popp, J., Wang, H., 2014. The influence of incline walking on joint mechanics. Gait Posture 39, 1017-1021.10.1016/j.gaitpost.2013.12.027

Hawker, G., Wright, J., Coyte, P., Paul, J., Dittus, R., Croxford, R., Katz, B., Bombardier, C., Heck, D., Freund, D., 1998. Health-related quality of life after knee replacement. The Journal of bone and joint surgery. American volume 80, 163-173.10.2106/00004623-199802000-00003

Heinlein, B., Kutzner, I., Graichen, F., Bender, A., Rohlmann, A., Halder, A.M., Beier, A., Bergmann, G., 2009. ESB Clinical Biomechanics Award 2008: Complete data of total knee replacement loading for level walking and stair climbing measured in vivo with a follow-up of 6–10 months. Clinical Biomechanics 24, 315-326

Hermens, H.J., Freriks, B., Disselhorst-Klug, C., Rau, G., 2000. Development of recommendations for SEMG sensors and sensor placement procedures. J Electromyogr Kinesiol 10, 361-374.10.1016/s1050-6411(00)00027-4

Hicks, J.L., Uchida, T.K., Seth, A., Rajagopal, A., Delp, S.L., 2015. Is my model good enough? Best practices for verification and validation of musculoskeletal models and simulations of movement. Journal of biomechanical engineering 137

Hong, S.W., Leu, T.H., Li, J.D., Wang, T.M., Ho, W.P., Lu, T.W., 2014. Influence of inclination angles on intra- and inter-limb load-sharing during uphill walking. Gait Posture 39, 29-34.10.1016/j.gaitpost.2013.05.023

Huang, C.H., Cheng, C.K., Lee, Y.T., Lee, K.S., 1996. Muscle strength after successful total knee replacement: a 6- to 13-year followup. Clin Orthop Relat Res 328, 147-154.10.1097/00003086-199607000-00023

Hummer, E., Thorsen, T., Weinhandl, J.T., Cates, H., Zhang, S., 2021. Knee joint biomechanics of patients with unilateral total knee arthroplasty during stationary cycling. J Biomech 115, 110111.10.1016/j.jbiomech.2020.110111

Hunt, M.A., Birmingham, T.B., Giffin, J.R., Jenkyn, T.R., 2006. Associations among knee adduction moment, frontal plane ground reaction force, and lever arm during walking in patients with knee osteoarthritis. J Biomech 39, 2213-2220.10.1016/j.jbiomech.2005.07.002

Hurwitz, D.E., Sumner, D.R., Andriacchi, T.P., Sugar, D.A., 1998. Dynamic knee loads during gait predict proximal tibial bone distribution. J Biomech 31, 423-430.10.1016/s0021-9290(98)00028-1

Khasian, M., Sharma, A., Fehring, T.K., Griffin, W.L., Mason, J.B., Komistek, R.D., 2020. Kinematic Performance of Gradually Variable Radius Posterior-Stabilized Primary TKA During Various Activities: An In Vivo Study Using Fluoroscopy. J Arthroplasty 35, 1101-1108.10.1016/j.arth.2019.10.053

Komnik, I., Peters, M., Funken, J., David, S., Weiss, S., Potthast, W., 2016. Non-Sagittal Knee Joint Kinematics and Kinetics during Gait on Level and Sloped Grounds with Unicompartmental and Total Knee Arthroplasty Patients. PLoS One 11, e0168566.10.1371/journal.pone.0168566

Kramers-de Quervain, I.A., Kämpfen, S., Munzinger, U., Mannion, A.F., 2012. Prospective study of gait function before and 2 years after total knee arthroplasty. The Knee 19, 622-627

Kurihara, Y., Ohsugi, H., Choda, K., Endo, Y., Tosaka, T., Matsuda, T., Tsuneizumi, Y., Tsukeoka, T., 2021. Relationships between early postoperative gait biomechanical factors and patient-reported outcome measures 6 months after total knee arthroplasty. The Knee 28, 354-361

Kurtz, S., Ong, K., Lau, E., Mowat, F., Halpern, M., 2007. Projections of primary and revision hip and knee arthroplasty in the United States from 2005 to 2030. The Journal of bone and joint surgery. American volume 89, 780-785.10.2106/JBJS.F.00222

Kuster, M.S., Wood, G.A., Stachowiak, G.W., Gachter, A., 1997. Joint load considerations in total knee replacement. J Bone Joint Surg Br 79, 109-113.10.1302/0301-620x.79b1.6978

Kutzner, I., Heinlein, B., Graichen, F., Bender, A., Rohlmann, A., Halder, A., Beier, A., Bergmann, G., 2010. Loading of the knee joint during activities of daily living measured in vivo in five subjects. J Biomech 43, 2164-2173.10.1016/j.jbiomech.2010.03.046

Kutzner, I., Stephan, D., Dymke, J., Bender, A., Graichen, F., Bergmann, G., 2013. The influence of footwear on knee joint loading during walking—in vivo load measurements with instrumented knee implants. J Biomech 46, 796-800

Lai, A.K.M., Arnold, A.S., Wakeling, J.M., 2017. Why are Antagonist Muscles Co-activated in My Simulation? A Musculoskeletal Model for Analysing Human Locomotor Tasks. Ann Biomed Eng 45, 2762-2774.10.1007/s10439-017-1920-7

Lange, G.W., Hintermeister, R.A., Schlegel, T., Dillman, C.J., Steadman, J.R., 1996. Electromyographic and kinematic analysis of graded treadmill walking and the implications for knee rehabilitation. The Journal of orthopaedic and sports physical therapy 23, 294-301.10.2519/jospt.1996.23.5.294

Lay, A.N., Hass, C.J., Gregor, R.J., 2006. The effects of sloped surfaces on locomotion: a kinematic and kinetic analysis. J Biomech 39, 1621-1628.10.1016/j.jbiomech.2005.05.005

Lerner, Z.F., DeMers, M.S., Delp, S.L., Browning, R.C., 2015. How tibiofemoral alignment and contact locations affect predictions of medial and lateral tibiofemoral contact forces. J Biomech 48, 644-650.10.1016/j.jbiomech.2014.12.049

Lerner, Z.F., Haight, D.J., DeMers, M.S., Board, W.J., Browning, R.C., 2014. The effects of walking speed on tibiofemoral loading estimated via musculoskeletal modeling. Journal of applied biomechanics 30, 197-205.10.1123/jab.2012-0206

Leroux, A., Fung, J., Barbeau, H., 2006. Postural adaptation to walking on inclined surfaces: II. Strategies following spinal cord injury. Clin Neurophysiol 117, 1273-1282.10.1016/j.clinph.2006.02.012

Levinger, P., Menz, H.B., Morrow, A.D., Feller, J.A., Bartlett, J.R., Bergman, N.R., 2013. Lower limb biomechanics in individuals with knee osteoarthritis before and after total knee arthroplasty surgery. J Arthroplasty 28, 994-999.10.1016/j.arth.2012.10.018

Lewek, M.D., Rudolph, K.S., Snyder-Mackler, L., 2004. Quadriceps femoris muscle weakness and activation failure in patients with symptomatic knee osteoarthritis. Journal of orthopaedic research : official publication of the Orthopaedic Research Society 22, 110-115.10.1016/S0736-0266(03)00154-2

Mandeville, D., Osternig, L.R., Chou, L.S., 2007. The effect of total knee replacement on dynamic support of the body during walking and stair ascent. Clin Biomech (Bristol, Avon) 22, 787-794.10.1016/j.clinbiomech.2007.04.002

Mandeville, D., Osternig, L.R., Lantz, B.A., Mohler, C.G., Chou, L.S., 2008. The effect of total knee replacement on the knee varus angle and moment during walking and stair ascent. Clin Biomech (Bristol, Avon) 23, 1053-1058.10.1016/j.clinbiomech.2008.04.011

Marouane, H., Shirazi-Adl, A., 2019. Sensitivity of medial-lateral load sharing to changes in adduction moments or angles in an asymptomatic knee joint model during gait. Gait Posture 70, 39-47.10.1016/j.gaitpost.2019.02.006

McClelland, J.A., Feller, J.A., Menz, H.B., Webster, K.E., 2014. Patterns in the knee flexion-extension moment profile during stair ascent and descent in patients with total knee arthroplasty. J Biomech 47, 1816-1821.10.1016/j.jbiomech.2014.03.026

McClelland, J.A., Webster, K.E., Feller, J.A., Menz, H.B., 2011. Knee kinematics during walking at different speeds in people who have undergone total knee replacement. The Knee 18, 151-155.10.1016/j.knee.2010.04.005

McIntosh, A.S., Beatty, K.T., Dwan, L.N., Vickers, D.R., 2006. Gait dynamics on an inclined walkway. J Biomech 39, 2491-2502.10.1016/j.jbiomech.2005.07.025

Meier, W., Mizner, R.L., Marcus, R.L., Dibble, L.E., Peters, C., Lastayo, P.C., 2008. Total knee arthroplasty: muscle impairments, functional limitations, and recommended rehabilitation approaches. The Journal of orthopaedic and sports physical therapy 38, 246-256.10.2519/jospt.2008.2715

Milner, C.E., 2008. Interlimb asymmetry during walking following unilateral total knee arthroplasty. Gait Posture 28, 69-73.10.1016/j.gaitpost.2007.10.002

Milner, C.E., O'Bryan, M.E., 2008. Bilateral frontal plane mechanics after unilateral total knee arthroplasty. Arch Phys Med Rehabil 89, 1965-1969.10.1016/j.apmr.2008.02.034

Miyazaki, T., Wada, M., Kawahara, H., Sato, M., Baba, H., Shimada, S., 2002. Dynamic load at baseline can predict radiographic disease progression in medial compartment knee osteoarthritis. Annals of the rheumatic diseases 61, 617-622.10.1136/ard.61.7.617

Mizner, R.L., Petterson, S.C., Snyder-Mackler, L., 2005. Quadriceps strength and the time course of functional recovery after total knee arthroplasty. The Journal of orthopaedic and sports physical therapy 35, 424-436.10.2519/jospt.2005.35.7.424

Morrison, J.B., 1970. The mechanics of the knee joint in relation to normal walking. J Biomech 3, 51-61.10.1016/0021-9290(70)90050-3

Mundermann, A., Dyrby, C.O., D'Lima, D.D., Colwell, C.W., Jr., Andriacchi, T.P., 2008. In vivo knee loading characteristics during activities of daily living as measured by an instrumented total knee replacement. Journal of orthopaedic research : official publication of the Orthopaedic Research Society 26, 1167-1172.10.1002/jor.20655

Ngai, V., Wimmer, M.A., 2015. Variability of TKR knee kinematics and relationship with gait kinetics: implications for total knee wear. Biomed Res Int 2015, 284513.10.1155/2015/284513

Nordin, M., Frankel, V.H., 2001. Basic biomechanics of the musculoskeletal system. Lippincott Williams & Wilkins.

Orishimo, K.F., Kremenic, I.J., Deshmukh, A.J., Nicholas, S.J., Rodriguez, J.A., 2012. Does total knee arthroplasty change frontal plane knee biomechanics during gait? Clinical Orthopaedics and Related Research® 470, 1171-1176

Ouellet, D., Moffet, H., 2002. Locomotor deficits before and two months after knee arthroplasty. Arthritis and rheumatism 47, 484-493.10.1002/art.10652

Pataky, T.C., 2010. Generalized n-dimensional biomechanical field analysis using statistical parametric mapping. J Biomech 43, 1976-1982.10.1016/j.jbiomech.2010.03.008

Pataky, T.C., Robinson, M.A., Vanrenterghem, J., 2013. Vector field statistical analysis of kinematic and force trajectories. J Biomech 46, 2394-2401.10.1016/j.jbiomech.2013.07.031

Pataky, T.C., Robinson, M.A., Vanrenterghem, J., 2016a. Region-of-interest analyses of one-dimensional biomechanical trajectories: bridging 0D and 1D theory, augmenting statistical power. PeerJ 4, e2652.10.7717/peerj.2652

Pataky, T.C., Vanrenterghem, J., Robinson, M.A., 2015. Zero- vs. one-dimensional, parametric vs. non-parametric, and confidence interval vs. hypothesis testing procedures in one-dimensional biomechanical trajectory analysis. J Biomech 48, 1277-1285.10.1016/j.jbiomech.2015.02.051

Pataky, T.C., Vanrenterghem, J., Robinson, M.A., 2016b. The probability of false positives in zero-dimensional analyses of one-dimensional kinematic, force and EMG trajectories. J Biomech 49, 1468-1476.10.1016/j.jbiomech.2016.03.032

Penny, W.D., Friston, K.J., Ashburner, J.T., Kiebel, S.J., Nichols, T.E., 2011. Statistical parametric mapping: the analysis of functional brain images. Elsevier.

Piazza, S.J., Delp, S.L., 2001. Three-dimensional dynamic simulation of total knee replacement motion during a step-up task. J Biomech Eng 123, 599-606.10.1115/1.1406950

Ramsay, J.O., 2004. Functional data analysis. Encyclopedia of Statistical Sciences 4

Rasnick, R., Standifird, T., Reinbolt, J.A., Cates, H.E., Zhang, S., 2016. Knee Joint Loads and Surrounding Muscle Forces during Stair Ascent in Patients with Total Knee Replacement. PLoS One 11, e0156282.10.1371/journal.pone.0156282

Redfern, M.S., DiPasquale, J., 1997. Biomechanics of descending ramps. Gait & Posture 6, 119-125

Reynolds, S., 2013. Does total knee arthroplasty reproduce natural knee mechanics. Université d'Ottawa/University of Ottawa.

Ro, D.H., Han, H.S., Lee, D.Y., Kim, S.H., Kwak, Y.H., Lee, M.C., 2018. Slow gait speed after bilateral total knee arthroplasty is associated with suboptimal improvement of knee biomechanics. Knee Surg Sports Traumatol Arthrosc 26, 1671-1680.10.1007/s00167-017-4682-8

Saari, T., Tranberg, R., Zugner, R., Uvehammer, J., Karrholm, J., 2005. Changed gait pattern in patients with total knee arthroplasty but minimal influence of tibial insert design: gait analysis during level walking in 39 TKR patients and 18 healthy controls. Acta Orthop 76, 253-260.10.1080/00016470510030661

Saxby, D.J., Modenese, L., Bryant, A.L., Gerus, P., Killen, B., Fortin, K., Wrigley, T.V., Bennell, K.L., Cicuttini, F.M., Lloyd, D.G., 2016. Tibiofemoral contact forces during walking, running and sidestepping. Gait Posture 49, 78-85.10.1016/j.gaitpost.2016.06.014

Sayeed, S.A., Sayeed, Y.A., Barnes, S.A., Pagnano, M.W., Trousdale, R.T., 2011. The risk of subsequent joint arthroplasty after primary unilateral total knee arthroplasty, a 10-year study. J Arthroplasty 26, 842-846.10.1016/j.arth.2010.08.016

Schipplein, O.D., Andriacchi, T.P., 1991. Interaction between active and passive knee stabilizers during level walking. Journal of orthopaedic research : official publication of the Orthopaedic Research Society 9, 113-119.10.1002/jor.1100090114

Schroeder, L.E., Peel, S.A., Leverenz, B.H., Weinhandl, J.T., 2021. Type of unanticipated stimulus affects lower extremity kinematics and kinetics during sidestepping. Journal of sports sciences 39, 618-628.10.1080/02640414.2020.1837481

Seireg, A., Arvikar, R.J., 1973. A mathematical model for evaluation of forces in lower extremeties of the musculo-skeletal system. J Biomech 6, 313-326.10.1016/0021-9290(73)90053-5

Shelburne, K.B., Torry, M.R., Pandy, M.G., 2006. Contributions of muscles, ligaments, and the ground-reaction force to tibiofemoral joint loading during normal gait. Journal of orthopaedic research : official publication of the Orthopaedic Research Society 24, 1983-1990.10.1002/jor.20255

Shimada, N., Deie, M., Hirata, K., Hiate, Y., Orita, N., Iwaki, D., Ito, Y., Kimura, H., Pappas, E., Ochi, M., 2016. Courses of change in knee adduction moment and lateral thrust differ up to 1 year after TKA. Knee Surg Sports Traumatol Arthrosc 24, 2506-2511.10.1007/s00167-015-3688-3

Shu, L., Li, S., Sugita, N., 2020. Systematic review of computational modelling for biomechanics analysis of total knee replacement. Biosurface and Biotribology 6, 3-11

Silder, A., Besier, T., Delp, S.L., 2012. Predicting the metabolic cost of incline walking from muscle activity and walking mechanics. J Biomech 45, 1842-1849.10.1016/j.jbiomech.2012.03.032

Simon, J.C., Della Valle, C.J., Wimmer, M.A., 2018. Level and Downhill Walking to Assess Implant Functionality in Bicruciate-and Posterior Cruciate–Retaining Total Knee Arthroplasty. The Journal of arthroplasty 33, 2884-2889

Smith, A.J., Lloyd, D.G., Wood, D.J., 2006. A kinematic and kinetic analysis of walking after total knee arthroplasty with and without patellar resurfacing. Clin Biomech (Bristol, Avon) 21, 379-386.10.1016/j.clinbiomech.2005.11.007

Standifird, T.W., Saxton, A.M., Coe, D.P., Cates, H.E., Reinbolt, J.A., Zhang, S., 2016. Influence of Total Knee Arthroplasty on Gait Mechanics of the Replaced and Non-Replaced Limb During Stair Negotiation. J Arthroplasty 31, 278-283.10.1016/j.arth.2015.06.052

Stansfield, B.W., Nicol, A.C., 2002. Hip joint contact forces in normal subjects and subjects with total hip prostheses: walking and stair and ramp negotiation. Clin Biomech (Bristol, Avon) 17, 130-139.10.1016/s0268-0033(01)00119-x

Steele, K.M., Demers, M.S., Schwartz, M.H., Delp, S.L., 2012. Compressive tibiofemoral force during crouch gait. Gait Posture 35, 556-560.10.1016/j.gaitpost.2011.11.023

Stensgaard Stoltze, J., Rasmussen, J., Skipper Andersen, M., 2018. On the biomechanical relationship between applied hip, knee and ankle joint moments and the internal knee compressive forces. International Biomechanics 5, 63-74

Sutherland, D.H., Olshen, R., Cooper, L., Woo, S.L., 1980. The development of mature gait. The Journal of bone and joint surgery. American volume 62, 336-353

Tarnita, D., Petcu, A.I., Dumitru, N., 2020. Influences of treadmill speed and incline angle on the kinematics of the normal, osteoarthritic and prosthetic human knee. Rom J Morphol Embryol 61, 199-208.10.47162/RJME.61.1.22

Vanrenterghem, J., Venables, E., Pataky, T., Robinson, M.A., 2012. The effect of running speed on knee mechanical loading in females during side cutting. J Biomech 45, 2444-2449.10.1016/j.jbiomech.2012.06.029

Vanwanseele, B., Parker, D., Coolican, M., 2009. Frontal knee alignment: three-dimensional marker positions and clinical assessment. Clin Orthop Relat Res 467, 504-509.10.1007/s11999-008-0545-4

Varacallo, M., Luo, T.D., Johanson, N.A., 2020. Total knee arthroplasty (TKA) techniques. StatPearls [Internet]

Wahid, F., Begg, R., McClelland, J.A., Webster, K.E., Halgamuge, S., Ackland, D.C., 2016. A multiple regression normalization approach to evaluation of gait in total knee arthroplasty patients. Clin Biomech (Bristol, Avon) 32, 92-101.10.1016/j.clinbiomech.2015.12.012

Walter, J.P., D'Lima, D.D., Colwell Jr, C.W., Fregly, B.J., 2010. Decreased knee adduction moment does not guarantee decreased medial contact force during gait. Journal of Orthopaedic Research 28, 1348-1354

Warmenhoven, J., Harrison, A., Robinson, M.A., Vanrenterghem, J., Bargary, N., Smith, R., Cobley, S., Draper, C., Donnelly, C., Pataky, T., 2018. A force profile analysis comparison between functional data analysis, statistical parametric mapping and statistical non-parametric mapping in on-water single sculling. J Sci Med Sport 21, 1100-1105.10.1016/j.jsams.2018.03.009

Wen, C., 2018. Influence of Cruciate Retaining, Posterior Stabilized and Bi-Cruciate Stabilized Total Knee Replacement Designs on Gait Mechanics during Ramp and Level Walking. Dissertation, University of Tennessee, TRACE: Tennessee Research And Creative Exchange.

Wen, C., Cates, H.E., Weinhandl, J.T., Crouter, S.E., Zhang, S., 2021. Knee biomechanics of patients with total knee replacement during downhill walking on different slopes. J Sport Health Sci.10.1016/j.jshs.2021.01.009

Wen, C., Cates, H.E., Zhang, S., 2019. Is knee biomechanics different in uphill walking on different slopes for older adults with total knee replacement? J Biomech 89, 40-47

Whyte, E.F., Richter, C., O'Connor, S., Moran, K.A., 2018. The effect of high intensity exercise and anticipation on trunk and lower limb biomechanics during a crossover cutting manoeuvre. Journal of sports sciences 36, 889-900.10.1080/02640414.2017.1346270

Wiik, A.V., Aqil, A., Tankard, S., Amis, A.A., Cobb, J.P., 2015. Downhill walking gait pattern discriminates between types of knee arthroplasty: improved physiological knee functionality in UKA versus TKA. Knee Surg Sports Traumatol Arthrosc 23, 1748-1755.10.1007/s00167-014-3240-x

Winby, C.R., Lloyd, D.G., Besier, T.F., Kirk, T.B., 2009. Muscle and external load contribution to knee joint contact loads during normal gait. J Biomech 42, 2294-2300.10.1016/j.jbiomech.2009.06.019

Winter, D.A., 2009. Kinetics: Forces and Moment of Force, Biomechanics and Motor Control of Human Movement. John Wiley & Sons, pp. 107-138.

Wylde, V., Dieppe, P., Hewlett, S., Learmonth, I., 2007. Total knee replacement: is it really an effective procedure for all? The Knee 14, 417-423

Yocum, D., Weinhandl, J.T., Fairbrother, J.T., Zhang, S., 2018. Wide step width reduces knee abduction moment of obese adults during stair negotiation. J Biomech 75, 138-146.10.1016/j.jbiomech.2018.05.002

Yoshida, Y., Mizner, R.L., Ramsey, D.K., Snyder-Mackler, L., 2008. Examining outcomes from total knee arthroplasty and the relationship between quadriceps strength and knee function over time. Clin Biomech (Bristol, Avon) 23, 320-328.10.1016/j.clinbiomech.2007.10.008

Zaghlol, R.S., Khalil, S.S., Attia, A.M., Dawa, G.A., 2020. Comparison of two different models of rehabilitation programs following total knee replacement operations. Egyptian Rheumatology and Rehabilitation 47, 1-9

Zeni Jr, J.A., Flowers, P., Bade, M., Cheuy, V., Stevens-Lapsley, J., Snyder-Mackler, L., 2019. Stiff knee gait may increase risk of second total knee arthroplasty. Journal of Orthopaedic Research® 37, 397-402

Zhao, D., Banks, S.A., D'Lima, D.D., Colwell, C.W., Jr., Fregly, B.J., 2007a. In vivo medial and lateral tibial loads during dynamic and high flexion activities. Journal of orthopaedic research : official publication of the Orthopaedic Research Society 25, 593-602.10.1002/jor.20362

Zhao, D., Banks, S.A., Mitchell, K.H., D'Lima, D.D., Colwell, C.W., Jr., Fregly, B.J., 2007b. Correlation between the knee adduction torque and medial contact force for a variety of gait patterns. Journal of orthopaedic research : official publication of the Orthopaedic Research Society 25, 789-797.10.1002/jor.20379

APPENDICES

Appendix C – Demographics

Table 6. Patient demographic information for the TKA group.

Subjects	Mass	Height	Age	Knee replacement side
S2	68.0	1.62	74	Right
S3	72.6	1.75	68	Left
S11	79.4	1.65	75	Right
S13	89.3	1.90	65	Left
S16	110.6	1.80	62	Right
S19	72.6	1.73	73	Right
S22	91.7	1.78	65	Left
S24	93.2	1.80	67	Left
S28	81.2	1.63	59	Left
Mean	84.3	1.7	67.6	
S.D.	13.4	0.1	5.5	

Table 7. Participant specific demographic information for the healthy control group.

Subjects	Mass	Height	Age
S17	76.5	1.73	72
S25	117.66	1.91	66
S27	102.1	1.90	62
S29	68.19	1.73	73
S30	66.5	1.68	69
S32	93.6	1.88	71
S33	54	1.68	75
S34	43.3	1.58	67
S35	66.22	1.78	73
	76.45	1.76	69.78
	23.78	0.11	4.15

Table 8. Patient-specific frontal plane mechanical axis angles (°) for the TKA group.

Subject	Replaced	Non-Replaced
S2	174.40	168.98
S3	176.89	182.88
S11	178.14	177.19
S13	173.69	169.77
S16	175.85	176.46
S19	175.61	171.50
S21	176.76	174.72
S24	186.64	185.01
S28	174.61	172.08
Mean	176.95	175.40
S.D.	3.89	5.62

Table 9. Patient-specific frontal plane mechanical axis angles (°) for the control group.

Subject	Left	Right
S17	178.3	177.8
S25	180.3	176.1
S27	182.1	183.6
S29	171.7	170.1
S30	174.7	173.9
S32	177.0	176.7
S33	178.0	177.4
S34	176.8	179.1
S35	175.3	175.3
Mean	177.1	176.7
S.D.	3.1	3.7

Appendix D – Muscle Activations and EMG

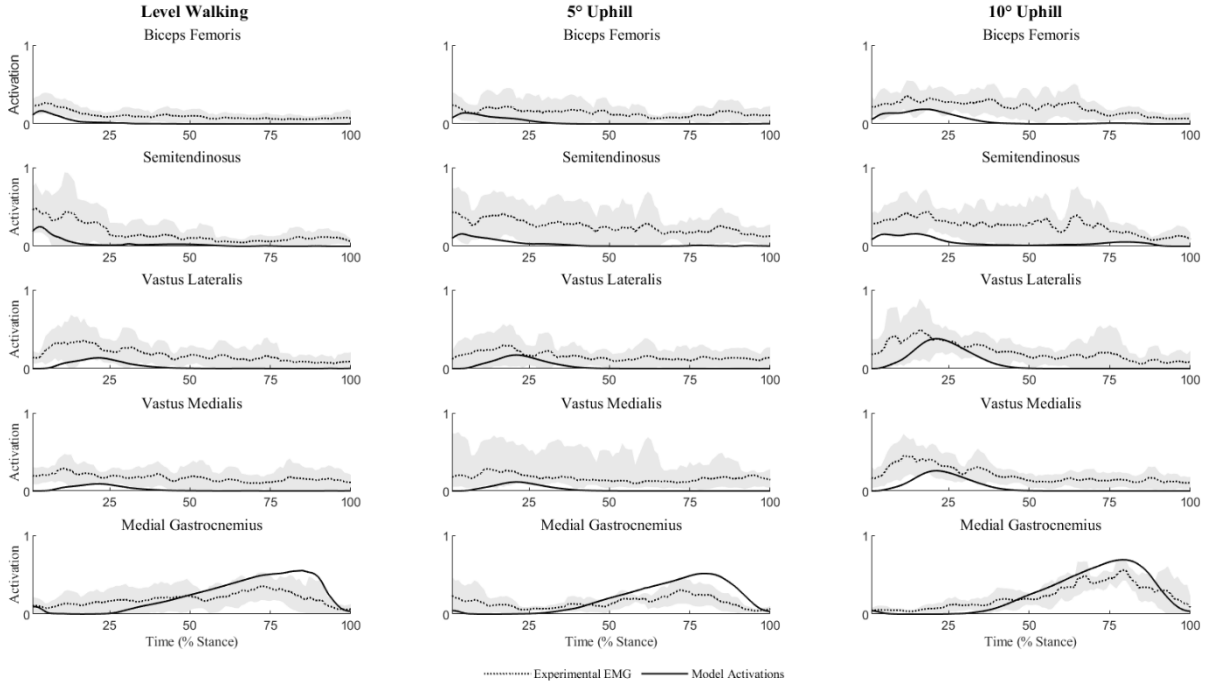

Figure 13. Muscle activations during level walking and uphill walking for the replaced limb.

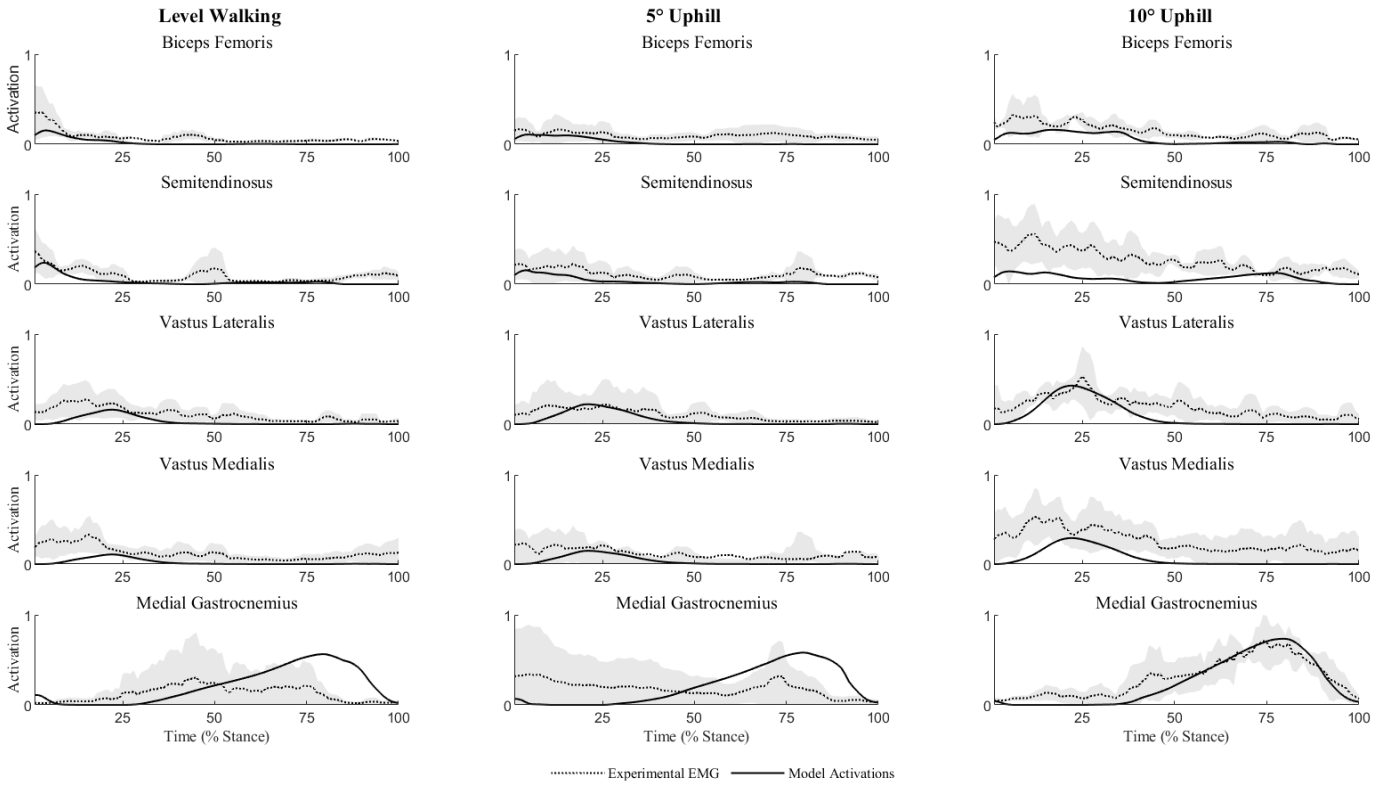

Figure 14. Muscle activations during level walking and uphill walking for the non-replaced limb.

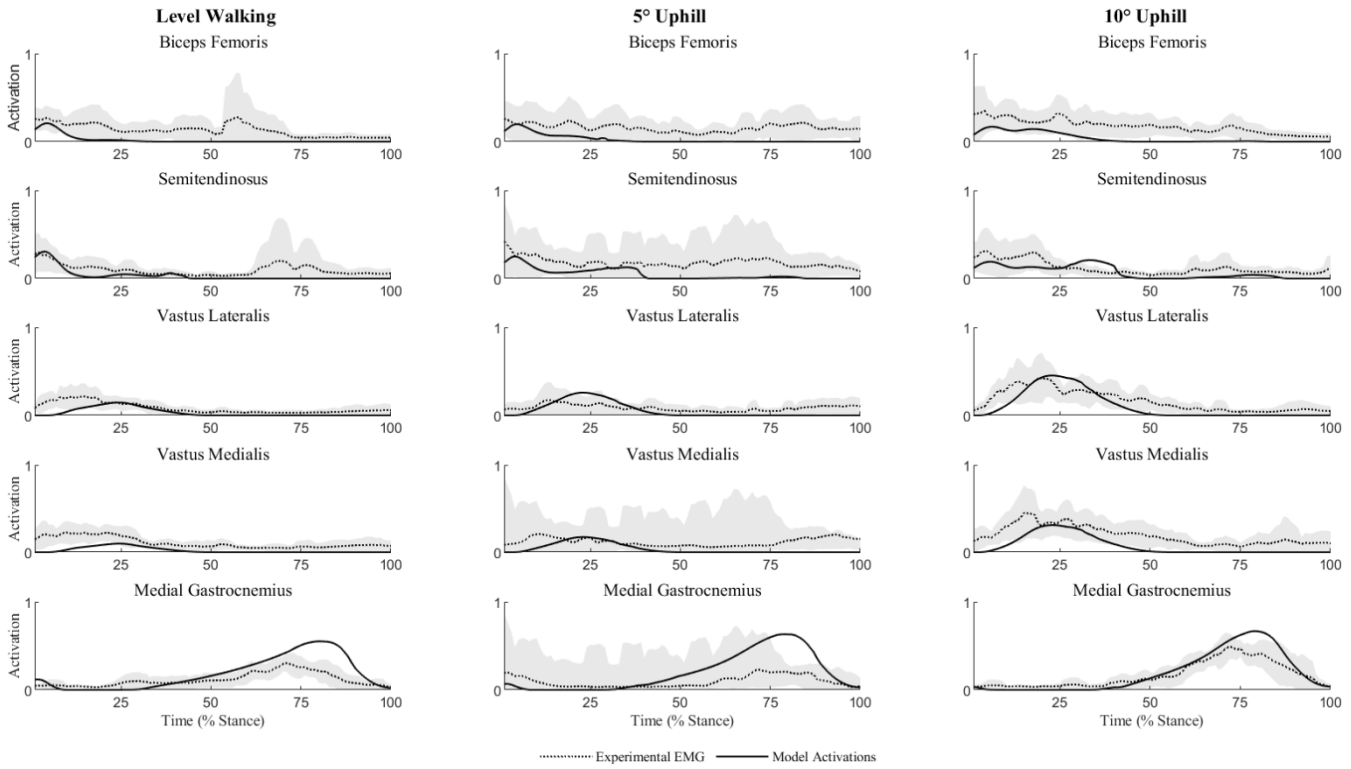

Figure 15. Muscle activations during level walking and uphill walking for the control limb.

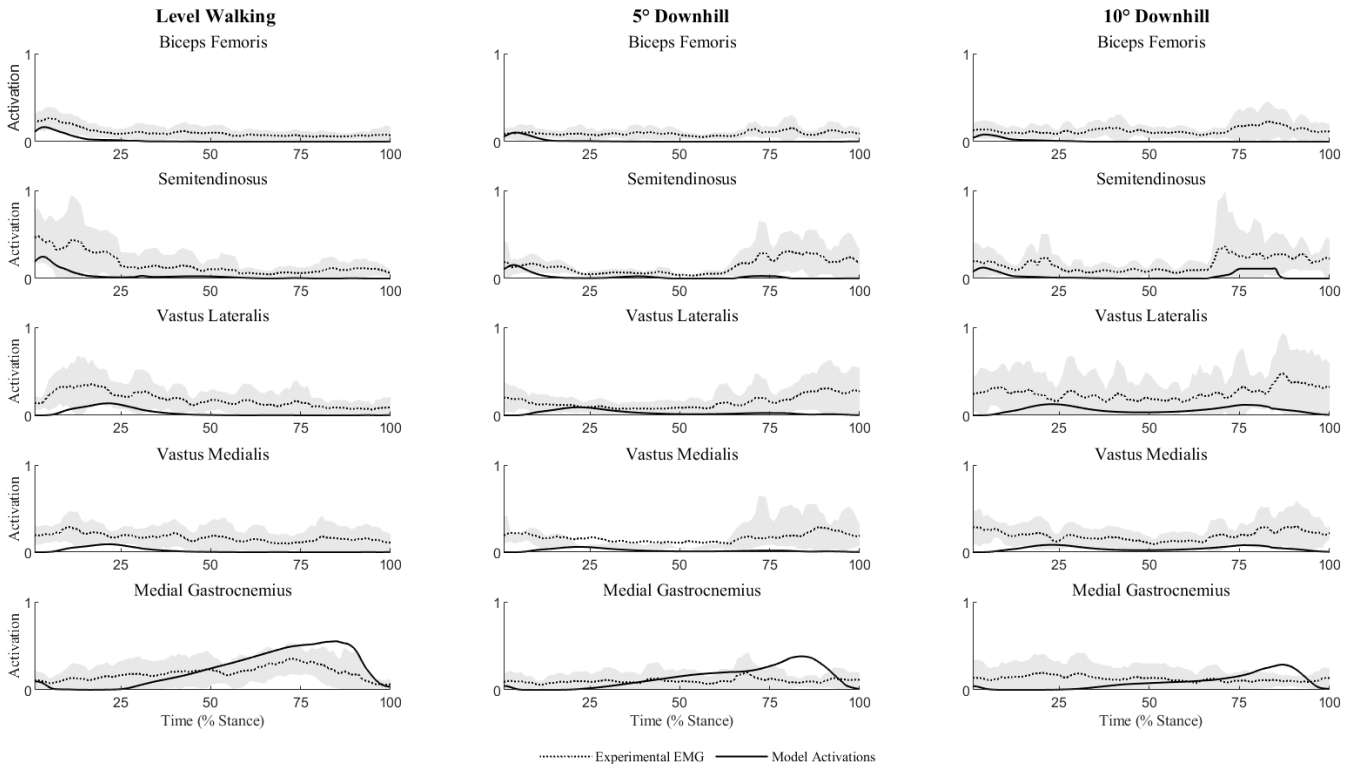

Figure 16. Muscle activations during level and downhill walking for the replaced limb.

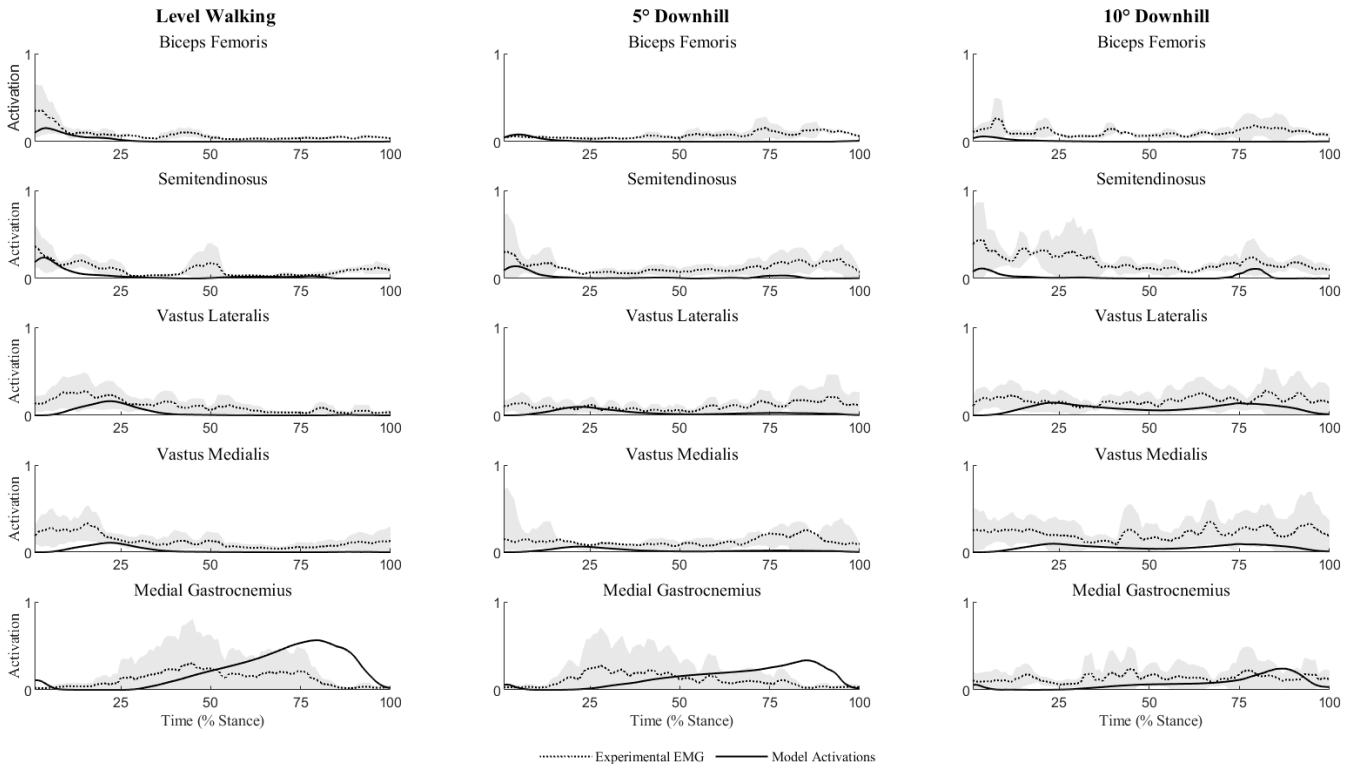

Figure 17. Muscle activations during level walking and downhill walking for the non-replaced limb.

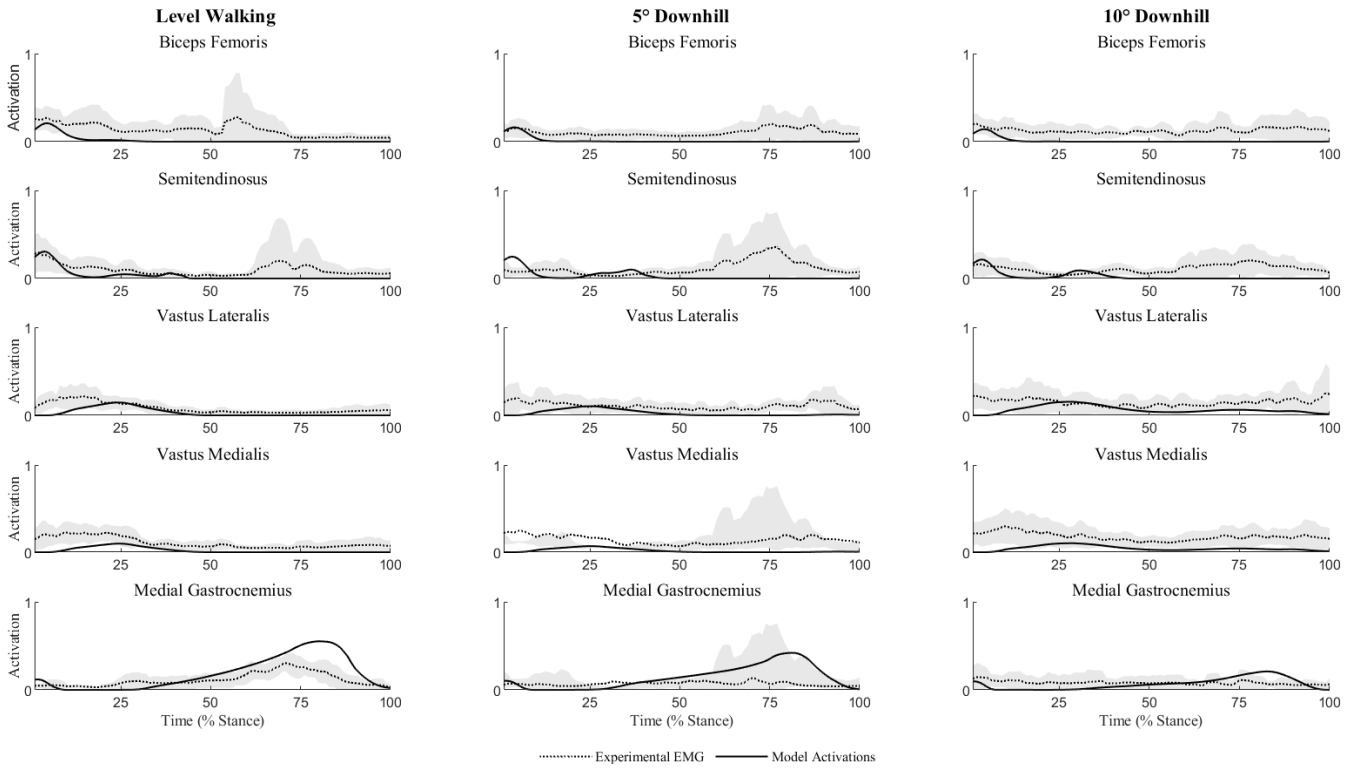

Figure 18. Muscle activations during level walking and downhill walking for the control limb.

Appendix E – Impulse

Table 10. Individual subject values for total stance phase TCF impulse for the replaced limb during level, uphill, and downhill walking.

Subject	Level	Up_5	Up_10	Down_5	Down_10
S2	1.53	1.51	2.02	1.27	1.40
S3	0.35	0.42	0.23	0.46	0.24
S11	1.70	1.97	1.74	1.85	2.00
S13	0.24	0.30	0.37	0.28	0.40
S16	1.61	1.66	2.27	1.78	2.65
S19	1.13	1.26	1.51	1.17	1.30
S22	0.21	0.21	0.31	0.28	0.76
S24	0.46	0.47	0.69	0.17	0.21
S28	0.36	0.41	0.44	0.61	0.48
Mean	0.84	0.91	1.06	0.87	1.05
SD	0.64	0.68	0.81	0.66	0.86

Table 11. Individual subject values for loading-response stance phase TCF impulse for the replaced limb during level, uphill, and downhill walking.

Subject	Level	Up_5	Up_10	Down_5	Down_10
S2	0.64	0.67	0.97	0.60	0.70
S3	0.02	0.03	0.01	0.32	0.18
S11	0.61	0.67	0.67	0.79	0.89
S13	0.02	0.02	0.03	0.02	0.33
S16	0.79	0.81	0.96	0.79	1.03
S19	0.44	0.55	0.72	0.48	0.57
S22	0.01	0.01	0.02	0.23	0.72
S24	0.07	0.07	0.07	0.05	0.08
S28	0.03	0.03	0.04	0.34	0.38
Mean	0.29	0.32	0.39	0.40	0.54
SD	0.32	0.35	0.43	0.29	0.32

Table 12. Individual subject values for push-off stance phase TCF impulse for the replaced limb during level, uphill, and downhill walking.

Subject	Level	Up_5	Up_10	Down_5	Down_10
S2	0.89	0.84	1.05	0.67	0.70
S3	0.32	0.38	0.22	0.14	0.05
S11	1.08	1.30	1.07	1.06	1.12
S13	0.22	0.28	0.34	0.27	0.07
S16	0.82	0.85	1.31	0.99	1.62
S19	0.69	0.71	0.79	0.68	0.73
S22	0.20	0.20	0.29	0.05	0.04
S24	0.39	0.40	0.62	0.12	0.13
S28	0.32	0.38	0.40	0.27	0.10
Mean	0.55	0.59	0.68	0.47	0.51
SD	0.33	0.36	0.40	0.39	0.57

Table 13. Individual subject values total stance phase TCF impulse for the non-replaced limb during level, uphill, and downhill walking.

Subject	Level	Up_5	Up_10	Down_5	Down_10
S2	1.33	1.33	1.67	1.24	1.93
S3	0.38	0.46	0.27	0.56	0.27
S11	1.71	1.76	2.16	1.72	2.00
S13	0.26	0.26	0.37	0.26	0.38
S16	2.36	2.35	3.74	1.92	2.55
S19	1.84	1.15	1.28	1.21	1.08
S22	0.17	0.18	0.26	0.27	0.35
S24	0.53	0.60	0.79	0.61	0.77
S28	0.36	0.30	0.34	0.47	0.53
Mean	0.99	0.93	1.21	0.92	1.10
SD	0.82	0.76	1.17	0.62	0.85

Table 14. Individual subject values for loading-response stance phase TCF impulse for the non-replaced limb during level, uphill, and downhill walking.

Subject	Level	Up_5	Up_10	Down_5	Down_10
S2	0.57	0.79	0.91	0.60	0.92
S3	0.02	0.02	0.02	0.44	0.21
S11	0.74	0.75	1.08	0.75	0.63
S13	0.01	0.02	0.03	0.18	0.31
S16	0.88	1.02	1.41	0.88	0.94
S19	1.20	0.45	0.61	0.52	0.50
S22	0.01	0.01	0.02	0.22	0.31
S24	0.07	0.06	0.06	0.51	0.64
S28	0.04	0.03	0.05	0.36	0.40
Mean	0.39	0.35	0.47	0.50	0.54
SD	0.46	0.41	0.55	0.23	0.26

Table 15. Individual subject values for push-off stance phase TCF impulse for the non-replaced limb during level, uphill, and downhill walking.

Subject	Level	Up_5	Up_10	Down_5	Down_10
S2	0.76	0.54	0.76	0.64	1.00
S3	0.36	0.44	0.25	0.12	0.05
S11	0.98	1.01	1.08	0.97	1.37
S13	0.25	0.24	0.34	0.08	0.07
S16	1.48	1.33	2.33	1.03	1.61
S19	0.64	0.70	0.67	0.69	0.58
S22	0.16	0.17	0.24	0.06	0.04
S24	0.47	0.54	0.73	0.10	0.13
S28	0.32	0.27	0.30	0.11	0.14
Mean	0.60	0.58	0.74	0.42	0.56
SD	0.42	0.38	0.66	0.41	0.62

Table 16. Individual subject values for total stance phase TCF impulse for the control limb during level, uphill, and downhill walking.

Subject	Level	Up_5	Up_10	Down_5	Down_10
S17	1.45	1.90	2.08	1.25	1.25
S25	0.34	0.46	0.27	0.56	0.22
S27	1.75	1.80	1.57	1.79	1.67
S29	0.26	0.36	0.41	0.24	0.33
S30	1.58	1.86	2.13	1.80	2.26
S32	1.25	1.33	1.43	1.21	1.21
S33	0.20	0.24	0.36	0.28	0.63
S34	0.46	0.40	0.93	0.63	0.92
S35	0.38	0.37	0.52	0.49	0.45
Mean	0.85	0.97	1.08	0.92	0.99
SD	0.64	0.73	0.75	0.61	0.67

Table 17. Individual subject values for loading-response stance phase TCF impulse for the control limb during level, uphill, and downhill walking.

Subject	Level	Up_5	Up_10	Down_5	Down_10
S17	0.57	1.14	0.95	0.54	0.61
S25	0.02	0.03	0.02	0.44	0.16
S27	0.65	0.63	0.63	0.79	0.71
S29	0.01	0.02	0.02	0.01	0.26
S30	0.73	0.87	0.92	0.79	0.90
S32	0.51	0.57	0.75	0.49	0.59
S33	0.01	0.01	0.02	0.24	0.58
S34	0.06	0.07	0.09	0.52	0.80
S35	0.02	0.02	0.05	0.38	0.34
Mean	0.29	0.37	0.38	0.47	0.55
SD	0.32	0.44	0.42	0.25	0.25

Table 18. Individual subject values for push-off stance phase TCF impulse for the control limb during level, uphill, and downhill walking.

Subject	Level	Up_5	Up_10	Down_5	Down_10
S17	0.87	0.76	1.13	0.71	0.63
S25	0.32	0.42	0.25	0.12	0.06
S27	1.10	1.17	0.94	1.00	0.96
S29	0.25	0.34	0.38	0.23	0.07
S30	0.85	0.99	1.21	1.02	1.36
S32	0.74	0.76	0.68	0.72	0.62
S33	0.20	0.23	0.33	0.04	0.04
S34	0.40	0.34	0.84	0.10	0.12
S35	0.36	0.35	0.47	0.11	0.12
Mean	0.57	0.60	0.69	0.45	0.44
SD	0.33	0.34	0.36	0.41	0.48

Appendix F – Statistical Parametric Mapping Results

Interaction, main effect, and post-hoc SPM{F} and SPM{t} tests for both uphill and downhill conditions.

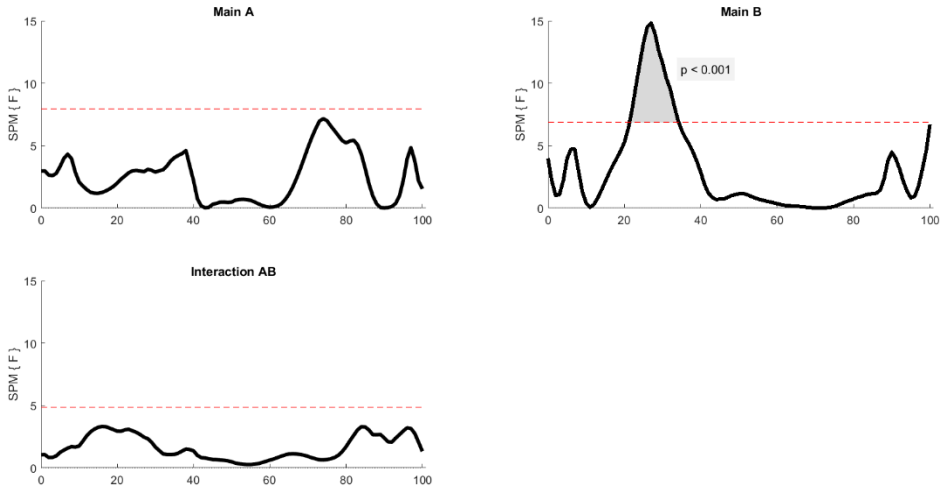

Figure 19. SPM interaction, main effect A (limb), and main effect B (slope)for TCF during uphill walking.

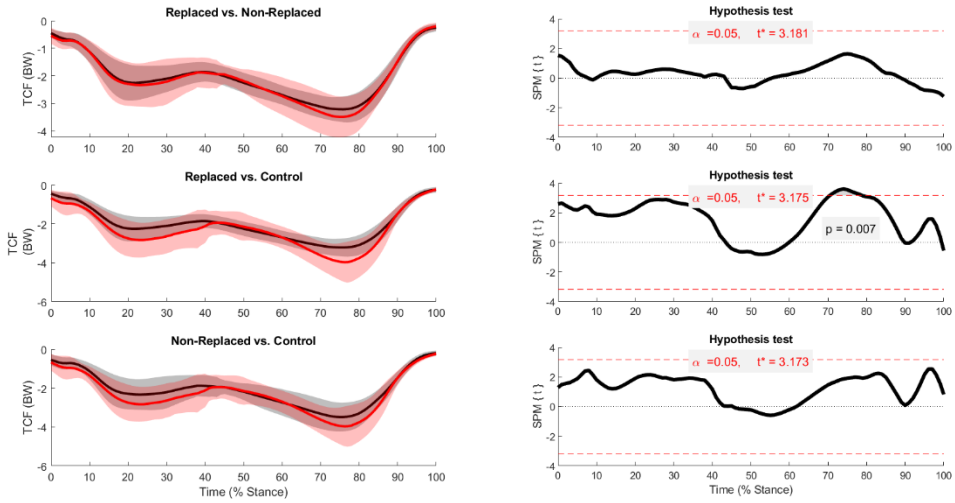

Figure 20. Main effect A (limb) post-hoc comparisons for TCF during uphill walking.

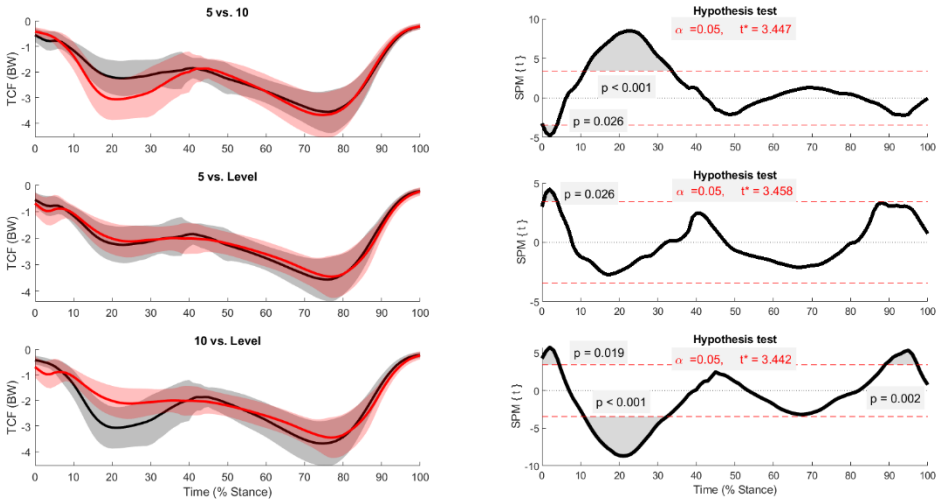

Figure 21. Main effect B (Slope) post-hoc comparisons for TCF during uphill walking.

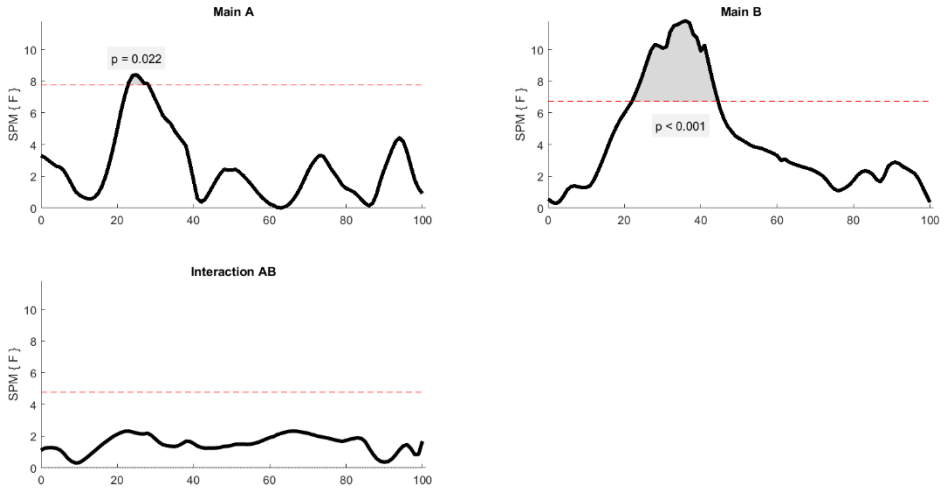

Figure 22. SPM interaction, main effect A (limb), and main effect B (slope) for MCF during uphill walking.

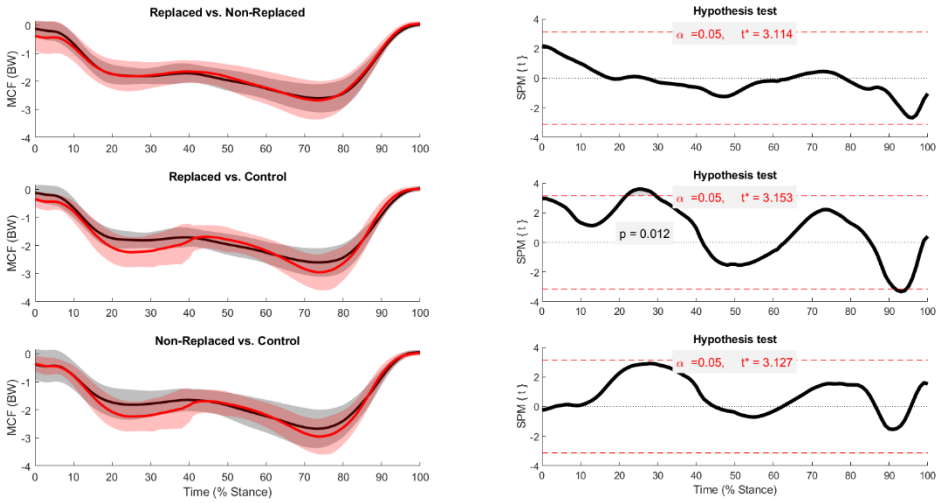

Figure 23. Main effect (Limb) post-hoc comparisons for MCF during uphill walking.

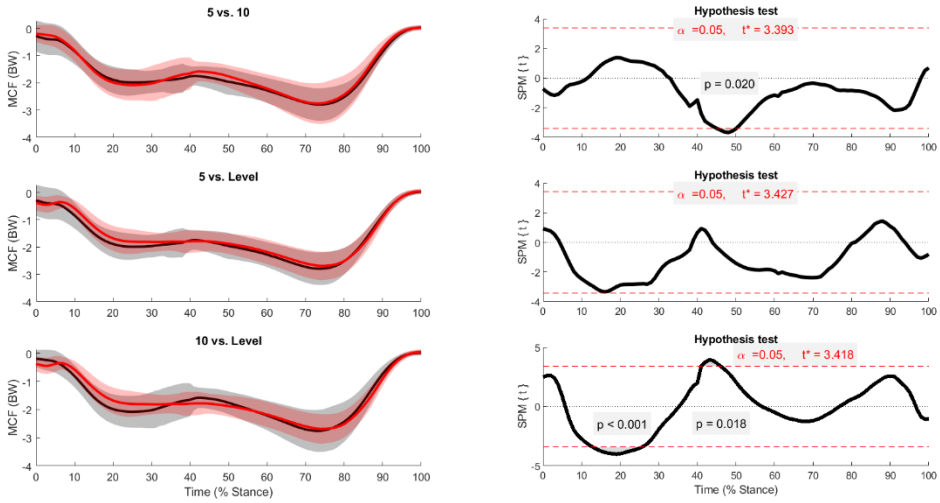

Figure 24. Main effect (Slope) post-hoc comparisons for MCF during uphill walking.

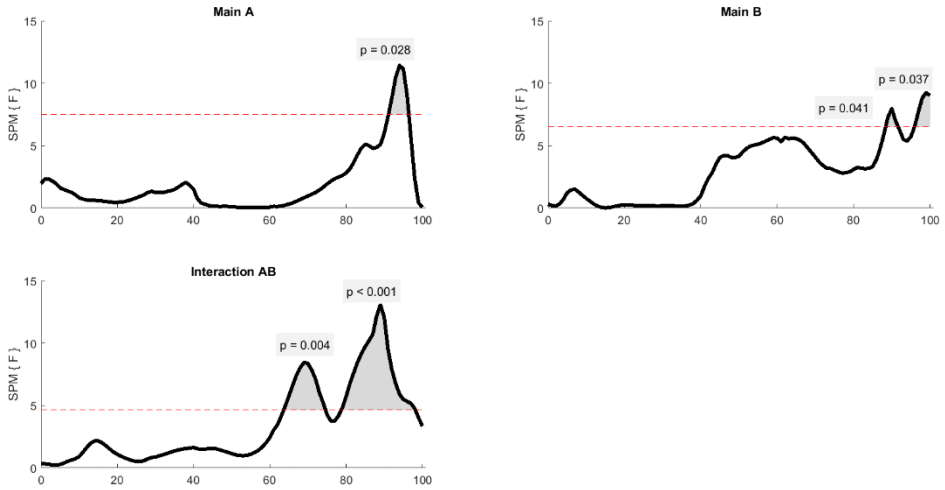

Figure 25. SPM interaction, main effect A (limb), and main effect B (slope) for LCF during uphill walking.

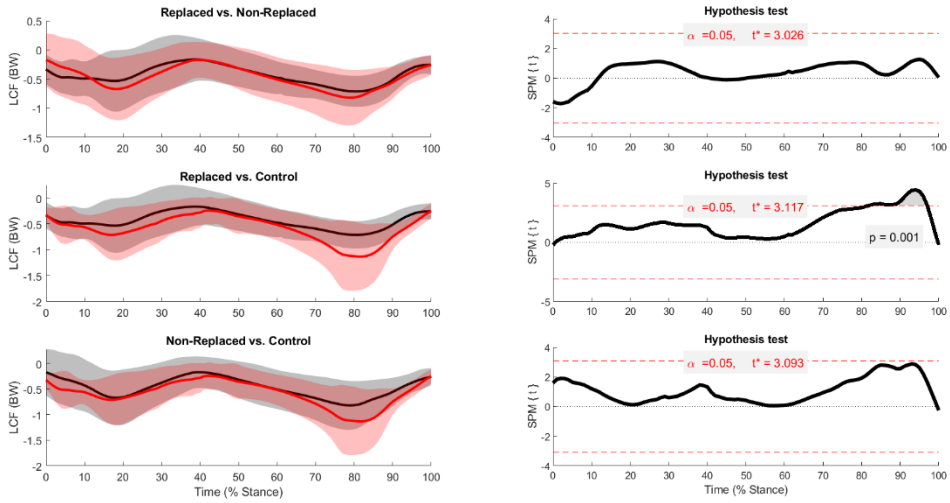

Figure 26. Main effect (Limb) post-hoc comparisons for LCF during uphill walking.

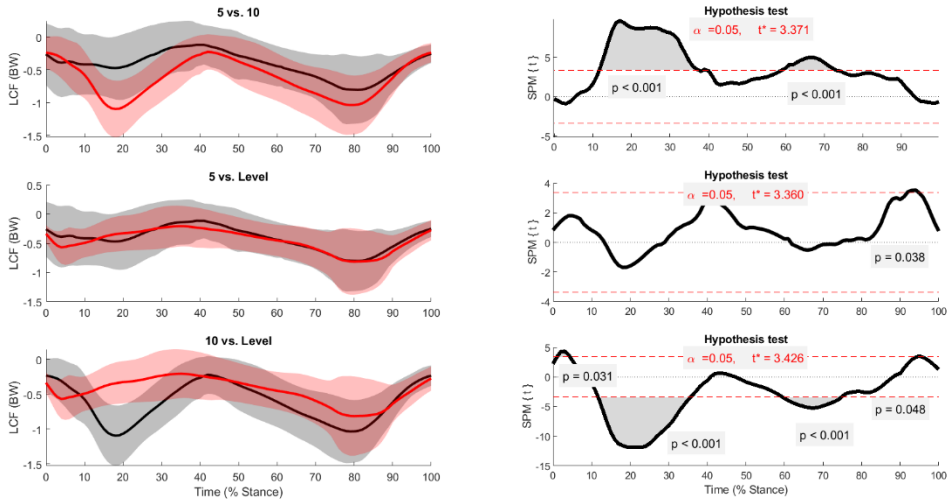

Figure 27. Main effect (Slope) post-hoc comparisons for LCF during uphill walking.

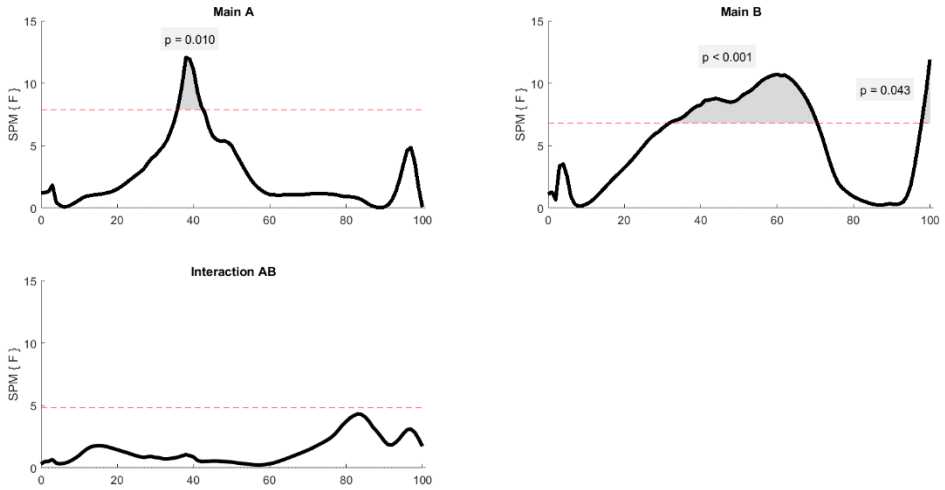

Figure 28. SPM interaction, main effect A (limb), and main effect B (slope) for knee extensor muscle force during uphill walking.

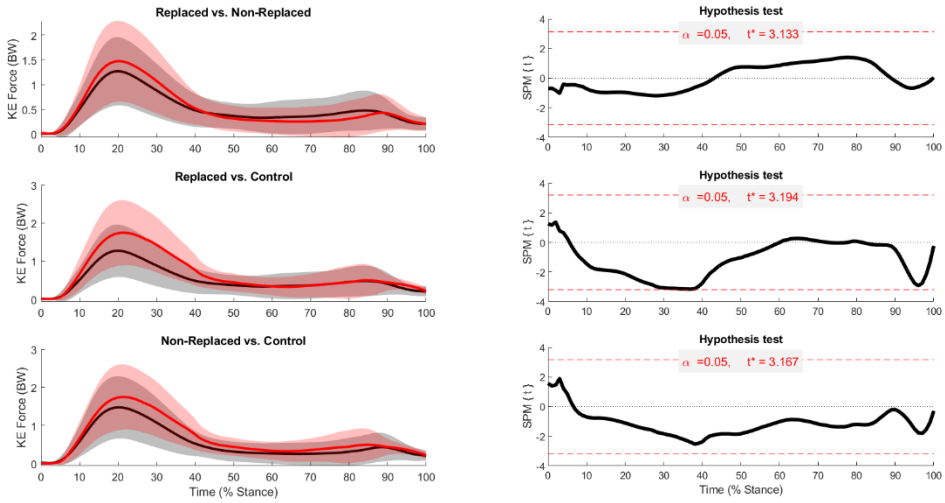

Figure 29. Main effect (Limb) post-hoc comparisons for knee extensor muscle force during uphill walking.

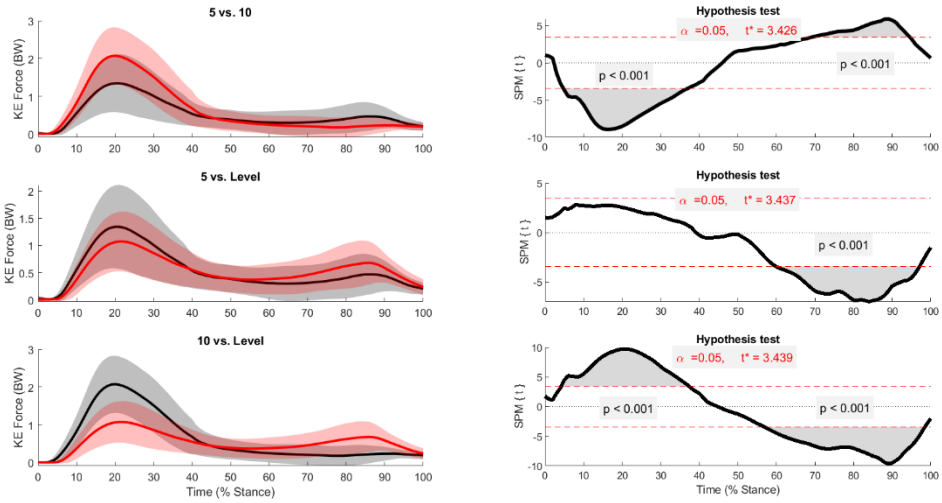

Figure 30. Main effect (Slope) post-hoc comparisons for knee extensor muscle force during uphill walking.

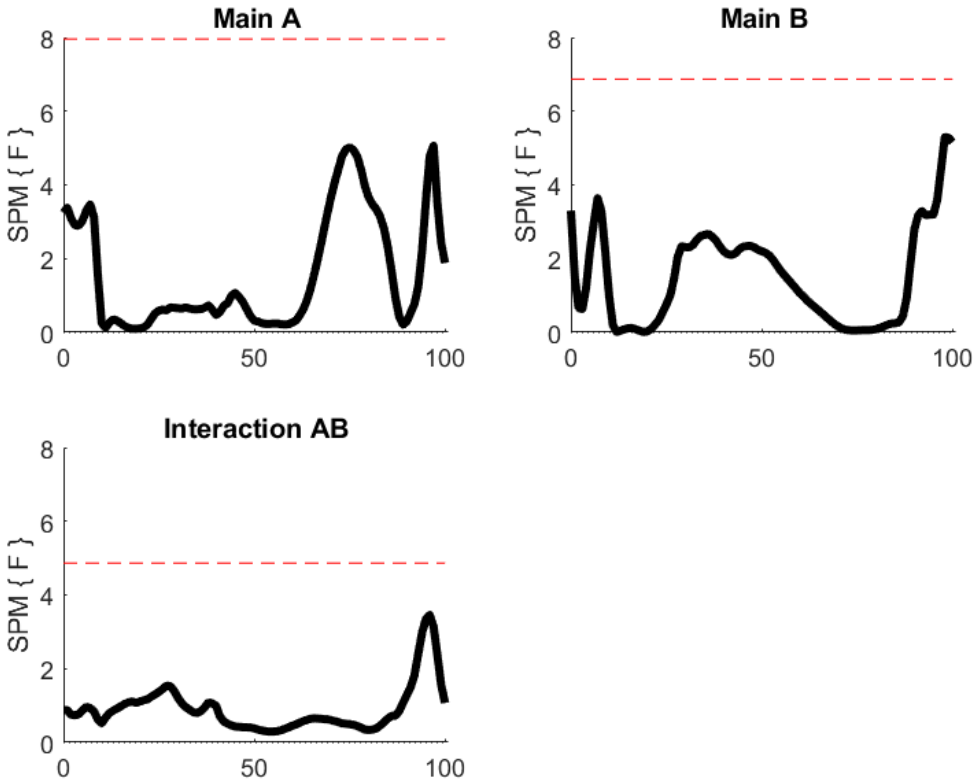

Figure 31. SPM interaction, main effect A (limb), and main effect B (slope) for knee flexor muscle force during uphill walking.

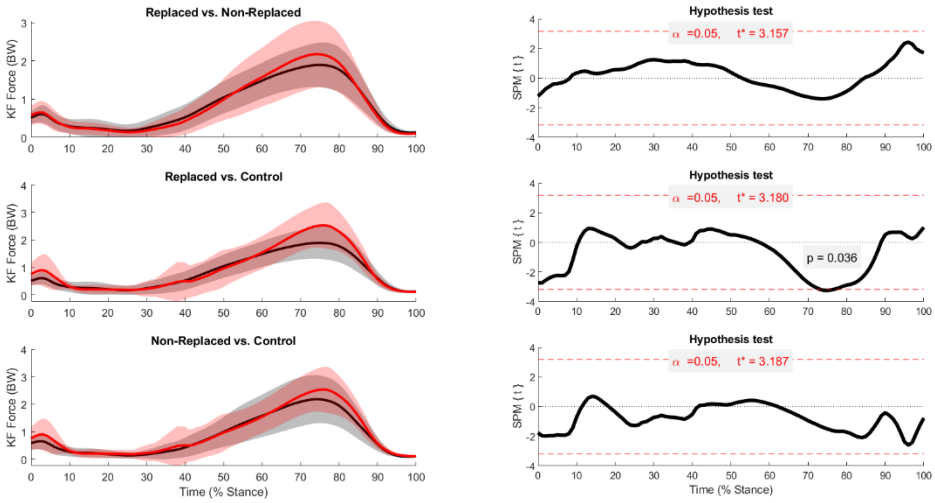

Figure 32. Main effect (Limb) post-hoc comparisons for knee flexor muscle force during uphill walking.

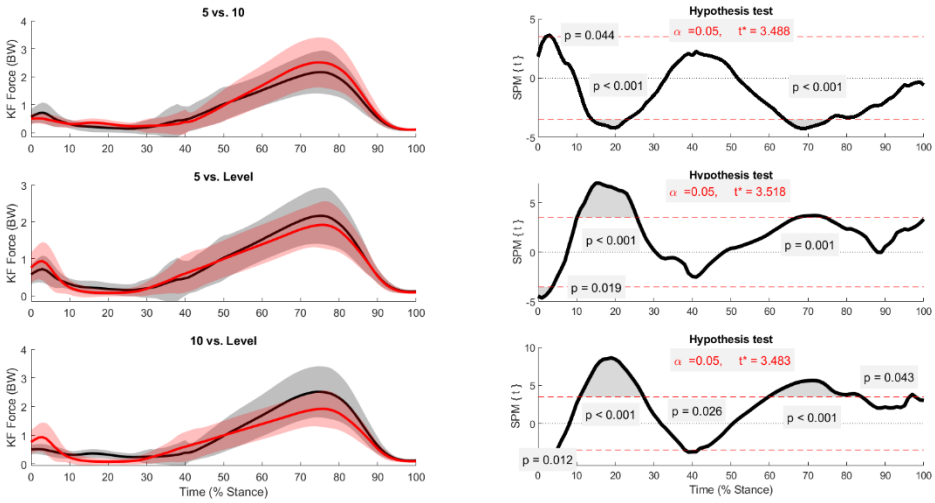

Figure 33. Main effect (Slope) post-hoc comparisons for knee flexor muscle force during uphill walking.

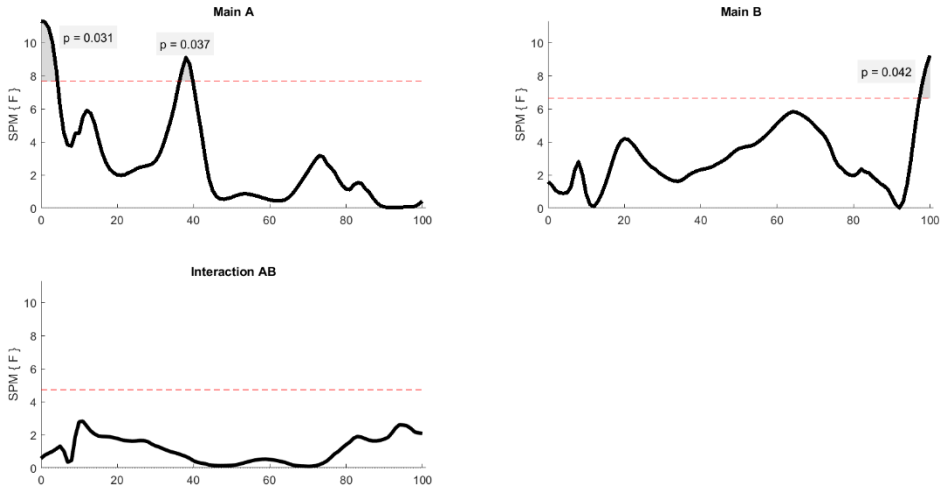

Figure 34 SPM interaction, main effect A (limb), and main effect B (slope) for TCF during downhill walking.

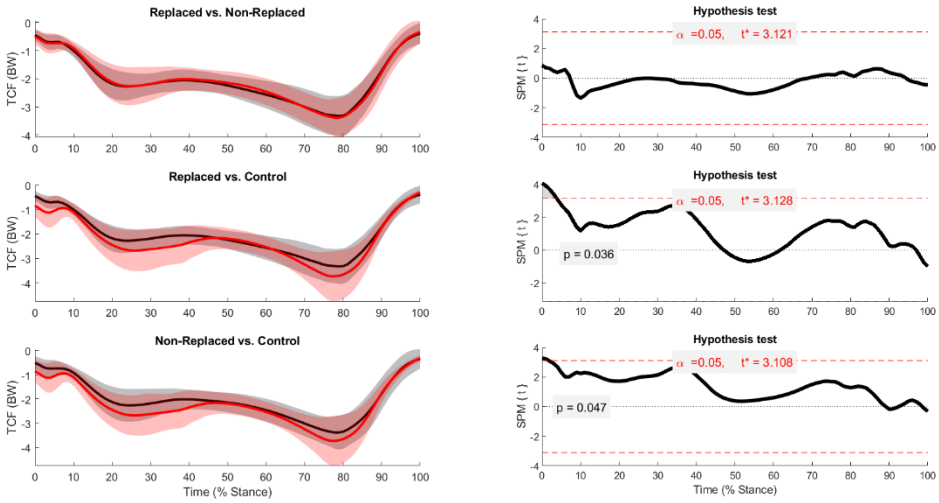

Figure 35. Main effect (Limb) post-hoc comparisons for TCF during downhill walking.

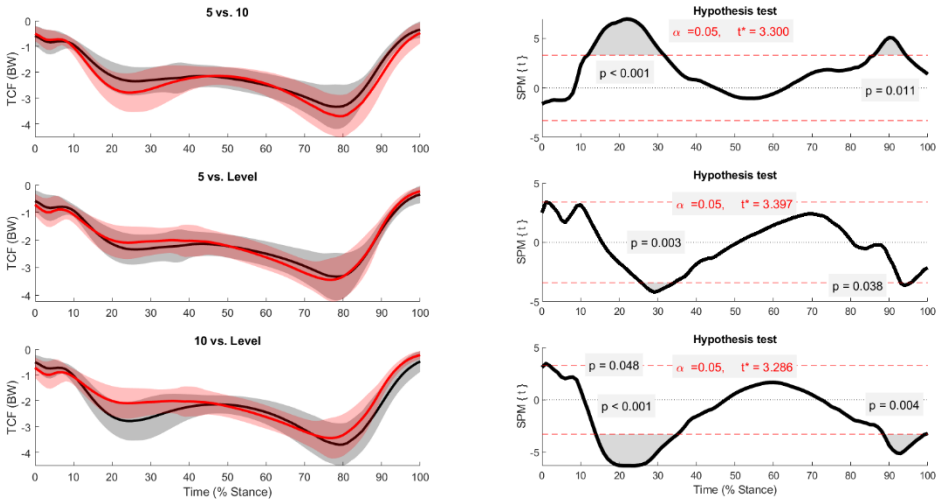

Figure 36. Main effect (Slope) post-hoc comparisons for TCF during downhill walking.

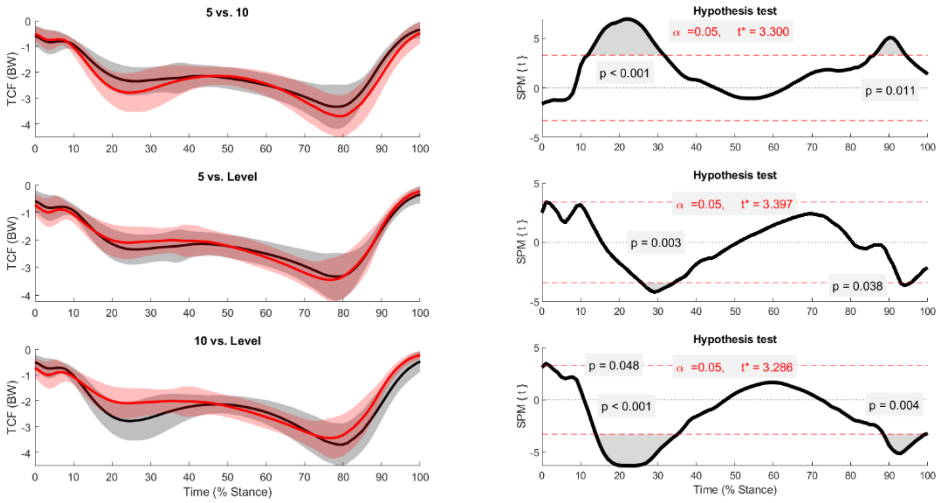

Figure 37. Main effect (Slope) post-hoc comparisons for TCF during downhill walking.

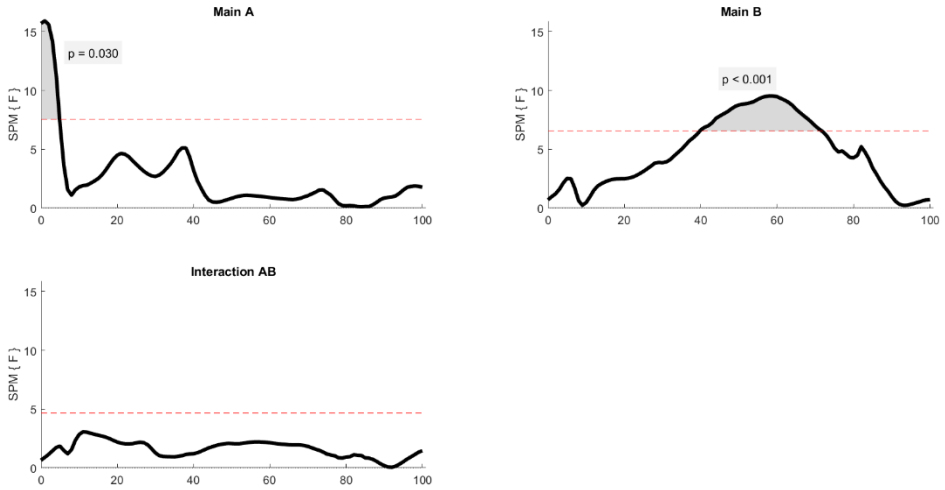

Figure 38. SPM interaction, main effect A (limb), and main effect B (slope) for MCF during downhill walking.

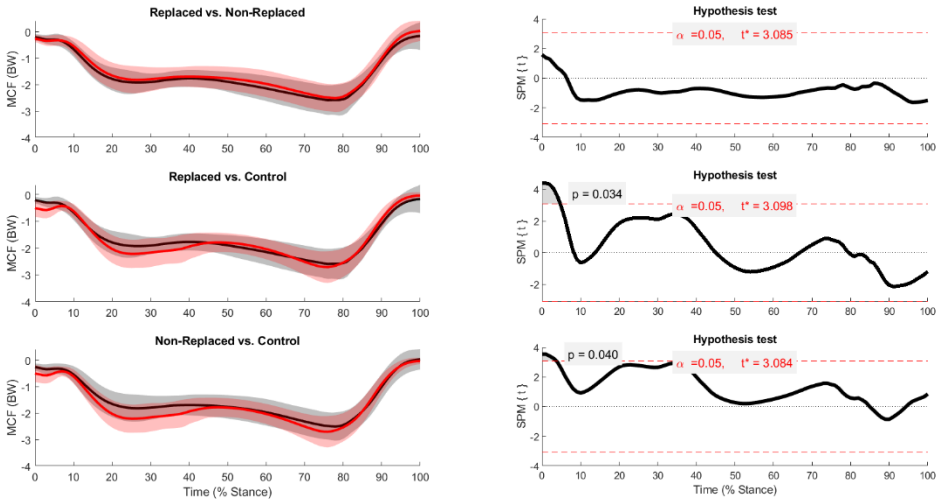

Figure 39. Main effect (Limb) post-hoc comparisons for MCF during downhill walking.

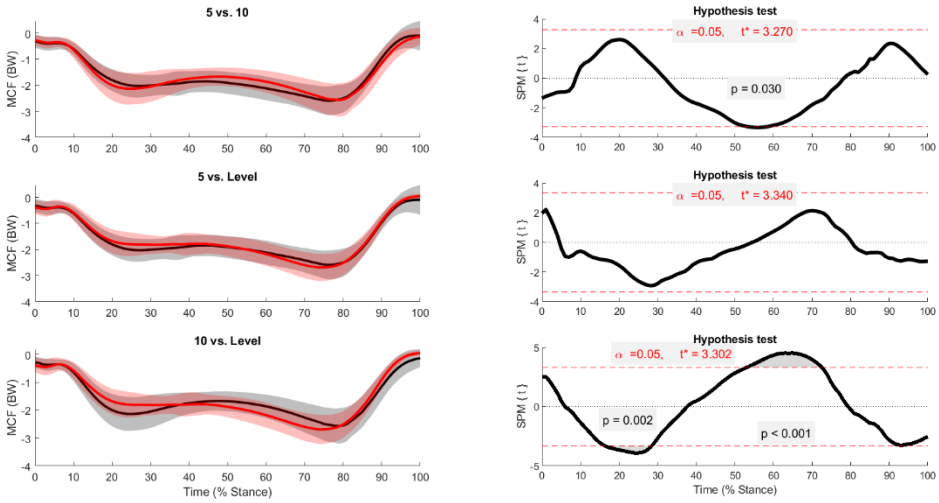

Figure 40. Main effect (Slope) post-hoc comparisons for MCF during downhill walking.

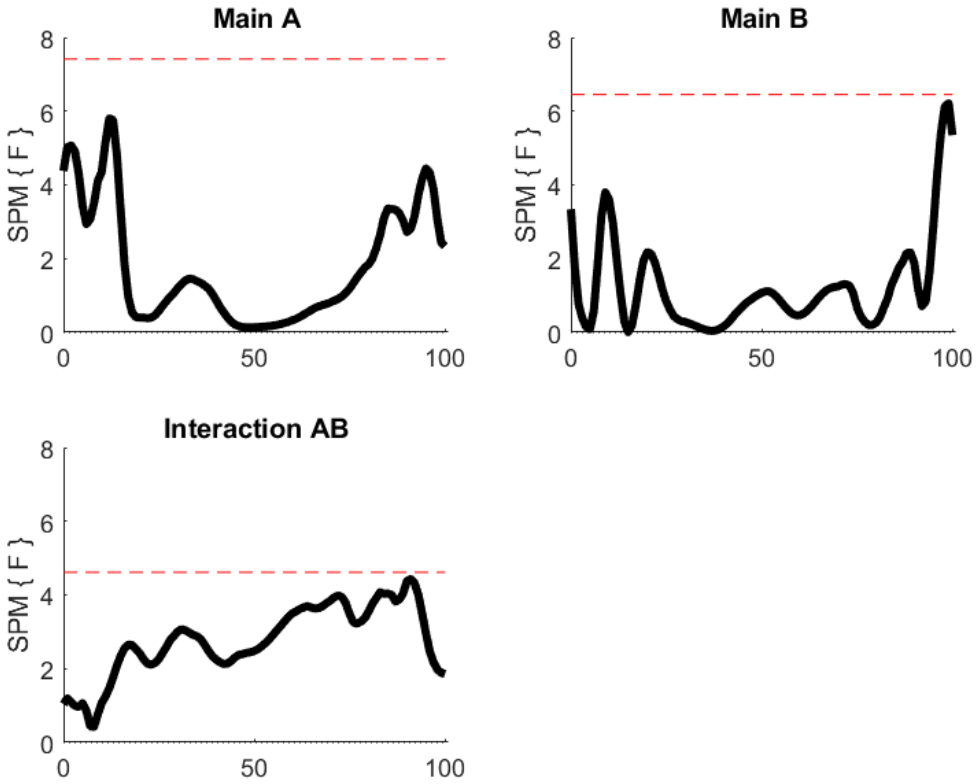

Figure 41. SPM interaction, main effect A (limb), and main effect B (slope) for LCF during downhill walking.

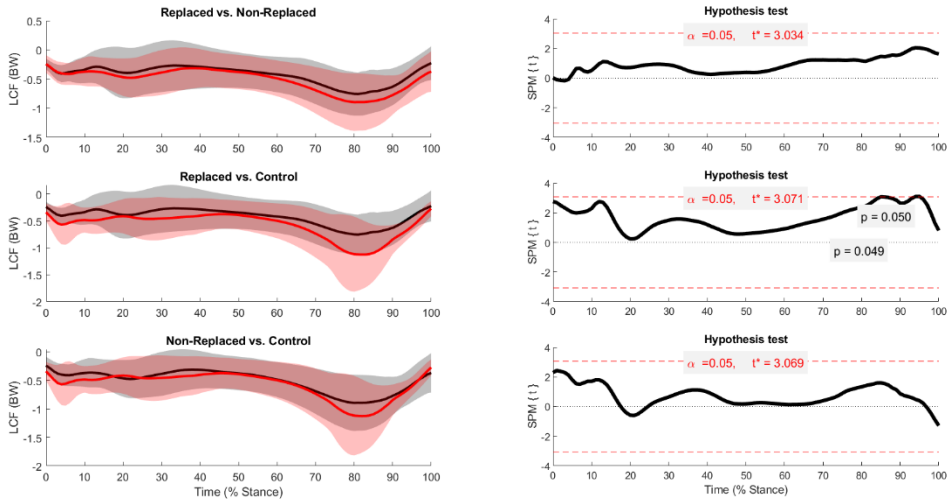

Figure 42. Main effect (Limb) post-hoc comparisons for LCF during downhill walking.

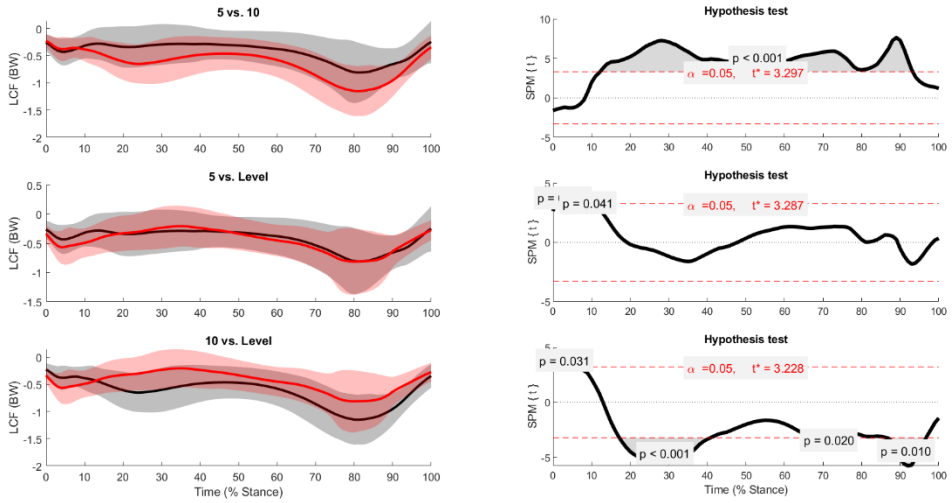

Figure 43. Main effect (Slope) post-hoc comparisons for LCF during downhill walking.

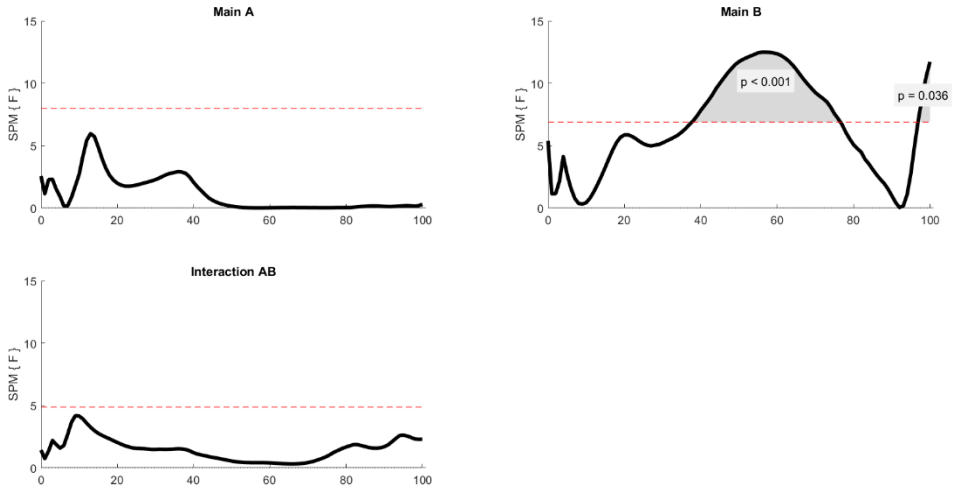

Figure 44. SPM interaction, main effect A (limb), and main effect B (slope) for knee extensor muscle forces during downhill walking.

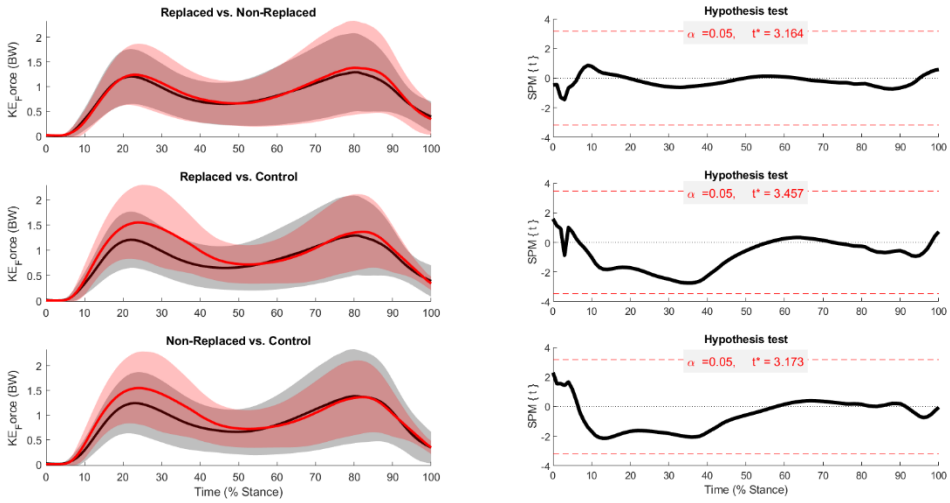

Figure 45. Main effect (Limb) post-hoc comparisons for knee extensor muscle forces during downhill walking.

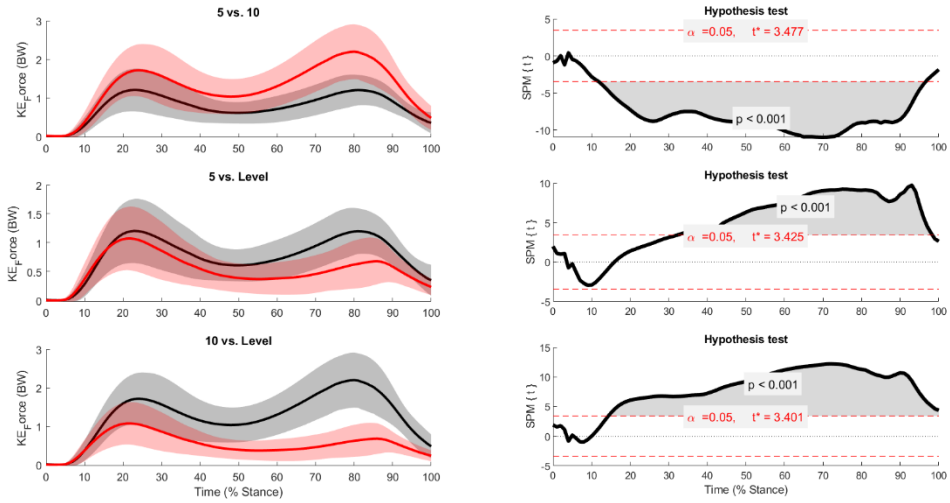

Figure 46. Main effect (Slope) post-hoc comparisons for knee extensor muscle forces during downhill walking.

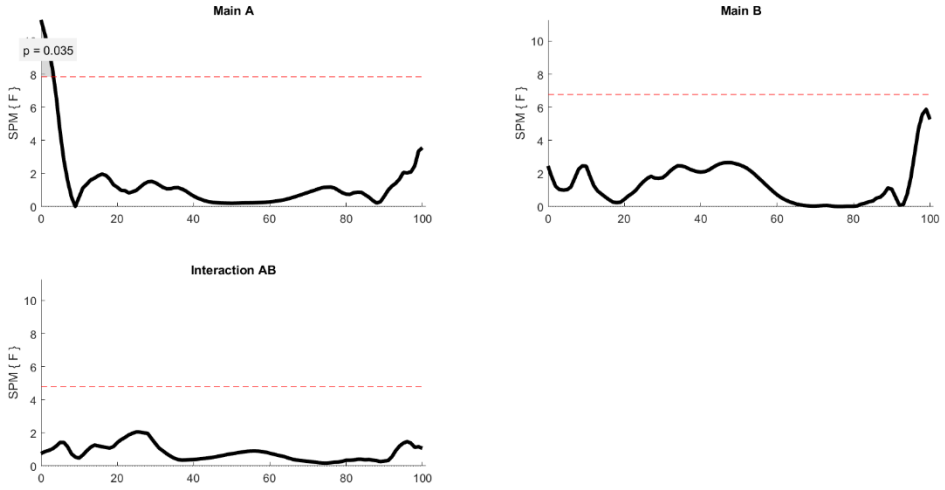

Figure 47. SPM interaction, main effect A (limb), and main effect B (slope) for knee flexor muscle force during downhill walking.

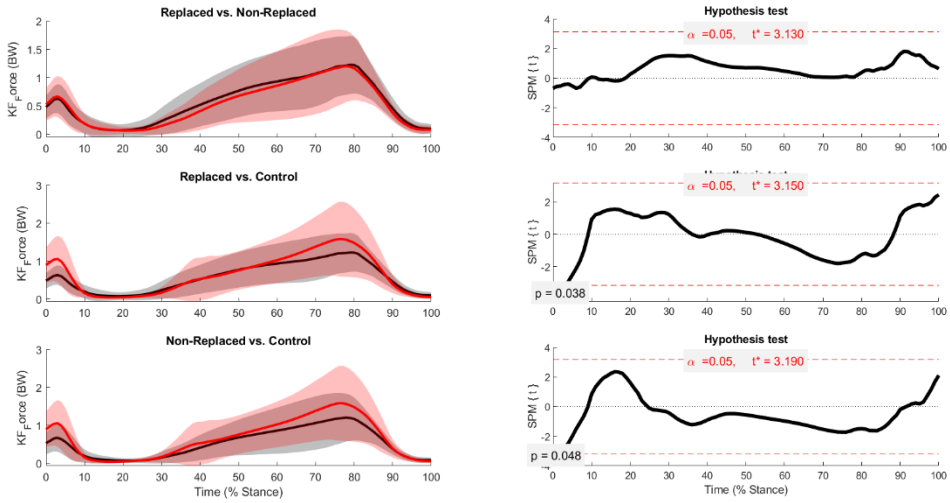

Figure 48. Main effect (Limb) post-hoc comparisons for knee flexor muscle forces during downhill walking.

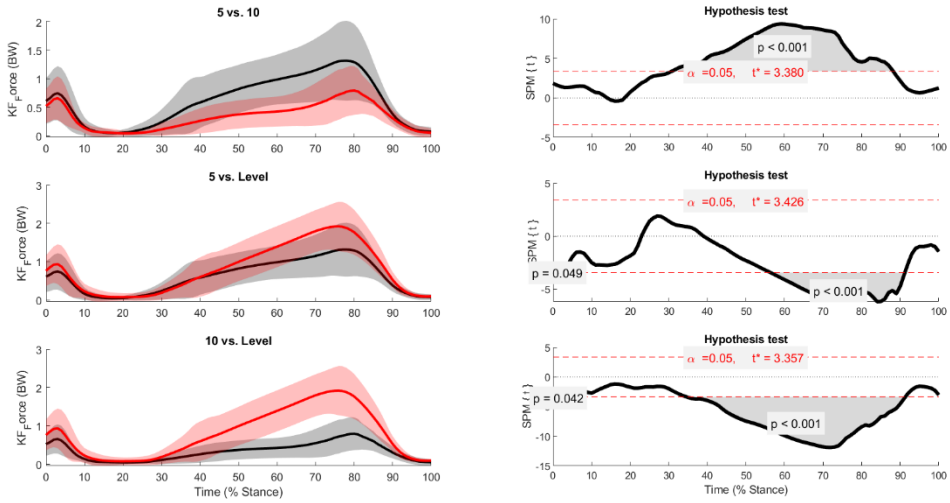

Figure 49. Main effect (Slope) post-hoc comparisons for knee flexor muscle forces during downhill walking.

Appendix G – Reserve Torque Actuator Comparisons

Table 19. Average reserve torque actuators of the hip joint during level walking for the replaced limb.

	Hip Flexion		Hip Abduction		Hip Rotation	
Subject	Hicks	Average	Hicks	Average	Hicks	Average
S2	-2.553	0.003	-3.727	-0.012	0.347	0.000
S3	-1.186	0.001	-3.968	-0.004	0.650	0.000
S11	-2.180	0.002	-4.938	-0.027	0.551	-0.003
S13	-1.592	0.003	-4.872	-0.027	0.613	0.029
S16	-3.643	-0.001	-6.695	-0.045	1.254	0.010
S19	-0.919	0.005	-4.030	-0.031	0.431	-0.010
S22	-2.052	0.005	-4.099	-0.015	0.452	-0.002
S24	-2.758	-0.001	-4.277	-0.010	1.199	-0.003
S28	-1.787	0.003	-5.011	-0.015	0.456	0.001
Mean	-2.074	0.002	-4.624	-0.021	0.661	0.002
S.D.	0.837	0.002	0.907	0.013	0.334	0.011

Table 20. Average reserve torque actuators of the knee joint during level walking for the replaced limb.

	Knee Angle		Ankle Angle	
Subject	Hicks	Average	Hicks	Average
S2	1.514	-0.003	-4.611	0.000
S3	1.763	-0.004	-0.087	0.003
S11	1.389	-0.006	-4.137	-0.001
S13	2.613	-0.005	-6.196	-0.007
S16	3.522	-0.005	-6.379	0.000
S19	2.319	-0.007	-5.303	0.001
S22	2.161	-0.005	-5.776	0.000
S24	3.439	0.000	-5.906	0.000
S28	0.543	-0.006	-4.489	0.002
Mean	2.140	-0.005	-4.765	0.000
S.D.	0.968	0.002	1.925	0.003

Table 21. Average reserve torque actuators of the hip joint during 5° uphill walking for the replaced limb.

	Hip Flexion		Hip Abduction		Hip Rotation	
Subject	Hicks	Average	Hicks	Average	Hicks	Average
S2	-4.352	-0.022	-3.406	-0.124	1.429	0.039
S3	-2.170	0.001	-3.387	-0.009	0.640	-0.001
S11	-2.016	0.000	-5.303	-0.016	0.775	-0.008
S13	-2.340	0.001	-5.123	-0.008	0.588	-0.002
S16	-5.517	-0.001	-5.532	-0.016	1.281	-0.002
S19	-0.908	0.002	-3.526	-0.011	0.396	-0.005
S22	-2.341	0.001	-4.578	-0.015	0.377	-0.002
S24	-2.996	-0.001	-3.659	-0.009	1.223	-0.003
S28	-2.861	0.003	-6.865	-0.016	3.865	-0.005
Mean	-2.833	-0.002	-4.598	-0.025	1.175	0.001
S.D.	1.362	0.008	1.209	0.037	1.081	0.014

Table 22. Average reserve torque actuators of the knee joint during 5° uphill walking for the replaced limb.

	Knee Angle		Ankle Angle	
Subject	Hicks	Average	Hicks	Average
S2	2.994	-0.003	-4.234	0.001
S3	1.619	-0.003	-5.242	0.000
S11	1.196	-0.003	-4.411	0.000
S13	2.090	-0.003	-5.969	-0.001
S16	1.939	-0.002	-6.627	0.000
S19	2.057	-0.003	-5.632	0.000
S22	1.316	-0.008	-4.831	0.003
S24	4.062	0.000	-6.439	-0.004
S28	1.543	-0.007	-4.748	0.000
Mean	2.091	-0.004	-5.348	0.000
S.D.	0.912	0.002	0.870	0.002

Table 23. Average reserve torque actuators of the hip joint during 10° uphill walking for the replaced limb.

	Hip Flexion		Hip Abduction		Hip Rotation	
Subject	Hicks	Average	Hicks	Average	Hicks	Average
S2	-3.683	-0.001	-2.574	-0.012	0.773	-0.003
S3	-2.496	-0.175	-3.367	-1.220	0.601	2.045
S11	-2.957	-0.003	-4.925	-0.031	0.843	-0.020
S13	-3.305	0.002	-4.171	-0.022	0.728	-0.012
S16	-5.572	-0.002	-4.254	-0.012	0.914	-0.004
S19	-1.112	0.003	-3.384	-0.024	0.598	-0.007
S22	-6.297	0.003	-25.534	-16.770	4.298	-3.593
S24	-3.917	-0.002	-3.955	-0.008	1.415	-0.003
S28	-3.794	0.001	-4.984	-0.015	1.251	-0.006
Mean	-3.682	-0.019	-6.350	-2.013	1.269	-0.178
S.D.	1.547	0.058	7.235	5.548	1.169	1.449

Table 24. Average reserve torque actuators of the knee joint during 10° uphill walking for the replaced limb.

	Knee Angle		Ankle Angle	
Subject	Hicks	Average	Hicks	Average
S2	3.137	-0.002	-4.817	-0.003
S3	1.483	-0.013	-5.581	-0.002
S11	1.627	-0.004	-4.417	-0.003
S13	2.702	-0.010	-7.221	-0.003
S16	2.765	-0.004	-6.847	0.000
S19	3.277	-0.004	-5.764	-0.001
S22	2.614	-0.006	-6.400	0.002
S24	4.347	0.001	-6.437	-0.002
S28	2.373	-0.008	-4.848	0.002
Mean	2.703	-0.006	-5.815	-0.001
S.D.	0.865	0.004	0.982	0.002

Table 25. Average reserve torque actuators of the hip joint during level walking for the non-replaced limb.

	Hip Flexion		Hip Abduction		Hip Rotation	
Subject	Hicks	Average	Hicks	Average	Hicks	Average
S2	-2.360	0.001	-2.405	-0.006	0.383	0.002
S3	-1.868	0.001	-2.589	-0.003	0.545	0.000
S11	-1.683	0.002	-4.415	-0.030	0.396	-0.004
S13	-1.523	0.004	-5.336	-0.016	0.383	0.003
S16	-4.145	0.001	-4.558	-0.010	1.016	-0.005
S19	-3.675	-0.022	-9.395	0.265	0.592	0.003
S22	-2.021	0.001	-4.372	-0.011	0.198	-0.001
S24	-1.768	0.001	-4.460	-0.016	0.850	-0.002
S28	-1.033	0.001	-4.804	-0.014	0.059	0.000
Mean	-2.230	-0.001	-4.704	0.018	0.492	0.000
S.D.	1.024	0.008	2.014	0.093	0.300	0.003

Table 26. Average reserve torque actuators of the knee joint during level walking for the non-replaced limb.

	Knee Angle		Ankle Angle	
Subject	Hicks	Average	Hicks	Average
S2	1.183	-0.002	-4.270	0.001
S3	1.418	-0.003	-0.060	0.002
S11	1.630	-0.010	-4.299	0.001
S13	1.493	-0.003	-6.526	-0.001
S16	3.753	-0.011	-6.915	0.002
S19	3.166	-0.005	-5.277	0.002
S22	1.307	-0.005	-5.100	0.001
S24	3.696	0.000	-6.535	-0.001
S28	0.445	-0.014	-4.439	0.004
Mean	2.010	-0.006	-4.825	0.001
S.D.	1.205	0.005	2.059	0.002

Table 27. Average reserve torque actuators of the hip joint during 5° uphill walking for the non-replaced limb.

	Hip Flexion		Hip Abduction		Hip Rotation	
Subject	Hicks	Average	Hicks	Average	Hicks	Average
S2	-0.908	0.002	-3.055	-0.001	0.060	0.000
S3	-2.348	0.000	-4.009	-0.020	0.859	0.038
S11	-2.835	0.001	-5.577	-0.018	0.788	-0.009
S13	-3.156	0.004	-5.858	-0.016	0.691	0.000
S16	-5.313	0.001	-4.780	-0.011	1.417	-0.005
S19	-1.713	0.001	-3.471	-0.006	0.578	-0.002
S22	-2.266	0.005	-3.068	-0.015	0.294	-0.010
S24	-3.864	0.002	-4.178	-0.014	0.765	-0.004
S28	-2.091	0.001	-4.514	-0.009	0.681	-0.007
Mean	-2.722	0.002	-4.279	-0.012	0.681	0.000
S.D.	1.288	0.002	1.012	0.006	0.377	0.015

Table 28. Average reserve torque actuators of the knee joint during 5° uphill walking for the non-replaced limb.

	Knee Angle		Ankle Angle	
Subject	Hicks	Average	Hicks	Average
S2	1.259	-0.002	-4.317	0.001
S3	1.937	-0.002	-4.055	-0.001
S11	1.576	-0.004	-4.871	0.000
S13	1.165	-0.004	-6.123	-0.008
S16	3.649	-0.006	-7.282	0.002
S19	2.324	-0.002	-5.181	0.001
S22	1.932	-0.016	-5.236	0.004
S24	2.904	0.000	-6.860	-0.001
S28	0.293	-0.009	-5.108	0.000
Mean	1.893	-0.005	-5.448	0.000
S.D.	0.993	0.005	1.095	0.003

Table 29. Average reserve torque actuators of the hip joint during 10° uphill walking for the non-replaced limb.

	Hip Flexion		Hip Abduction		Hip Rotation	
Subject	Hicks	Average	Hicks	Average	Hicks	Average
S2	-3.052	0.000	-2.152	-0.008	0.719	0.002
S3	-2.094	-0.061	-3.348	-0.160	0.978	0.638
S11	-3.311	0.001	-5.543	-0.203	1.177	-0.149
S13	-3.342	0.002	-4.399	-0.011	0.863	-0.003
S16	-4.845	0.000	-4.230	-0.010	1.208	-0.004
S19	-1.870	0.001	-3.613	-0.018	0.728	-0.005
S22	-3.358	0.001	-3.921	-0.014	0.968	-0.005
S24	-5.038	0.001	-4.557	-0.016	1.417	-0.004
S28	-2.971	0.000	-4.094	-0.011	0.691	-0.001
Mean	-3.320	-0.006	-3.984	-0.050	0.972	0.052
S.D.	1.065	0.021	0.929	0.075	0.253	0.225

Table 30. Average reserve torque actuators of the knee joint during 10° uphill walking for the non-replaced limb.

	Knee Angle		Ankle Angle	
Subject	Hicks	Average	Hicks	Average
S2	3.196	-0.001	-4.456	0.001
S3	2.574	-0.002	-4.874	-0.001
S11	2.791	-0.007	-5.091	-0.002
S13	2.521	-0.005	-7.022	-0.001
S16	5.144	-0.016	-7.242	0.003
S19	2.760	-0.005	-5.830	0.002
S22	6.160	-0.485	-5.886	0.511
S24	4.454	0.001	-6.629	-0.001
S28	0.701	-0.008	-4.995	0.001
Mean	3.367	-0.059	-5.781	0.057
S.D.	1.633	0.160	1.005	0.170

Table 31. Average reserve torque actuators of the hip joint during level walking for the control limb.

	Hip Flexion		Hip Abduction		Hip Rotation	
Subject	Hicks	Average	Hicks	Average	Hicks	Average
S17	-2.965	0.004	-4.347	-0.016	0.383	-0.004
S25	-2.588	0.004	-6.953	-0.017	1.447	0.001
S27	-3.500	0.000	-6.016	-0.011	1.587	-0.001
S29	-1.383	0.002	-3.357	-0.008	0.473	-0.001
S30	-2.494	0.006	-3.623	-0.020	0.374	-0.013
S32	-5.013	0.425	-4.047	-0.329	0.383	0.157
S33	-1.894	0.003	-3.017	-0.017	0.827	-0.002
S34	-0.397	0.003	-2.029	-0.009	0.188	0.002
S35	-0.712	0.004	-4.462	-0.015	0.464	-0.001
Mean	-2.327	0.050	-4.206	-0.049	0.681	0.015
S.D.	1.436	0.141	1.506	0.105	0.504	0.053

Table 32. Average reserve torque actuators of the knee joint during level walking for the control limb.

	Knee Angle		Ankle Angle	
Subject	Hicks	Average	Hicks	Average
S17	0.862	-0.006	-4.744	0.000
S25	4.467	-0.005	-7.667	0.000
S27	5.148	-0.001	-7.136	-0.001
S29	1.457	-0.002	-4.228	0.000
S30	1.752	-0.008	-3.846	0.002
S32	3.182	-0.300	-6.408	0.001
S33	2.508	-0.004	-3.741	0.001
S34	0.533	-0.002	-2.753	0.000
S35	1.223	-0.004	-3.920	0.000
Mean	2.348	-0.037	-4.938	0.000
S.D.	1.619	0.099	1.711	0.001

Table 33. Average reserve torque actuators of the hip joint during 5° uphill walking for the control limb.

	Hip Flexion		Hip Abduction		Hip Rotation	
Subject	Hicks	Average	Hicks	Average	Hicks	Average
S17	-2.571	0.002	-3.588	-0.014	0.648	-0.010
S25	-4.014	0.003	-5.583	-0.015	1.700	-0.001
S27	-4.8257	-0.0008	-5.8671	-0.0094	1.6943	-0.001
S29	-1.341	0.001	-3.126	-0.007	0.512	-0.001
S30	-2.670	0.002	-3.241	-0.021	0.874	-0.013
S32	-5.148	0.007	-3.581	-0.020	0.420	0.004
S33	-2.141	0.002	-2.359	-0.016	0.699	-0.007
S34	-0.719	0.003	-1.688	-0.009	0.353	0.000
S35	-1.080	0.003	-3.503	-0.011	0.345	0.000
Mean	-2.723	0.002	-3.615	-0.014	0.805	-0.003
S.D.	1.618	0.002	1.352	0.005	0.534	0.005

Table 34. Average reserve torque actuators of the knee joint during 5° uphill walking for the control limb.

	Knee Angle		Ankle Angle	
Subject	Hicks	Average	Hicks	Average
S17	1.732	-0.006	-5.291	0.000
S25	6.196	-0.006	-8.375	0.000
S27	5.7675	-0.0004	-6.7813	-0.0009
S29	1.504	-0.002	-4.158	0.000
S30	2.561	-0.004	-4.210	0.000
S32	2.468	-0.008	-6.659	-0.001
S33	2.306	-0.005	-3.587	0.001
S34	1.082	-0.003	-3.093	0.000
S35	0.716	-0.004	-4.175	0.000
Mean	2.704	-0.004	-5.148	0.000
S.D.	1.962	0.003	1.762	0.001

Table 35. Average reserve torque actuators of the hip joint during 10° uphill walking for the control limb.

	Hip Flexion		Hip Abduction		Hip Rotation	
Subject	Hicks	Average	Hicks	Average	Hicks	Average
S17	-2.735	0.001	-3.396	-0.012	0.827	-0.008
S25	-5.253	0.001	-5.631	-0.012	1.742	-0.004
S27	-5.394	-0.002	-5.642	-0.008	1.886	-0.001
S29	-2.769	0.000	-3.029	-0.009	0.563	-0.005
S30	-3.051	0.002	-2.528	-0.018	0.778	-0.005
S32	-3.084	0.004	-4.179	-0.021	0.421	0.010
S33	-2.115	0.001	-2.431	-0.014	0.824	-0.006
S34	-0.723	0.002	-1.942	-0.013	0.562	0.002
S35	-3.007	0.000	-4.696	-0.010	1.169	-0.003
Mean	-3.125	0.001	-3.719	-0.013	0.975	-0.002
S.D.	1.448	0.002	1.385	0.004	0.523	0.005

Table 36. Average reserve torque actuators of the knee joint during 10° uphill walking for the control limb.

	Knee Angle		Ankle Angle	
Subject	Hicks	Average	Hicks	Average
S17	2.546	-0.004	-5.686	-0.001
S25	7.922	-0.003	-7.842	0.000
S27	6.295	0.000	-7.163	-0.001
S29	1.358	-0.001	-4.656	0.000
S30	2.948	-0.004	-4.937	0.000
S32	2.828	-0.007	-6.221	0.000
S33	2.524	-0.004	-4.008	0.000
S34	1.525	-0.002	-2.803	-0.001
S35	3.630	-0.002	-4.248	-0.001
Mean	3.509	-0.003	-5.285	0.000
S.D.	2.194	0.002	1.600	0.001

Table 37. Average reserve torque actuators of the hip joint during 5° downhill walking for the replaced limb.

	Hip Flexion		Hip Abduction		Hip Rotation	
Subject	Hicks	Average	Hicks	Average	Hicks	Average
S2	-2.696	0.002	-3.762	-0.011	0.436	0.002
S3	-2.170	0.001	-3.387	-0.009	0.640	-0.001
S11	-1.449	0.000	-4.849	-0.008	0.749	0.003
S13	-2.144	0.001	-4.887	-0.009	0.626	0.017
S16	-2.993	-0.001	-5.383	-0.008	0.779	0.002
S19	-0.777	0.002	-3.592	-0.010	0.333	-0.002
S22	-1.702	0.002	-5.535	-0.013	0.213	0.000
S24	-1.440	0.000	-3.970	-0.006	1.014	0.000
S28	-1.226	0.000	-4.547	-0.019	0.959	0.032
Mean	-1.844	0.001	-4.435	-0.010	0.639	0.006
S.D.	0.716	0.001	0.789	0.004	0.272	0.011

Table 38. Average reserve torque actuators of the knee joint during 5° downhill walking for the replaced limb.

	Knee Angle		Ankle Angle	
Subject	Hicks	Average	Hicks	Average
S2	1.602	-0.002	-3.792	0.000
S3	1.619	-0.003	-5.242	0.000
S11	2.571	0.000	-3.758	-0.001
S13	2.985	0.000	-5.855	-0.003
S16	3.006	0.000	-5.650	0.000
S19	1.697	-0.002	-5.058	0.001
S22	1.788	-0.004	-5.143	0.002
S24	4.501	0.001	-5.956	-0.003
S28	1.377	-0.002	-4.172	0.001
Mean	2.350	-0.001	-4.958	0.000
S.D.	1.018	0.002	0.853	0.002

Table 39. Average reserve torque actuators of the hip joint during 10° downhill walking for the replaced limb.

	Hip Flexion		Hip Abduction		Hip Rotation	
Subject	Hicks	Average	Hicks	Average	Hicks	Average
S2	-2.066	0.001	-4.152	-0.009	0.614	0.004
S3	-1.097	-0.096	-3.985	-1.308	0.567	0008
S11	-1.837	0.000	-4.931	-0.008	0.844	0.004
S13	-1.579	0.001	-4.686	-0.005	0.640	0.006
S16	-3.447	-0.001	-5.622	-0.008	1.078	0.004
S19	-1.375	0.003	-4.025	-0.010	0.390	-0.001
S22	-0.800	0.002	-4.194	-0.009	0.614	0.001
S24	-1.019	0.000	-3.859	-0.005	1.137	0.001
S28	-0.802	-0.009	-4.781	-0.065	0.884	0.124
Mean	-1.558	-0.011	-4.471	-0.159	0.752	0.780
S.D.	0.836	0.032	0.577	0.431	0.249	2.285

Table 40. Average reserve torque actuators of the knee joint during 10° downhill walking for the replaced limb.

	Knee Angle		Ankle Angle	
Subject	Hicks	Average	Hicks	Average
S2	2.845	-0.001	-3.528	-0.001
S3	2.883	-0.001	-4.162	0.002
S11	3.423	0.000	-3.304	0.000
S13	4.505	0.000	-5.293	-0.002
S16	5.723	0.001	-4.676	0.000
S19	1.924	-0.001	-4.751	0.001
S22	2.555	-0.001	-4.555	0.000
S24	5.247	0.001	-5.326	-0.002
S28	3.236	-0.001	-4.076	0.002
Mean	3.593	0.000	-4.408	0.000
S.D.	1.284	0.001	0.707	0.001

Table 41. Average reserve torque actuators of the hip joint during 5° downhill walking for the non-replaced limb.

	Hip Flexion		Hip Abduction		Hip Rotation	
Subject	Hicks	Average	Hicks	Average	Hicks	Average
S2	-2.956	0.003	-3.568	-0.006	0.898	0.009
S3	-1.459	-0.004	-2.788	-0.018	0.479	0.092
S11	-0.576	0.001	-5.003	-0.012	0.374	0.001
S13	-1.094	0.003	-4.679	-0.003	0.165	0.001
S16	-2.280	0.001	-5.421	-0.008	1.112	0.002
S19	-1.096	0.002	-3.794	-0.005	0.585	-0.002
S22	-1.288	0.004	-4.359	-0.013	0.424	0.000
S24	-1.340	0.001	-4.905	-0.014	0.939	0.000
S28	-0.848	0.001	-7.552	-0.073	0.659	0.068
Mean	-1.437	0.001	-4.674	-0.017	0.626	0.019
S.D.	0.739	0.002	1.353	0.021	0.306	0.035

Table 42. Average reserve torque actuators of the knee joint during 5° downhill walking for the non-replaced limb.

	Knee Angle		Ankle Angle	
Subject	Hicks	Average	Hicks	Average
S2	3.089	0.000	-3.838	0.000
S3	2.284	0.000	-4.079	0.000
S11	1.810	-0.003	-3.972	0.000
S13	1.172	-0.001	-6.340	0.000
S16	3.348	0.000	-6.707	0.001
S19	2.181	-0.001	-4.836	0.001
S22	2.102	-0.005	-5.223	0.000
S24	4.254	0.000	-6.280	-0.003
S28	2.088	-0.008	-4.170	0.001
Mean	2.481	-0.002	-5.049	0.000
S.D.	0.926	0.003	1.137	0.001

Table 43. Average reserve torque actuators of the hip joint during 10° downhill walking for the non-replaced limb.

	Hip Flexion		Hip Abduction		Hip Rotation	
Subject	Hicks	Average	Hicks	Average	Hicks	Average
S2	-1.948	0.001	-2.988	-0.004	1.075	0.006
S3	-1.022	0.002	-3.141	-0.006	0.491	0.003
S11	-1.186	0.001	-4.351	-0.009	0.699	0.001
S13	-1.744	0.002	-4.725	-0.011	0.583	0.001
S16	-2.647	0.001	-5.481	-0.008	1.273	0.002
S19	-0.994	0.002	-3.891	-0.004	0.580	0.000
S22	-1.002	0.002	-3.695	-0.008	0.591	0.003
S24	-1.337	0.001	-5.308	-0.014	1.336	0.003
S28	-0.759	0.001	-5.697	-0.522	0.700	0.662
Mean	-1.405	0.001	-4.364	-0.065	0.814	0.076
S.D.	0.602	0.000	1.007	0.171	0.324	0.220

Table 44. Average reserve torque actuators of the knee joint during 10° downhill walking for the non-replaced limb.

	Knee Angle		Ankle Angle	
Subject	Hicks	Average	Hicks	Average
S2	4.196	0.001	-3.371	-0.001
S3	3.688	0.001	-4.923	-0.001
S11	3.872	0.000	-4.073	0.001
S13	5.210	0.000	-4.626	0.000
S16	6.428	0.000	-5.952	0.001
S19	2.168	0.000	-4.260	0.001
S22	2.490	-0.002	-4.596	0.000
S24	5.522	0.001	-5.925	-0.003
S28	1.865	-0.007	-4.009	-0.008
Mean	3.938	-0.001	-4.637	-0.001
S.D.	1.581	0.002	0.861	0.003

Table 45. Average reserve torque actuators of the hip joint during 5° downhill walking for the control limb.

	Hip Flexion		Hip Abduction		Hip Rotation	
Subject	Hicks	Average	Hicks	Average	Hicks	Average
S17	-2.077	0.002	-3.915	-0.010	0.650	-0.002
S25	-3.057	0.579	-6.241	-1.585	0.269	0.950
S27	-2.980	-0.001	-5.897	-0.008	1.751	0.001
S29	-0.807	0.002	-3.171	-0.007	0.596	0.002
S30	-1.973	0.004	-3.165	-0.014	0.303	-0.006
S32	-3.504	0.008	-3.978	-0.019	0.464	0.001
S33	-1.722	0.005	-2.373	-0.015	0.482	-0.002
S34	-0.721	0.002	-1.973	-0.008	0.296	0.003
S35	-0.591	0.002	-3.916	-0.010	0.329	0.001
Mean	-1.937	0.067	-3.848	-0.186	0.571	0.105
S.D.	1.086	0.192	1.439	0.525	0.463	0.317

Table 46. Average reserve torque actuators of the knee joint during 5° downhill walking for the control limb.

	Knee Angle		Ankle Angle	
Subject	Hicks	Average	Hicks	Average
S17	2.486	-0.002	-4.194	0.000
S25	0.709	-0.941	-6.764	-0.008
S27	6.320	0.000	-6.345	-0.001
S29	1.842	-0.001	-3.517	0.000
S30	2.036	-0.005	-3.350	0.001
S32	3.758	-0.008	-5.448	0.001
S33	2.124	-0.005	-3.329	0.000
S34	1.306	-0.001	-2.652	0.000
S35	1.090	-0.002	-3.392	0.000
Mean	2.408	-0.107	-4.332	-0.001
S.D.	1.714	0.313	1.482	0.003

Table 47. Average reserve torque actuators of the hip joint during 10° downhill walking for the control limb.

	Hip Flexion		Hip Abduction		Hip Rotation	
Subject	Hicks	Average	Hicks	Average	Hicks	Average
S17	-1.727	0.000	-3.994	-0.007	0.717	-0.001
S25	-2.116	0.001	-5.886	-0.009	1.733	0.005
S27	-2.498	-0.001	-6.187	-0.007	1.888	0.005
S29	-1.491	0.001	-3.145	-0.006	0.617	0.003
S30	-1.657	0.003	-3.137	-0.011	0.401	-0.003
S32	-3.038	0.006	-4.964	-0.016	0.528	0.004
S33	-1.198	0.003	-3.097	-0.013	0.585	0.002
S34	-0.410	0.002	-1.895	-0.007	0.396	0.009
S35	-0.543	0.001	-3.755	-0.009	0.805	0.002
Mean	-1.631	0.002	-4.007	-0.009	0.852	0.003
S.D.	0.856	0.002	1.417	0.003	0.561	0.003

Table 48. Average reserve torque actuators of the knee joint during 10° downhill walking for the control limb.

	Knee Angle		Ankle Angle	
Subject	Hicks	Average	Hicks	Average
S17	3.652	0.000	-3.590	0.000
S25	8.519	0.001	-5.222	0.000
S27	7.240	0.001	-5.730	-0.001
S29	2.389	0.000	-3.497	0.001
S30	3.367	-0.002	-3.265	0.001
S32	4.149	-0.005	-4.488	0.000
S33	2.690	-0.002	-3.080	0.000
S34	2.506	0.000	-2.436	0.000
S35	3.029	0.000	-3.124	0.000
Mean	4.171	-0.001	-3.826	0.000
S.D.	2.199	0.002	1.088	0.000

VITA

Tanner A. Thorsen was born in Provo, UT in 1987 to Byron and Sidney Thorsen and is the eldest of five children. He grew up in Arlington, TX, where he graduated from James W. Martin High School in 2005. After graduation, Tanner attended Brigham Young University where he graduated with a Bachelor of Science degree in Exercise Science in 2011. In 2018, Tanner completed a master's degree at The University of Tennessee, Knoxville in Kinesiology with a concentration in Biomechanics. Tanner completed his educational pursuits at the University of Tennessee, Knoxville, earning a Doctor of Philosophy in Kinesiology and Sport Studies with a concentration in Biomechanics in 2021. Tanner has accepted a tenure-track, assistant professor position at The University of Southern Mississippi in Hattiesburg, MS.